

Institute of Experimental Pharmacology and Toxicology
(Director: Prof. Dr. Thomas Eschenhagen)
Center for Experimental Medicine
University Medical Center Hamburg-Eppendorf

Development of an *in vitro* assay system for protein phosphatase inhibitor-1 antagonists

Dissertation

to obtain the academic degree
Doctor rerum naturalium (Dr. rer. nat.)

Submitted to the Department of Chemistry
Faculty of Mathematics, Informatics and Natural Sciences
University of Hamburg

By

Hannieh Sotoud

Hamburg 2012

“I never know what I think about something until I read what I have written on it”

William Faulkner

Day of the disputation: 13.07.2012

1. Referee: Prof. Dr. Peter Heissig

2. Referee: Prof. Dr. Thomas Eschenhagen

Declaration

I declare that the work reported in the dissertation submitted to the University of Hamburg and entitled,

“Development of an *in vitro* assay system for protein phosphatase inhibitor-1 antagonists”

was realized in person in the Institute of Experimental Pharmacology and Toxicology under the supervision of Prof. Dr. Thomas Eschenhagen. All sources of information as well as the results obtained in collaboration with other people are pointed out.

The dissertation has not been submitted in whole or in part for a degree at any other University.

Hannieh Sotoud

Hamburg May 2012

Contents

1	Introduction	1
1.1	Chronic heart failure and therapy.....	1
1.2	Serine/threonine phosphatases	3
1.2.1	Protein phosphatase 1 (PP1).....	5
1.2.2	I-1 as a specific regulator of PP1	9
1.3	Physiology and pathophysiology of the β -adrenoceptor signaling cascade	10
1.3.1	Cellular mechanisms of cardiac contraction.....	10
1.3.2	Role of β -adrenergic system in regulating of cardiac contraction.....	12
1.3.3	Physiological and pathophysiological roles of I-1 in the heart.....	16
1.4	I-1 as a new therapeutic target in heart failure.....	18
1.4.1	Screening of small molecules for drug discovery	20
1.4.2	Assay systems for Ser/Thr phosphatase activities.....	23
1.5	Objective	25
2	Materials	27
2.1	Antibodies.....	27
2.2	Bacterial strain	27
2.3	Buffers & solutions.....	27
2.4	Cell culture media	29
2.5	Compounds with risk phrases (R) and security advices (S).....	29
2.6	Enzymes	33
2.7	Equipments.....	33
2.8	Kits.....	36
3	Methods	37
3.1	Preparation of I-1 protein	37
3.1.1	Bacterial expression of I-1 protein	37
3.1.2	Site-directed mutagenesis of I-1	39
3.1.3	PKA phosphorylation/thiophosphorylation of I-1	42
3.1.4	Biotinylation of I-1	42
3.2	Surface plasmon resonance (SPR) measurements.....	43
3.3	Phosphatase assay development	44
3.3.1	pNPP as a chromogenic substrate	44
3.3.2	DiFMUP as a fluorogenic substrate	45
3.3.3	Phosphatase inhibitors in the colorimetric and fluorescence assays	46
3.3.4	The synthetic peptides of I-1	48
3.4	Cell culture.....	49
3.4.1	Preparation of HEK 293 cells.....	49

3.4.2	Preparation and treatment of NRCMs.....	50
3.4.3	Preparation and treatment of EHTs	52
3.4.4	Preparation and treatment of AMCMs	53
3.5	Immunohistological staining and confocal microscopy	54
3.5.1	Immunohistological staining of NRCMs	54
3.5.2	Immunofluorescence staining of EHTs	55
3.5.3	Confocal laser scanning microscopy	55
3.6	Video-optical measurements of AMCMs.....	55
3.7	Protein preparations and analysis.....	58
3.7.1	Preparation of cell and tissue homogenates	58
3.7.2	Quantification of protein using Bradford's method	59
3.7.3	SDS-PAGE and Western blot	60
3.8	Screening of compounds in the PP1-I-1 assay	61
3.8.1	<i>In silico</i> selected compounds	62
3.8.2	Determination of Z'- factor for the fluorescence assay	63
3.8.3	High-throughput screening.....	63
3.9	Determination of endogenous phosphatase activity	68
3.9.1	Measurement of phosphatase activities in the radioactive assay	68
3.9.2	Measurement of phosphatase activities in the fluorescence assay	69
3.10	Statistical analysis	69
4	Results	70
4.1	Development of PP1-I-1 assay systems	70
4.1.1	Preparation of I-1 recombinant protein.....	70
4.1.2	Development and characterization of the colorimetric assay	72
4.1.3	Development and characterization of the fluorescence assay	75
4.2	Investigation of PP1-I-1 interactions using mutant I-1 proteins.....	79
4.3	Investigation of I-1 peptides for PP1-I-1 interaction inhibition	83
4.3.1	Characterization of I-1 peptides	83
4.3.2	Effects of I-1 ^{SPRKIQFTV} in cardiac cells.....	86
4.4	Screening of small molecules	93
4.4.1	Screening of <i>in silico</i> selected compounds	94
4.4.2	High-throughput screening (HTS)	97
4.4.2.1	Determination of Z'-factor for the fluorescence assay.....	97
4.4.2.2	Single-point measurements of HTS	98
4.4.2.3	Kinetic measurements of HTS	103
4.5	Determination of endogenous PP1 activity in the fluorescence assay.....	106
5	Discussion	111
5.1	Development of a non-radioactive phosphatase assay facilitates the monitoring of PP1/I-1 activity	111
5.2	The I-1 N-terminal KIQF motif and Thr-P ³⁵ are essential for PP1 binding and inhibition	114

5.3	The binding site of the KIQF motif is a promising druggable target for PP1/I-1 interaction inhibitors.....	116
5.4	High throughput screening using the fluorescence assay would be an appropriate system to detect small molecule inhibitors for PP1/I-1 interaction	120
5.5	Determination of endogenous PP1 activity in the fluorescence assay is challenging.....	124
6	Summary.....	127
7	Zusammenfassung	129
8	References.....	132
9	Appendix.....	149
9.1	Abbreviations	149
9.2	Amino acid abbreviations.....	153
9.3	Indication of particular risks (R)	154
9.4	Indication of safety precautions (S).....	156
9.5	Curriculum vitae	159
9.6	Congress participations	160
10	Acknowledgement	162

1 Introduction

1.1 Chronic heart failure and therapy

Heart failure (HF) is a major problem worldwide causing a reduced quality of life, high mortality and frequent hospitalization. The definition of HF is the inability of the heart to supply adequate blood flow and therefore oxygen delivery to peripheral tissues and organs leading to reduced exercise capacity, fatigue, and shortness of breath. The crude prevalence of heart failure is 0.3-2.4% in general population with an increase of 3-13% for people over 56 years (Cowie et al. 1997). In the Framingham Study, a large epidemiologic study conducted in the United States, the median survival of patients with HF was only 1.7 years for men and 3.2 years for women, with only 25% of men and 38% of women surviving 5 years (Ho et al. 1993). Not only the high mortality, but also the reduced life quality and frequent hospitalizations, are the remarkable health and social complications of HF. Hypertensive and ischemic heart disease are considered as the most common reasons of HF. The primary abnormality is impairment of left ventricular function, leading to a fall in cardiac output (Jackson et al. 2000). Consequently, several compensatory mechanisms take place to maintain intact cardiac output. These mechanisms include: (1) the Frank-Starling relationship, whereby an increase in preload and thus length of the sarcomeres leads to an increase in contractility, (2) an increased release of catecholamine and other neurohormonal factors by adrenergic cardiac nerves and the adrenal medulla, causing an increase in heart rate and contractility, and (3) myocardial hypertrophy with or without cardiac chamber dilatation (Chiariello & Perrone-Filardi 1999). However, all of these adaptive mechanisms, over time, become maladaptive and trigger progression of HF (Fig 1.1).

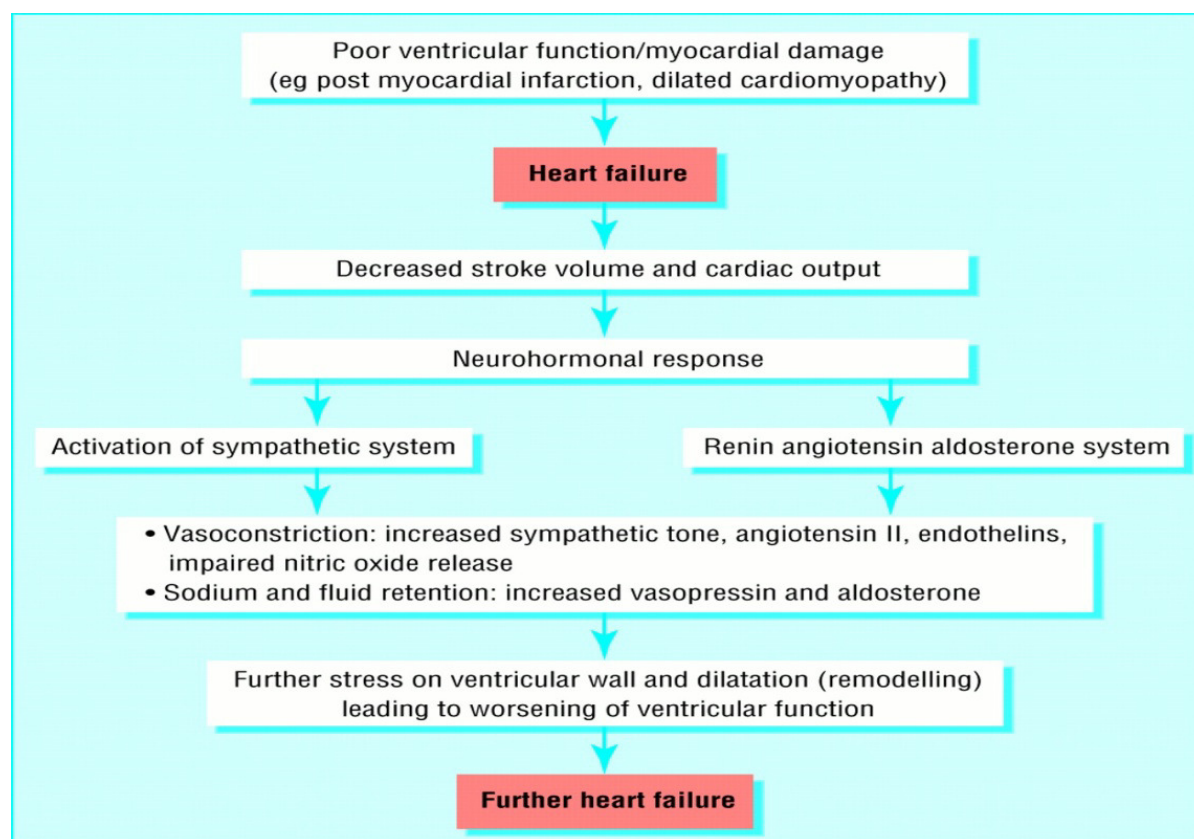


Figure 1.1 Neurohormonal and compensatory mechanisms in heart failure. The decrease in cardiac output leads to activation of several neurohormonal compensatory mechanisms aimed at improving the mechanical environment of the heart (Jackson et al. 2000).

Whereas up to 40 years ago HF was managed with diuretics and digitalis glycosides, the cornerstones of therapy for HF patients with systolic dysfunction today include ACE inhibitors or angiotensin II type 1 receptor antagonists (ARBs), β -blockers, and aldosterone antagonists, which have significantly improved survival (Morrissey et al. 2011). Historically, inotropic drugs that enhance contraction at a given ventricular volume were sought in order to enhance the Ca^{2+} signal that activates contraction. However, many of the early drugs such as digoxin overload cardiac muscle cells with Ca^{2+} , increasing both energy consumption and the risk of arrhythmias. Phosphodiesterase (PDE) inhibitors mimic the effect of sympathetic stimulation via β -adrenergic receptors and greatly increase energy consumption by the heart during the normal physiological 'fight-or-flight' response. In heart failure, this increase in energy consumption can worsen the patient's prognosis (Stevenson 2003; Bers & Harris 2011). Consequently, the current standard drugs in HF are not positive inotropic agent. ACE inhibitors and ARBs inhibit the renin-angiotensin system and β -

blockers block β -adrenergic signal pathway, and thereby protect the heart at the tissue and cellular level leading to reduced myocardial damage and improved systolic function of the heart (Delgado & Willerson 1999). However, on the way to find new therapeutic interventions, blockade of endothelin receptor (Teerlink 2002), TNF α and interleukin-1 antagonizing (Anker & Coats 2002) and central sympathetic inhibition (Cohn et al. 2003) were not beneficial in HF. Table 1.1 shows several medical therapies for treatment of chronic heart failure that failed in clinical phases. Limited therapeutic options for severe HF, and an inability to substantially and consistently reverse pathologic remodeling and myocardial dysfunction in most HF patients emphasize the requirement for new therapeutic strategies in HF (Feldman et al. 2005). In order to afford this demand, understanding of pathological pathways involved in HF is essential to identify potential therapeutic targets.

Table 1.1 Examples of drugs tested unsuccessfully in heart failure

Drug name	Year	Side-effects
Milrinone (PDEI)	1991	Increased mortality
Flosequinan (?)	1993	Increased mortality
Pimobendan (PDEI)	1996	Trend towards increased mortality (dose?)
Vesnarinone (?)	1998	Increased mortality. arrhythmias
Omapatrilat (dual)	2002	Angioneurotic edema . no clear advantage
Moxonidin (anti-SNS)	2003	Increased mortality (dose?)
Infliximab (TNF α)	2003	Increased mortality (dose?)
Etanercept (TNF α)	2004	Trend towards increased mortality
Bosentan (ET-1)	2005	Liver-Toxicity. but CHF-improvement over time ?
Etomoxir (CPT I)	2007	Liver-Toxicity
Rosuvastatin	2007	No benefit
ARB + ACEI	2003/2008	No benefit. more ADR

1.2 Serine/threonine phosphatases

Reversible protein phosphorylation is recognized as a major mechanism regulating the physiology of plant and animal cells, specifically cell division, cell differentiation, neuronal activity, muscle contraction and metabolic functions (see reviews by Herzig

& Neumann 2000; Shi 2009; Virshup & Shenolikar 2009). Steady-state phosphorylation reflects the balance between the activity of protein kinases and phosphatases. Since about 3% of all human genes encode protein kinases or phosphatases (Hunter 1995), it is not unlikely that about one third of all mammalian proteins are reversibly phosphorylated (Depaoli-Roach et al. 1994). In eukaryotic cells, phosphorylation mainly occurs on the three hydroxyl-containing amino acids serine, threonine and tyrosine, of which serine is the predominant target (86%; Olsen et al. 2006). However, while the human genome encodes an almost equal number of tyrosine kinases and phosphatases (90 vs. 107), the number of catalytic subunits of serine/threonine phosphatases is much lower than that of Ser/Thr kinases (40 vs. 428; Moorhead et al. 2007). Decades of research have discovered that Ser/Thr phosphatases do not exist freely in the cells, but are multimeric enzymes formed by a shared catalytic subunit and a large number of regulatory subunits. When holoenzymes are considered, Ser/Thr phosphatases and kinases show a similar diversity (Cohen 2002; Virshup & Shenolikar 2009). Recent studies classified Ser/Thr phosphatases into three structurally unrelated groups (Fig 1.2): I) phosphoprotein phosphatases (PPPs), II) metal-dependent protein phosphatases (PPMs) and III) aspartate-based phosphatases represented by FCP/SCP (TFIIF-associating component of RNA polymerase II CTD phosphatase/small CTD phosphatase. PPP family include PP1, PP2A, PP2B (calcineurin), PP4, PP5, PP6 and PP7, which have similar catalytic domains. PP2C and pyruvate dehydrogenase phosphatase are representative of PPMs. PP1 and PP2A are the most abundant Ser/Thr phosphatases. Their functions and structures have been extensively studied.

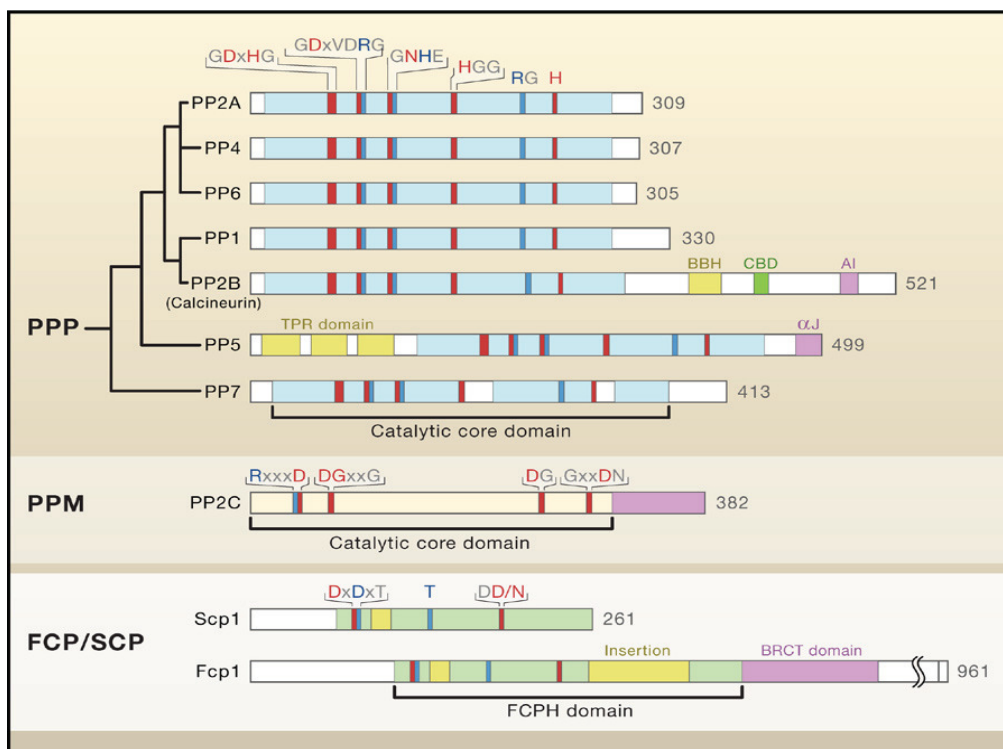


Figure 1.2 The three families of Ser/Thr phosphatases. The catalytic core domains of representative family members of PPP, PPM and aspartate-based phosphatases were compared (Shi 2009).

1.2.1 Protein phosphatase 1 (PP1)

PP1 (35-37 kDa) is a ubiquitously expressed Ser/Thr phosphatase. The highly conserved structure during evolution emphasizes the essential role of PP1 in cellular processes including cell cycle, synaptic plasticity, muscle contraction, gene transcription and metabolism see reviews by (Cohen 2002; Ceulemans & Bollen 2004). In mammalian cells, three genes encode four isoforms of PP1 catalytic subunit PP1 α , PP1 β (δ), PP1 γ_1 & PP1 γ_2 (Cohen 1988). All of these isoforms possess distinct tissue distribution and subcellular localization leading to a preferential binding to regulatory subunits and individual function (Alessi et al. 1992; MacMillan et al. 1999). For instance, the β -isoform is supposed to be the dominant form of PP1c in the sarcoplasmic reticulum according to the findings from specific PP1c isoforms knockdown in the cardiomyocytes (Aoyama et al. 2011). The catalytic subunit of PP1 is not free in the living organisms and accomplishes its diverse activities in a complex with more than 100 known regulatory subunits (Ceulemans et al. 2002). These regulators determine PP1 subcellular localization, substrate specificity and fine-

tuning of activity. Without sharing structural similarities, regulatory subunits are divided into two general groups: I) modulators, which target PP1c to distinct subcellular location or substrate and II) regulators that do not determine the targets of PP1c, including inhibitors, chaperones and activators (Cohen 2002). Two types of PP1 inhibitors are protein inhibitors and natural small molecular toxins. The toxins such as microcystin, okadaic acid (OA), calyculin A and tautomycin inhibit PP1 activity potently, but not specifically. In contrast, PP1 is specially inhibited by the three acid- and heat-stable protein inhibitors inhibitor-1 (I-1), dopamine- and cyclic-AMP-regulated phosphoprotein of molecular weight 32,000 (DARPP-32) and inhibitor-2 (I-2). In contrast to I-2, phosphorylation of I-1 and DARPP-32 by PKA on Thr³⁵ and Thr³⁴, respectively, is essential to convert them into potent inhibitors of PP1 (Aitken & Cohen 1982; Foulkes et al. 1983).

The first crystal structures of PP1 complexes with microcystin and tungstate were reported by Goldberg et al. (1995) and Egloff et al. (1995), respectively. The catalytic subunit shows a globular compact fold with β -sandwich that excludes only the COOH and NH₂ terminus. The active site is situated at the bifurcation point of an extended Y-shaped groove on the surface of the molecule (Fig 1.3). Two metal ions (presumably Mn²⁺ & Fe²⁺) are positioned in the active site, contributing to catalysis of substrate by enhancing the nucleophilicity of metal-bound water and the electrophilicity of the phosphorus atom. The arms of the surface grooves are termed I) acidic groove, II) hydrophobic groove, and III) C-terminus groove (Egloff et al. 1995; Goldberg et al. 1995). A loop between β_{12} and β_{13} sheets overhangs the active site, which is essential for either enzymatic activity or binding to the regulators (Xie et al. 2006).

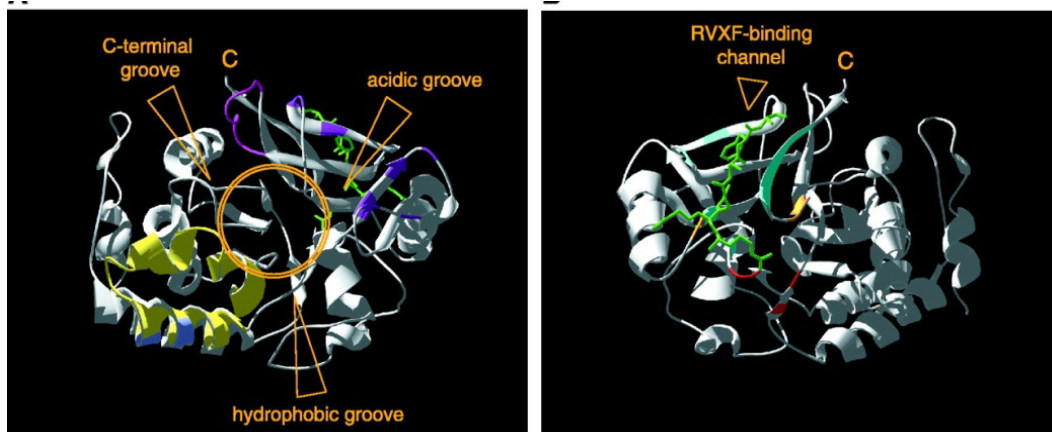


Figure. 1.3 The molecular surface of PP1. PP1 γ (ribbons) bound to an RVxF-containing peptide. The left panel shows the frontal view of PP1 with the catalytic site (encircled) and the three grooves that emanate from the catalytic site. The β_{12}/β_{13} loop is drawn in magenta and the acidic groove in purple. The right panel demonstrates the dorsal view of the same structure. The RVxF-containing peptide is rendered as a green sticks representation (Ceulemans & Bollen 2004).

The crystal structures of PP1 complexes with microcystin (Goldberg et al. 1995), OA (Maynes et al. 2001) and calyculin A (Kita et al. 2002) implicated similar inhibition mode of PP1c by toxins via targeting of the active site and the β_{12}/β_{13} loop. Although these toxins are able to inhibit other members of PPP family, the IC_{50} varies within the group (the IC_{50} of OA for PP1 and PP2A is 40 nM and 1 nM, respectively). In contrast, protein inhibitors are specific for a single PPP family member (Dancheck et al. 2008). The early studies of PP1 targeting subunits G_M , G_L , and M_{110} identified a highly conserved consensus RVxF as a general binding motif (Fig 1.3). RVxF, in which x is any amino acid except large hydrophobic residues (Wakula et al. 2003), mediates the interaction of regulatory subunits with a hydrophobic pocket of PP1 molecular surface distal from active site (Egloff et al. 1997; Ceulemans & Bollen 2006). RVxF is present in >90% of PP1 interactors determining their binding to PP1c without influencing the activity (Bollen et al. 2010). It is proposed that this motif promotes the interaction of secondary binding sites that are responsible for PP1 activity and specificity. Fig 1.4 showed representative PP1 complexes containing RVxF motif. The binding of M_{110} to PP1c is mediated by RVxF motif, but the induced activity/specificity is modulated by additional interactions (Tóth et al. 2000). Similarly, inhibition of PP1c by AKAP220 occurs with consensus bindings to the RVxF and a secondary interaction site (Schillace et al. 2001). The binding of functional interaction sites seems to be weak and therefore requires the support of the RVxF consensus.

RVxF has been found in many regulators of PP1 such as myosin phosphatase targeting subunit (MYPT1; Terrak et al. 2004), spinophilin and neurabin (Terry-Lorenzo et al. 2002), nuclear inhibitor of PP1 (NIPP1; Beullens et al. 1999), I-1 and its neuronal homologue, DARPP-32 (Barford et al. 1998). Interestingly, some of the regulators that do not possess an RVxF motif (~10%) interact with PP1c also via the RVxF binding site. Human factor C1 (HFC) is an example of such proteins (Ajuh et al. 2000). More experiments including gene disruption, inhibitory peptides, mutational analyses and *in vivo* data are required to understand the modulation and function of PP1 diverse complexes, individually. Indeed, detection of small molecules that allosterically activate or inhibit PP1 activities could be valuable in treatment of several diseases.

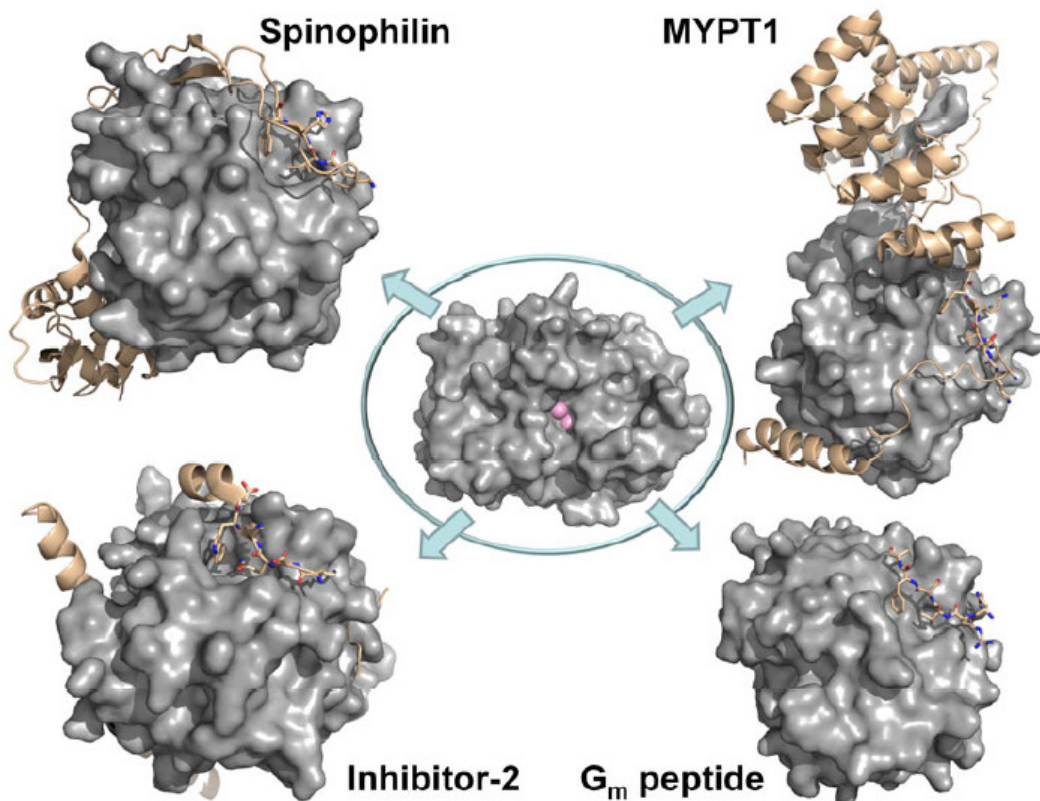


Figure 1.4 The structures of PP1 holoenzymes. PP1 catalytic subunit (gray surface) alone (in the center) and in complex with its different regulators (right and left panels) have been shown. The metals ions are depicted as pink spheres in the active site. The regulators are shown as beige ribbons and their RVxF motifs are highlighted as sticks (Peti et al. 2012).

1.2.2 I-1 as a specific regulator of PP1

Protein phosphatase 1 inhibitor-1 (I-1) is a 171 amino acid heat and acid stable protein that was first purified from rabbit skeletal muscle by Nimmo and Cohen (1978a). However its ubiquitous expression has been reported by several laboratories (MacDougall et al. 1989; Elbrecht et al. 1990; Hemmings et al. 1992). The apparent molecular weight of I-1 on SDS-PAGE (26-28 kDa) is higher than the calculated one (18-19 kDa). This discrepancy might be due to a low degree of order in this protein (Endo et al. 1996). I-1 has no tertiary structure and belongs to the family of intrinsically unstructured proteins (IUPs; Huang et al. 2000). I-1 inhibits PP1 activity selectively and potently ($IC_{50} \sim 1$ nM) after PKA phosphorylation on Thr³⁵ (Cohen 1989; Shenolikar & Nairn 1991). Regulation of PP1 activity by I-1 occurs in the cytosol of skeletal muscle, heart, kidney, brain, and liver, under control of the hormonal signaling, particularly cAMP mediated pathways (Herzig & Neumann 2000). The N-terminus of I-1 is highly conserved between rat, rabbit and human (Endo et al. 1996). Although precise molecular details of the interactions of I-1 with PP1 are not yet available, it is proposed that the 50 amino acid-N-terminal of I-1 containing the common binding motif, RVxF (KIQF) and phosphorylated Thr³⁵ are inevitable to bind and inhibit PP1 activity (Kwon et al. 1997; Watanabe et al. 2001). Also, four consecutive arginines that precede the phosphothreonine in I-1 are proposed to interact with multiple acidic residues lining in acidic groove (Goldberg et al. 1995; Connor et al. 1998; Terrak et al. 2004). Moreover, contact with β_{12} - β_{13} loop has been reported to be crucial for PP1-I-1 interaction (Connor et al. 1998; Huang et al. 1999). This might facilitate the placement of phospho-Thr³⁵ in the active site of PP1 and thereby inhibiting the enzymatic activity. While the N-terminus domain of I-1 is responsible for PP1 inhibition, the C-terminus seems to function as an anchoring domain that binds to other proteins, particularly growth arrest and DNA damage-inducible protein (GADD34), and forms heteromeric complexes (Weiser et al. 2004). I-1-GADD34-PP1 complex is the cross-talk between cAMP signal and eIF2 α for regulation of protein translation (Connor et al. 2001). The roles of I-1 in glycogen metabolism (Poulter et al. 1988), muscle contractility (Chisholm & Cohen 1988; Neumann et al. 1991), cell growth (Walker et al. 1992), neuronal plasticity (Mulkey et al. 1994) and heart function (Neumann et al. 1991; El-Armouche et al. 2003a) have

been studied. However, the structural details of PP1-I-1 complex remain to be elucidated, particularly via crystallographic studies.

1.3 Physiology and pathophysiology of the β -adrenoceptor signaling cascade

1.3.1 Cellular mechanisms of cardiac contraction

Each time that the heart beats, ventricular contraction is triggered by a wave of electricity (action potential), which originates from the heart's natural pacemaker in the top of right atrium, called sinoatrial (SA) node. The impulse spread throughout the atria causing atrial contraction and then travels into the ventricles via atrioventricular (AV) node generating ventricular contraction (Klabunde 2007).

The action potential results in contraction of single myocardial muscle cells (cardiomyocytes). Each cardiomyocyte is filled with hundreds of rod-like myofibrils, which are composed of the sarcomeres. During contraction, the thin actin filament and the thick myosin filament slide over each other and then they pull together the two ends of the sarcomere. The thick filament consists of hundreds of myosin molecules. Each myosin contains two heads, which have ATPase sites and provide the required energy for actin-myosin cross bridge formation. The thin filament is composed of actin, tropomyosin and troponin complex. The sarcomere is bound on either side by the Z-line to which actin is attached. Myosin extends from the center towards either direction (Opie 2008). The interaction of actin and myosin is initiated by increasing intracellular calcium level. The troponin complex in the thin filament consists of three subunits; troponin C (TnC), troponin inhibitor (TnI) and troponin T (TnT). TnC is the calcium sensitive subunit and contains four Ca^{+2} binding sites. TnI is the inhibitory subunit that binds actin in the relaxed state, thereby preventing actin-myosin contraction. Troponin T (TnT) is involved in the attachment of the troponin complex to the thin filament, binding tropomyosin and actin. The binding of intracellular Ca^{+2} by TnC induces a conformational change in the troponin complex, which causes TnI to release actin, subsequently allowing actin to interact with myosin, resulting in muscle contraction (Opie 2008).

Regulation of cytosolic Ca^{2+} is mainly carried out by proteins in the sarcolemma and sarcoplasmic reticulum (SR), the analogue of endoplasmic reticulum in muscle cells. The sarcolemma is a complex membrane that forms a tubular network (T tubules)

extending the extracellular space into the interior of the cell. The action-potential wave opens the tubular voltage-dependent L-type Ca^{2+} channels (LTCC) that are in close proximity to the SR. Ca^{2+} ions enter the cardiomyocytes and after reaching the junctional area between LTCC and SR trigger the release of a large amount of Ca^{2+} from SR through calcium release channels called ryanodine receptors (RyR2). This process is termed Calcium-Induced-Calcium-Release (CICR). RyR2 is a megacomplex protein consisting of Ca^{2+} release channel and several regulatory proteins that are localized to the junctional complex (Bers 2002a; Opie 2008). The SR is the Ca^{2+} store of the myocytes and contains Ca^{2+} at a millimolar level. This high intra-SR Ca^{2+} concentration along with Ca^{2+} intruded upon LTCC stimulate the opening of RyR2 to release SR Ca^{2+} (Bers 2002b). Thereby, the cytosolic concentration of Ca^{2+} increases about 100 (from 10^{-7} to 10^{-5} M) fold resulting in the interaction of Ca^{2+} with TnC to trigger the contractile process (Fig 1.5).

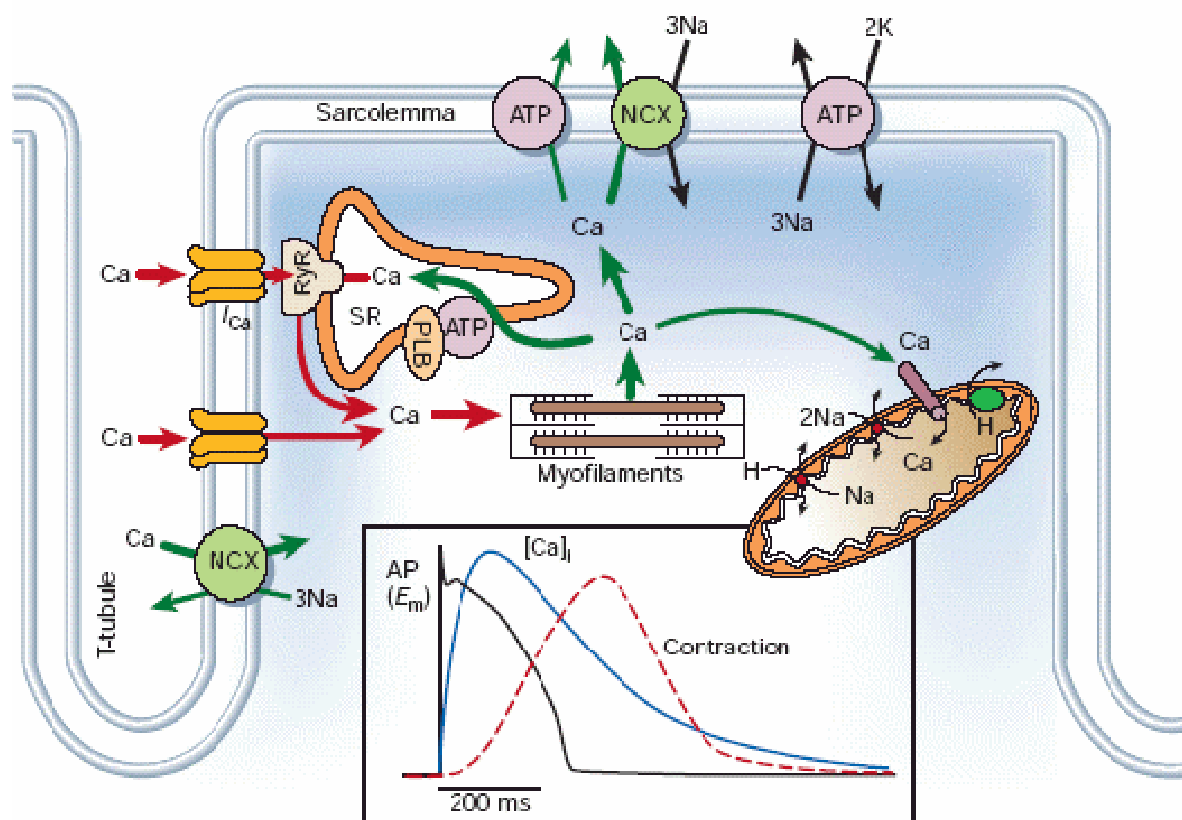


Figure 1.5 Scheme of calcium role in cardiac contractility. Electrical excitation at the sarcolemmal membrane activates voltage-gated Ca^{2+} channels, and the resulting Ca^{2+} entry activates Ca^{2+} release from the sarcoplasmic reticulum (SR) via ryanodine receptors (RyRs), resulting in contractile element activation. Inset shows the time course of an action potential (E_m), Ca^{2+} transient and contraction (Bers 2002a).

To initiate the next contraction, cytosolic calcium concentration must be reduced allowing the Ca^{2+} dissociation from TnC. Four mechanisms govern Ca^{2+} transport out of the cytosol: I) SR Ca^{2+} -ATPase (SERCA), II) sarcolemmal $\text{Na}^{+}/\text{Ca}^{2+}$ exchange (NCX), III) sarcolemmal Ca^{2+} -ATPase and IV) mitochondrial Ca^{2+} uniport. The same amount of Ca^{2+} that enters during a contraction should be extruded during relaxation to keep the steady state (Bers 2002a).

The activity of SERCA is regulated by a 27 kDa-pentamer protein called phospholamban (PLB) that is located on the SR membrane. PLB is an endogenous inhibitor of SERCA. Data from animal models with either knockout (KO; Luo et al. 1994) or overexpressed PLB (Kadambi et al. 1996) indicated the essential role of PLB in regulation of SR function and subsequently cardiac contractility. Two major protein kinases, cAMP-dependent protein kinase A (PKA) and Ca^{2+} /calmodulin-dependent protein kinase II (CaMKII) control the activity of PLB by phosphorylation on distinct sites, which result in disinhibition of SERCA (Wegener et al. 1989). Phosphorylation of PLB on both Ser¹⁶ and Thr¹⁷ by PKA and CaMKII, respectively, leads to increased SR calcium uptake (Bers 2002a). The phosphorylation state of PLB can be reversed by protein phosphatase activity (Kranias & Di Salvo 1986; Ahmad et al. 1989). Calcium is stored in the SR bound to a highly charged storage protein termed calsequestrin (CSQ) during the relaxation phase (Opie 2008).

1.3.2 Role of β -adrenergic system in regulating of cardiac contraction

The sympathetic nervous system is the most powerful accelerator of the cardiac contraction-relaxation cycle (Bers 2002a). In the cardiomyocytes three subtypes of β -adrenoceptors (ARs) are expressed: β_1 -ARs, the most abundant, β_2 - and probably β_3 -ARs (Bylund et al. 1994). The ratio of β_1 to β_2 -ARs in a human heart is approximately 70:30 (Brodde 1991). Despite predominant expression of β_1 -ARs, stimulation of both β_1 and β_2 -ARs almost equally mediates increases of cardiac contractility (inotropism), frequency (chronotropism), rate of relaxation (lusitropism) and impulse conduction through AV node (dromotropism; Brodde & Michel 1999; El-Armouche et al. 2003b). The role of β_3 -AR is still unclear (Brodde et al. 2006). The binding of catecholamines to β -AR activates a GTP binding protein (G_s), leading to increased cAMP production via adenylyl cyclases (ACs). The increased intracellular cAMP in turn activates PKA to phosphorylate several cardiac proteins, including

LTCC, RyR2, TnI, myosin binding protein C (MyBP-C) and PLB and thereby regulates cardiac contraction (see reviews by Rapundalo 1998; El-Armouche & Eschenhagen 2009). PKA phosphorylations of LTCC at Ser¹⁹²⁸ and RyR2 at Ser²⁸⁰⁸ increase cytosolic Ca²⁺ levels and thereby induce stronger contractility (positive inotropy). Phosphorylations of myofilament proteins, TnI (Ser^{23/24}) and MyBP-C (Ser²⁸²), decrease myofilament Ca²⁺ sensitivity and thereby promote relaxation kinetics (positive lusitropy; Cazorla et al. 2006; Stelzer et al. 2007). Phosphorylation of PLB at Ser¹⁶ enhances the rate and amount of Ca²⁺ uptake into the SR and thereby induces a positive lusitropic effect (Fig 1.6; Lindemann et al. 1983; Wegener et al. 1989). Several evidences indicate that PKA phosphorylation of Ser¹⁶ triggers the phosphorylation of Thr¹⁷ by CaMKII leading to amplification of the effects induced by PLB phosphorylation (Lindemann & Watanabe 1985; Wegener et al. 1989; Vittone et al. 1990). Similarly, concomitant phosphorylation of RyR2 at Ser²⁸¹⁵ by CaMKII and at Ser²⁸⁰⁹ by PKA, in a fight-or-flight response, leads to maximal SR Ca²⁺ release and thereby maximal contractile force (Wehrens et al. 2004; Opie 2008).

The cAMP mediated phosphorylation events are compensated by cAMP phosphodiesterases (PDEs; Fischmeister et al. 2006) and Ser/Thr protein phosphatases, mainly PP1 and PP2A (MacDougall et al. 1991; Lüss et al. 2000).

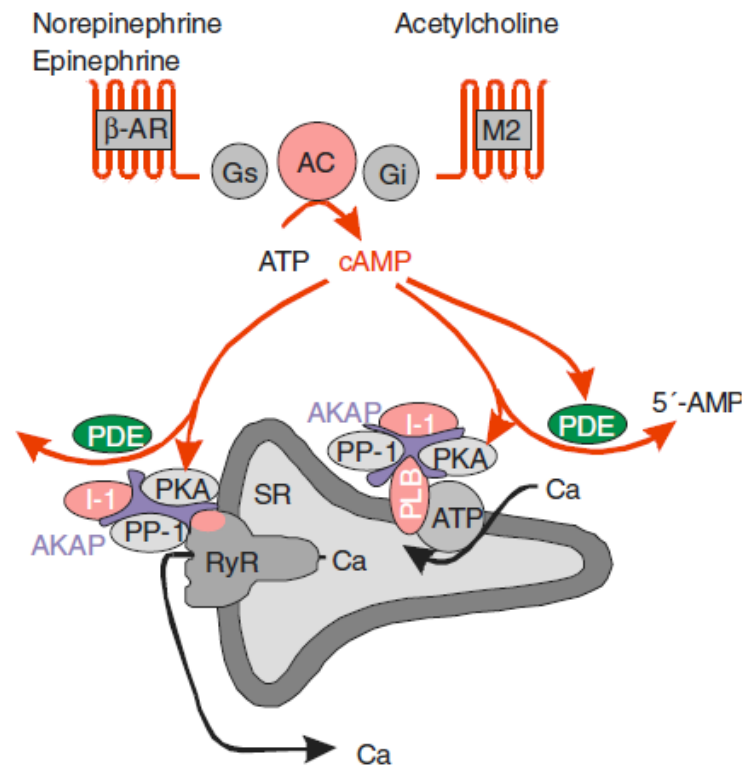


Figure 1.6 The SR as an effector compartment in the cAMP/PKA signaling pathway. β -adrenergic/cAMP/PKA-dependent phosphorylation of RyR and PLB regulates intracellular Ca^{2+} transient causing increase in cardiac output (El-Armouche & Eschenhagen 2009).

Desensitization of β -adrenergic signal transduction is a major hallmark of HF leading to attenuated cardiac responsiveness to adrenergic neurotransmitters (Bristow et al. 1982; Eschenhagen 2008). Although, short-term stimulation of β -AR increases cardiac output, long-term stimulation in chronic HF results in suppression of responsiveness (Fig 1.7; Lohse et al. 2003). This is due to reduced β -AR density, uncoupling of β -AR from G_s arising from increased β -adrenergic kinase (GRK2) and increased G_i protein and mRNA (El-Armouche et al. 2003b; El-Armouche & Eschenhagen 2009). Clinical studies have reported a direct correlation of chronic activation of the adrenergic nervous system and shortened survival (Kaye et al. 2004). During progressive HF, the β -AR signaling pathway undergoes stereotypic alterations (Lefkowitz et al. 2000). Subsensitivity of the β -adrenoceptor pathway can be interpreted either as a beneficial mechanism protecting against catecholamine toxicity or as a maladaptive program exaggerating contractile dysfunction (El-Armouche 2003a; Lohse et al. 2003). Evidence indicates that in contrast to β_2 -ARs, β_1 -ARs through G_s signaling have proapoptotic effects (Communal et al. 1999), which emphasizes the protective effect of β_1 -ARs desensitization. The molecular alterations

in chronic HF downstream of PKA comprise hypophosphorylation of PLB, TnI and MyBP-C, contributing to impaired relaxation (Bartel et al. 1996). Hypophosphorylation of PLB leading to dysfunction of SERCA might be due to either reduction in cAMP in the SR compartment or an increase in PP1 activity (Port & Bristow 2001). In contrast, LTCC and RyR have been reported to be hyperphosphorylated (Schröder et al. 1998; Marx et al. 2000) leading to pathophysiological enhancement of cytosolic Ca^{2+} . Hyperphosphorylation of LTCC and subsequently hyperactivity of single-channels arising from decreased dephosphorylation rate may be contributed to altered subcellular distribution of PP1 (Schröder et al. 1998). PKA hyperphosphorylation of RyR2 results in dysregulation of RyR2 channel providing the “leaky RyR2” (diastolic SR Ca^{2+} release; Marx et al. 2000). The altered calcium homeostasis during chronic desensitization of β -adrenergic signal transduction mechanisms leads to an increased intracellular Ca^{2+} concentration during diastole (Feldman et al. 2005). One of the consequences of increased cytoplasmic Ca^{2+} might be induction of fetal genes, which may contribute to contractile dysfunction and pathologic hypertrophy (Lowes et al. 2002).

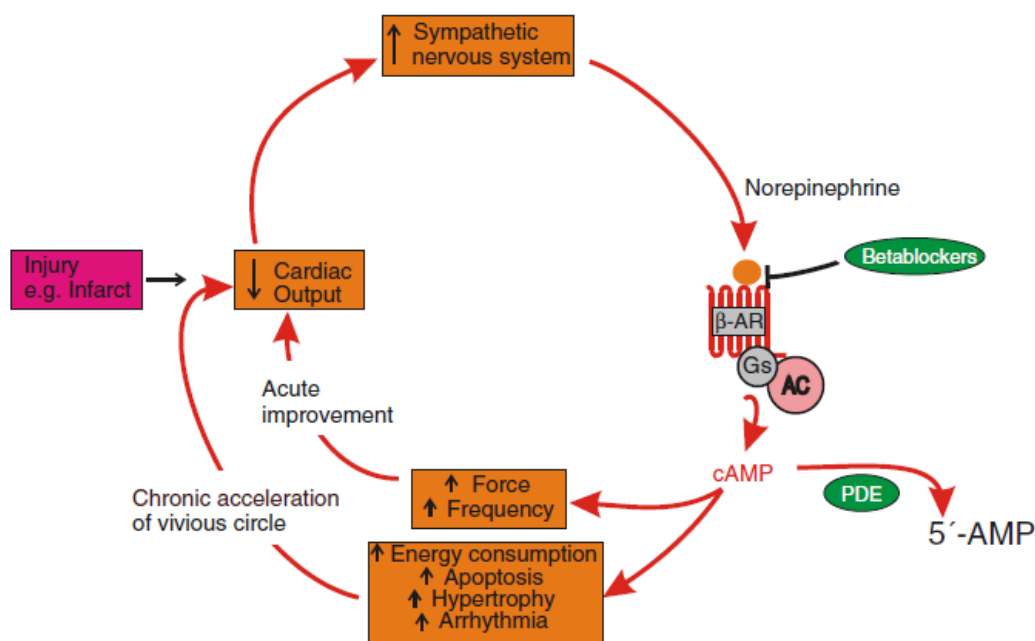


Figure. 1.7 Vicious circle in heart failure. Cardiac injury leads to reduced contractility resulting in activation of the sympathetic nervous system. Acutely, norepinephrine stabilizes the heart rate and force through β_1 -AR stimulation. However, continuous overstimulation of β -AR converts the physiological condition to a pathophysiological response. In heart failure, the signaling cascade is normally desensitized in response to chronic norepinephrine stimulation, an adaptation that can be viewed as mainly beneficial (Eschenhagen 2008).

1.3.3 Physiological and pathophysiological roles of I-1 in the heart

Neumann et al. (1991) demonstrated the presence of I-1 in the heart and its phosphorylation upon β -adrenergic stimulation, which indicates I-1 involvement in β -adrenergic signal cascade. Another evidence for hormonal regulation of I-1 was the observation that I-1 phosphorylation in rabbit skeletal muscle increased from 31% to 70% after adrenaline injection (Foulkes et al. 1980). However, the low expression level of I-1 and lack of a sensitive antibody retarded understanding of I-1 physiological roles, in detail. The acid resistance property of I-1 facilitates its enrichment in a trichloroacetic acid (TCA) extract (Foulkes et al. 1980). Using this strategy, I-1 was detected in cardiomyocytes (Gupta et al. 1996). Overexpression of I-1 sensitized cardiomyocytes to β -adrenergic agonists, indicating an amplifier role of I-1 in the β -adrenergic signal cascade (Fig 1.8; El-Armouche et al. 2003a). β -adrenergic stimulation increases cardiac contractility as a consequence of PKA phosphorylation of several cardiac proteins that regulate intracellular Ca^{2+} homeostasis. PP1 reverses this effect by dephosphorylating of phosphoproteins (MacDougall et al. 1991). I-1 is also a substrate of PKA and after phosphorylation on Thr³⁵ becomes active and antagonizes PP1 effect, preferentially on PLB (El-Armouche & Eschenhagen 2009). I-1 is dephosphorylated by other members of Ser/Thr phosphatases such as PP2A and PP2B (Hemmings et al. 1984). Activation of PP2B occurs following increases in cytosolic Ca^{2+} level leading to deactivation of I-1 and increased PP1 activity. We showed that inhibition of PP2A and PP2B activities in cardiomyocytes with OA and cyclosporine A, respectively, results in significant increases of I-1-PThr³⁵ and PLB-PSer¹⁶ (El-Armouche et al. 2006a). Interestingly, cell fractionation studies demonstrated that cardiac I-1 is mostly (78%) associated with the SR (Gupta et al. 2003). This is compatible with a role of I-1 in regulating of SR phosphoproteins like PLB. I-1 can also be phosphorylated at Ser⁶⁷ by PKC α , causing attenuation of I-1 activity toward PP1 (Braz et al. 2004). Thus, PKC α knockdown in both cardiomyocytes and engineered heart tissues (EHTs) demonstrated improved contractility (El-Armouche et al. 2007b). This situation has been showed to be associated with suppressed I-1 activity and decreased PLB phosphorylation (Braz et al. 2004; Rodriguez et al. 2006).

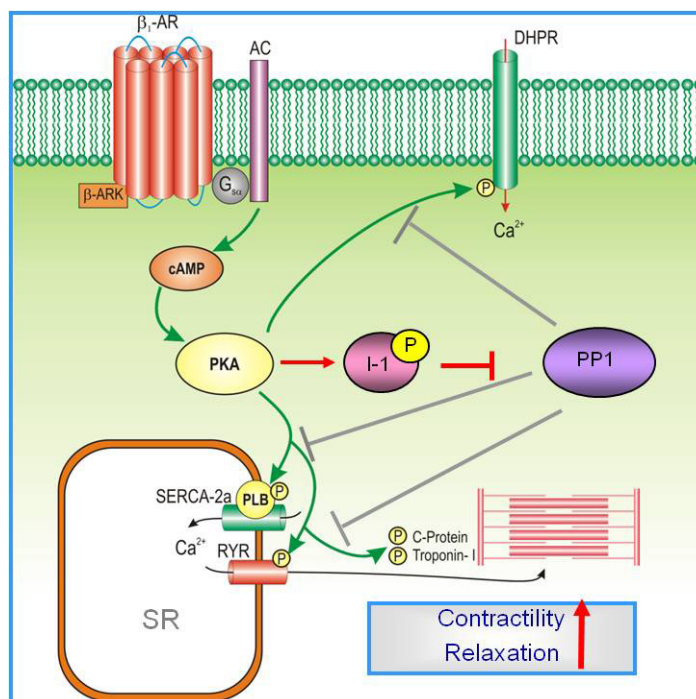


Figure 1.8 Scheme of I-1 as an amplifier of β-adrenergic signaling. β-adrenergic stimulation activates PKA, which in turn phosphorylates cardiac proteins leading to increased contractility. This PKA phosphorylation step can be reversed by phosphatases in the heart, of which type-1 phosphatases are predominating. Inhibitor-1 is a substrate of PKA and inhibits type-1 phosphatase potentially only in its phosphorylated state. The consequence of this inhibition is amplifying the PKA-mediated effects on protein phosphorylation and contractility.

In HF I-1 is like the β₁-adrenoceptors downregulated and hypophosphorylated, *in vitro* and *in vivo* (El-Armouche et al. 2003a; El-Armouche et al. 2004). This feature is consistent with PP1 hyperactivity in human failing hearts (Neumann et al. 1997). Reduction in I-1 protein and phosphorylation levels in failing hearts were accompanied with reduced phosphorylation of cardiac proteins such as PLB (El-Armouche et al. 2004). Indeed, drastically decrease in I-1 phosphorylation (up to 77%) in HF could be due to the depressed cAMP-PKA signaling via β-adrenergic desensitization (El-Armouche et al. 2003a). On the other hand, the increased level of PP2B in HF (Molkentin et al. 1998), might also contribute to I-1 hypophosphorylation. Whether hypoactivity of I-1 and following hyperactivity of PP1 in HF is a maladaptive or protective mechanism, is still under discussion (El-Armouche et al. 2011).

1.4 I-1 as a new therapeutic target in heart failure

β -blockers improve life quality and reduce mortality of patients with HF (Delgado & Willerson 1999). However, the negative chronotropic and inotropic effects of β -blockers could induce undesired reductions in contractility (Teerlink 2002). Therefore, they are not recommended in acute myocardial infarction or unstable angina (Anker & Coats 2002). In severe patients with chronic obstructive pulmonary dysfunction (COPD), only selective β -blockers can be carefully used (Cohn et al. 2003). All β -blockers are contraindicated in patients with asthma (Feldman et al. 2005). The other problem of β -blockers is that guideline recommended target doses cannot be reached in all patients due to hypotension, dizziness or fatigue. Moreover, genetic polymorphisms of β -ARs and other proteins of the β -adrenergic signal cascade lead to interindividual variability of the responsiveness to β -blockers (Klabunde 2007). Therefore, new therapeutic interventions with more selectivity to block detrimental aspects of β -blockers are interesting.

Carr et al. (2002) showed that either overexpression of PP1 catalytic subunit or ablation of I-1 in animal models were associated with decreased PLB phosphorylation and subsequently cardiac dysfunction. Accordingly, they applied an adenovirus to overexpress constitutive active I-1 in failing human cardiomyocytes, representing PP1 inhibition as a therapeutic target. Pathak et al. (2005) demonstrated that gene-transfer of constitutive active I-1 leads to chronic suppression of PP1 associating with increased cardiac function. In apparent contrast, our group demonstrated that I-1 ablation protected mice against detrimental effects induced by catecholamines (Fig 1.9 B; El-Armouche et al. 2008). Overexpression of full-length I-1 led to increase of PP1c, as an adverse compensatory mechanism (El-Armouche et al. 2008). Furthermore, conditional overexpression of constitutively active I-1 in I-1 knockout mice (TG I-1c) demonstrated improved contractility under basal condition in young mice, but cardiac dysfunction aging and after catecholamine infusion (Fig 1.9 A; Wittköpper et al. 2010).

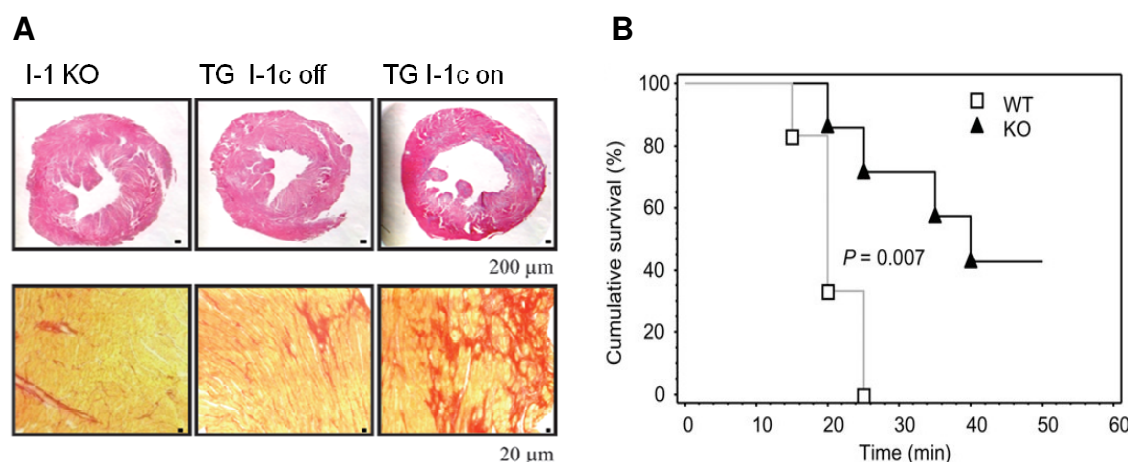


Figure 1.9 Isoprenaline-induced detrimental effects in I-1 KO versus overexpressed TG I-1c mice. **A)** Representative H & E-stained (upper row) and sirius red-stained (lower row) paraffin sections demonstrate dilation of the hearts and fibrosis extent, respectively, in I-1 KO and conditional (on and Off) transgenic mice with I-1c overexpression after isoprenaline infusion for 14 days (Wittköpper et al. 2010). **B)** Survival after isoprenaline infusion in n=6 WT and n=7 I-1 KO mice (El-Armouche et al. 2008).

These findings suggested that I-1 blockade could be a new therapeutic approach in HF. It would represent a partial blockade of the β -adrenergic system without affecting the whole cAMP pathway. Some of the anticipated differences of I-1 blockade compared to β -blockers could be: I) no modulation of heart rate. I-1 KO and I-1c mice showed similar heart rate under basal condition and after β -adrenergic stimulation (El-Armouche et al. 2008; Wittköpper et al. 2010). The reason is very likely that the regulation of pacemaker channels by cAMP occurs upstream of I-1, and therefore is unaffected by I-1. II) No relaxation deficit. It has been shown that I-1 has no effect on PKA-mediated phosphorylations of the myofilament proteins Tnl and MyBP-C and thereby no effect on Ca^{2+} sensitivity (Wegener et al. 1989). III) Mild negative inotropic effect. Since I-1 does not modulate LTCC, its blockade leads to less depression of cardiac contractility than β -blockers. However, at this point advantages or disadvantages of inhibition as β -blocker remain purely theoretical. A gene therapy approach using siRNA has been performed aiming at I-1 knockdown in mouse heart, but the results were inconclusive due to low gene transfer and knockdown efficiency (Neuber et al. unpublished). An attractive approach would therefore be the development of a small molecule inhibitor of I-1. Identification of such compounds not only provides a new pharmacologic intervention, could also clarify the oppositional concepts of I-1 as a target in HF.

1.4.1 Screening of small molecules for drug discovery

The concept of drug discovery is based on physiological readouts or target identification (Sams-Dodd 2005). Following target identification, a validation process is carried out to investigate if its modulation in a pathological pathway has therapeutic effects. Therefore, well-understanding of biological processes is important for identification of disease new targets. Transgenic animals (KO or KI) or cell-based disease models are broadly used for target validations (Fig 1.10).

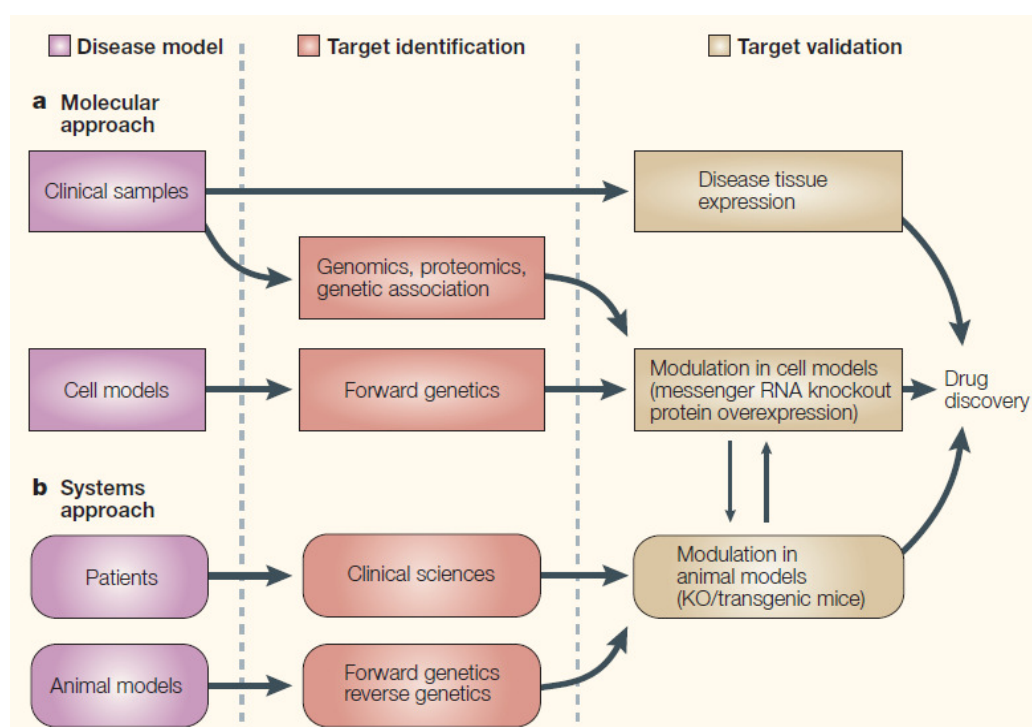


Figure 1.10 Target-based drug discovery. Identification of novel targets and early validation to confirm their involvement in disease processes carried out using two strategies: **a** Molecular approach, which attempts to understand the cellular mechanisms contributing in disease of interest, **b** System approach, is based on clinical findings and animal models (Lindsay 2003).

The term “drugability” describes how well a target is effective and accessible for drugs, especially small molecules (Dobson 2004). Recognition of one disease target makes it possible to find other upstream or downstream targets with potential fewer side effects and better drugability (Eckstein 2008). Fig 1.11 illustrates the different groups of drug targets according to biochemical criteria. The analysis shows that among ~500 molecular targets, cell-surface receptors, particularly G protein-coupled

receptors represent the largest group of current drug targets (45%; Drews 2000; Christopoulos 2002).

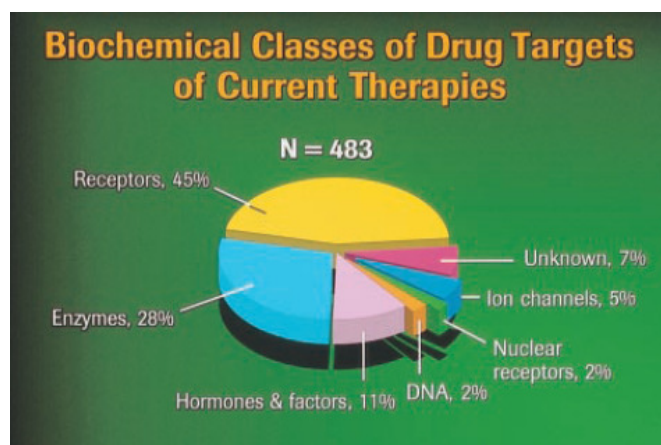


Figure 1.11 Comprehensive analysis of molecular targets for current drugs (Goodman 1996).

Following determination of an appropriate target the development of an appropriate assay is a critical step in the drug discovery pathway. Classically, large numbers of compounds are first tested in an *in vitro* assay to pick out some promising candidates. *In vitro* assays are biochemical systems consisting of recombinant or isolated reagents. In any case, an eligible assay for screening approaches should be physiologically relevant to the target, robust with reproducible results, sensitive, time and cost-effective and automatable. The rate of hit finding in a primary screen varied from 0.1 to 5%, depending on the given cutoff parameters and dynamic range of the assay (Eckstein 2008).

Over the past decades, high-throughput screening (HTS) has been used extensively to make the assessment of chemical libraries faster. The term HTS is used when assays are run in a 96-, 384- or 1536-well format. Increasing miniaturization and automation facilitate screening of up to 100,000 compounds daily. The statistical parameters such as signal-to-noise, Z- and Z'-factors are used for quality evaluation of an assay for HTS. Therefore, sometimes the final HTS form differs from its original assay format. Nowadays, virtual (*in silico*) screening has become an important component of drug discovery pipeline, from hit identification to lead optimization. Employment of structural properties of protein, DNA and RNA, obtained from x-ray crystallography or nuclear magnetic resonance (NMR) enables filtering out the majority of compounds with low chance to be a hit. One successful example of using virtual screening was the detection of HIV protease inhibitors (Kitchen et al. 2004; Chang et al. 2010). The obtained hits from a primary screen are usually retested and

confirmed by studying dose-response relationships. After validation of selectivity and efficacy, a hit becomes a “lead”. The lead compounds proceed to biological investigations in animals. Chemical refinements improve the efficacy, stability, delivery and toxicity of the leads. When a lead becomes a “new drug candidate”, it goes to the development phase consisting of preclinical studies. Following a successful preclinical development, the compound files as “investigational new drug” (IND) and enters clinical trials, which are the most critical and expensive parts of drug discovery pathway (Eckstein 2008). Fig 1.12 shows the outline of drug development process.

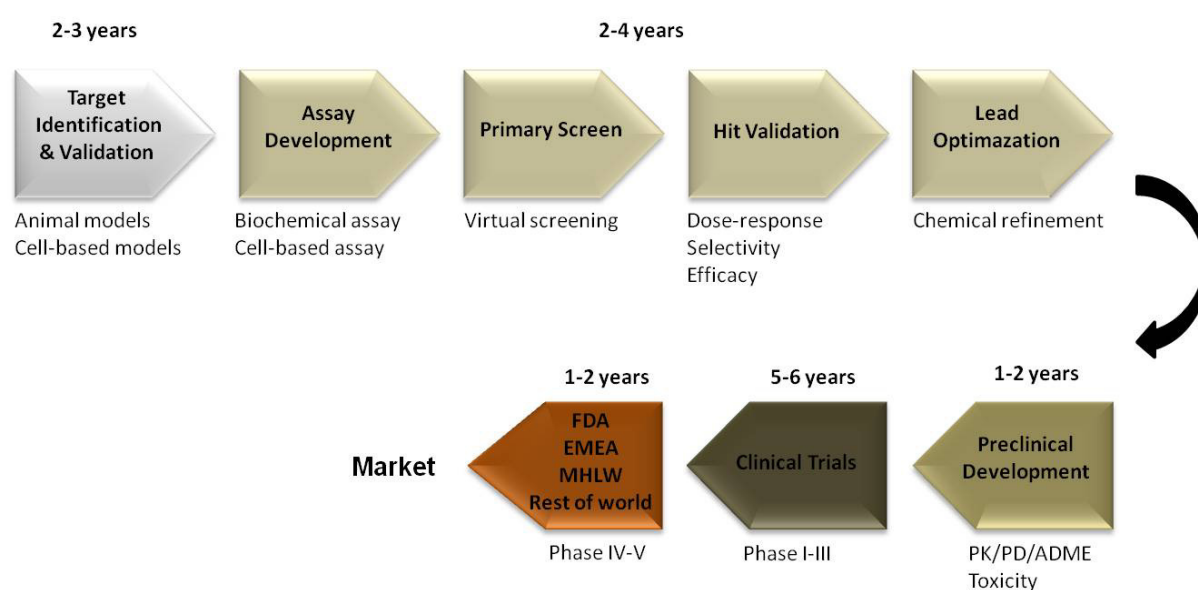


Figure 1.12 Drug discovery from bench to market.

About 90% of NCEs fail in the clinical phase. On average, the development of a new drug takes ~12 years (Smith 2002; Eckstein 2008). Despite a lot of advances in drug screening and increased investments in research and development (R&D), the numbers of FDA approved new drugs is falling down over the past few years (Fig 1.13). In this regard, drug development process demands better understanding of potential targets, as well as more advertence to quality of assays and compounds. Since 2000, pharmaceutical companies have become interested in cooperation with academics (Baker 2010). The idea of integration of academics into industry-like has been substantially grown, The partnership with academics in R&D researches has the potential to ameliorate the drug discovery approaches including target validation, assay optimization and small molecule profiling (Baker 2010).

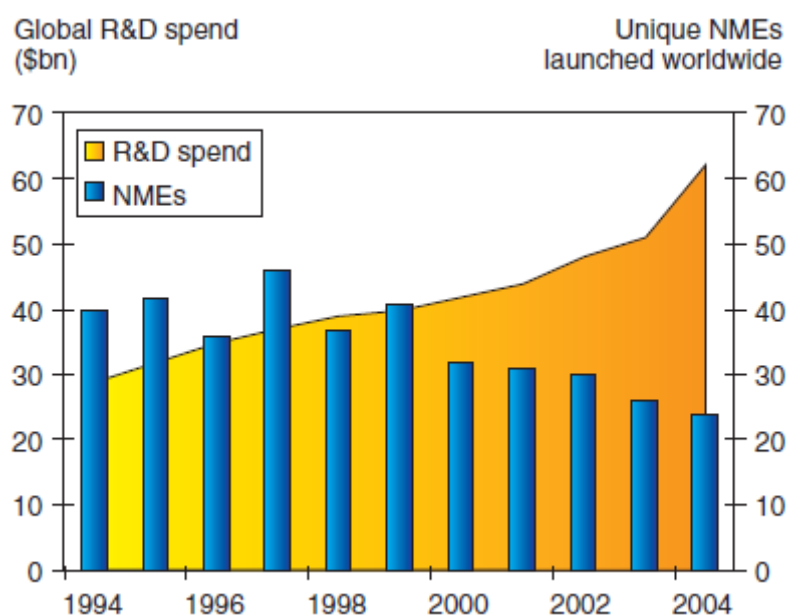


Figure 1.13 Decreased rate of new drug approval despite increased R&D spending by pharma companies (Hoekema 2007).

1.4.2 Assay systems for Ser/Thr phosphatase activities

Assay development follows target validation in the drug discovery pathway. Therefore the focus of this chapter introduces the available assays for Ser/Thr phosphatases. In the early studies, Ingebritsen & Cohen (1983) divided Ser/Thr phosphatases into two groups based on their substrate sensitivity and inhibition properties. Type 1 phosphatase (PP1) dephosphorylates only the β -subunit of phosphorylase kinase and is inhibited by inhibitor proteins, I-1 and I-2. Type 2 phosphatases including PP2A, PP2B and PP2C dephosphorylate the α -subunit of phosphorylase kinase and are resistant against I-1 and I-2. The investigations of several proteins, involved in carbohydrate metabolism, lipid synthesis, protein synthesis and some other phosphoproteins, indicated broad and overlapping substrate specificities for PP1, PP2A and PP2C. However, PP2B dephosphorylates only few phosphoproteins including phosphorylase kinase, I-1 and myosin light chains (Ingebritsen & Cohen 1983). Whereas the activities of PP1 and PP2A are independent of divalent cations, PP2B and PP2C have absolute requirements for Ca^{2+} and Mg^{2+} , respectively (Cohen et al. 1989). PP1 and PP2A are the only enzymes that act on glycogen phosphorylase, significantly (Ingebritsen & Cohen 1983). Therefore, phosphorylase a has become the most common substrate to

determine activities of PP1 and PP2A in combination with I-1 or I-2 to distinguish PP1 activity from PP2A. Afterwards, Cohen et al. (1989) introduced an improved phosphatase assay by addition of OA, which inhibits PP2A activity more potent than PP1. The combination of inhibitor proteins with OA allowed quantification of PP1 and PP2A activities in two different ways with higher accuracy. The activity that is sensitive to protein inhibitors and/or insensitive to low nanomolar concentrations of OA was considered as PP1 activity. While the ratio of phosphatase activity that is resistant to I-1 or I-2 and inhibited by low nM OA was accounted for PP2A. The phosphorylase phosphatase activity is measured by the release of radioactive inorganic phosphate from [^{32}P]-labeled substrate. However, [^{32}P]-phosphorylase a has to prepared freshly prior to the assay, using phosphorylase kinase and [^{32}P]-ATP. Up to now, this radioactive-based system is the most relevant assay for detection and quantification of PP1 activity, either as free catalytic subunit or as holoenzyme. Meanwhile, other synthetic radioactive substrates have been developed including [^{32}P]-phosphohistone and [^{32}P]-phosphopeptides (Honkanen et al. 1990; Honkanen 1993). Although such phosphoproteins closely mimic physiological substrates, they are expensive to produce and not suitable for HTS. The trend to non-radioactive assays led to the development of chromogenic and fluorogenic substrates. Baykov et al. (1988) utilized malachite green and molybdate to measure free alkaline phosphate. This method was extended to determine activity of protein phosphatases by quantification of released phosphate after forming complex with malachite green and molybdate (Geladopoulos et al. 1991). The other chromogenic substrate, p-nitrophenyl phosphate (pNPP), was commonly used for alkaline phosphatase activity, however was also shown to be a good substrate for PP1 and PP2A (Takai et al. 1995). Since An & Carmichael (1994) described pNPP for the detection of natural toxins like microcystin and nodularin, several laboratories adapted this system as an alternative method instead of mouse bioassay, ELISA or HPLC to determine toxins with PP1 and PP2A inhibitory effects (Ward et al. 1997; Metcalf et al. 2001; Bouaícha et al. 2002). The first fluorogenic substrate, 4-methylumbelliferyl phosphate (MUP) was described in 1965 by Fernley and Walkeras for alkaline phosphatases. Subsequently, Mountfort et al. (1999) & Vieytes et al. (1997) demonstrated the advantages of using MUP and PP2A over other standard methods for detection of OA in shellfish and mussel. However, using MUP, the

enzymatic activity should be carried out in a basic milieu to achieve maximum sensitivity. Therefore, a fluorinated MUP derivative, 6, 8-difluoro-4-methylumbelliferyl phosphate (DiFMUP) has been developed that acts in all acidic, neutral and basic pH. The high activities of PP1 and PP2A against DiFMUP facilitate measurement of very tiny amounts of both enzymes (Fontal et al. 1999). Development of selective assay systems for PP2A and tyrosine phosphatases (PTPs) has been described by Pastula et al. (2003). Application of fluorescent-labeled phosphopeptides as substrate for PP1 and PP2A has been shown by Noble et al. (2003). Although DiFMUP and PNPP have been employed for PP1 quantification (Fontal et al. 1999), better non-radioactive assays for PP1 are still needed. One reason is that available non-radioactive substrates are nonspecifically cleaved by all PP making the determination of endogenous phosphatases difficult. To sort out this problem, phosphatase inhibitors can be employed. General phosphatase inhibitors like NaF and Na_3VO_4 are commonly used to roughly distinguish the different type of phosphatases. Despite inhibiting many phosphatases, Na_3VO_4 preferentially inhibits the activities of tyrosine phosphatases (Gordon 1991). Natural toxins that target Ser/Thr phosphatases including OA, calyculin A, tautomycin and microcystin are useful tools for investigation of cellular phosphatase activities and phosphorylation events (Neumann et al. 1994; El-Armouche et al. 2006a; Lankoff et al. 2006). Many of these compounds share structural similarities, and several have become readily available for research purposes (Swingle et al. 2009).

1.5 Objective

The underlying hypothesis of this work is that a therapeutic window exist downstream in the β -adrenergic signaling cascade in which interventions could extend or replace classical beta-blockers by “partial subcellular beta-blockade”. Based on our previous findings from I-1 KO or transgenic overexpressed mice (El-Armouche et al. 2008; Wittköpper et al. 2010), pharmacological blockade of I-1 may represent a new therapeutic target in treating HF.

In the current study we attempted to identify and characterize I-1 inhibitory compounds using an appropriate screening system. Therefore, we sought to develop a reliable, non-radioactive and cost-efficient *in vitro* PP1-I-1 assay system in a multi-well-format. This assay should afford the screening of a library to find compounds

that antagonize the inhibitory effect of I-1 on PP1 activity and thereby indirectly enhance it. Such an activating would β -adrenergic signals intracellularly. Different I-1 peptides were tested in this assay to confirm structure prediction models and to delineate the residues critical for PP1/I-1 interactions. In addition, we investigated the properties of our assay as a tool for determination of PP1 activity in tissue/cell extracts.

2 Materials

2.1 Antibodies

Alexa Fluor® 546 goat anti-rabbit IgG, Invitrogen, NY, USA

α -actinin, Sigma-Aldrich, Steinheim, Germany

β -actin Sigma-Aldrich, Steinheim, Germany

cMyBP-C (C0C2-domains), Mathias Gautel, King's College London, UK

CSQ, Dianova, Hamburg, Germany

I-1, El-Armouche et al. 2003, Germany

Mouse IgG, peroxidase conjugate, Sigma-Aldrich, Steinheim, Germany

Rabbit IgG, peroxidase conjugate, Sigma-Aldrich, Steinheim, Germany

PLB, Badrilla, Leeds, UK

Phospho PLB-Ser¹⁶, Badrilla, Leeds, UK

Phospho PLB-Thr¹⁷, Badrilla, Leeds, UK

Protein phosphatase 1 (PP1) catalytic subunit, Upstate

2.2 Bacterial strain

E. Coli BL21, Invitrogen

E. Coli XL-1 Blue MRF, Stratagene

2.3 Buffers & solutions

Antibody solution

50 mM Tris-HCl, 1% BSA, 0.5% triton X-100, 0.01% NaN₃

Block buffer

50 mM Tris-HCl, pH 7.4, 10% active FCS, 1% BSA, 0.5% Triton X-100, 0.01% NaN₃

Blot buffer (1x)

25 mM Tris-base, 190 mM glycine, 20% methanole

CBFHH

136.9 mM NaCl, 5.4 mM KCl, 0.8 mM MgSO₄ (7x H₂O), 5.5 mM glucose, 0.4 mM KH₂PO₄, 0.3 mM Na₂HPO₄ (7x H₂O) and 20 mM HEPES, pH 7.5

Coomassie

0.2% coomassie brilliant blue G250, 25% isopropanol, 10% acetic acid

Digestion buffer

Perfusion buffer (fresh) plus 0.0125 CaCl₂ (2x H₂O), 0.075 mg/mL Liberase TM

DNase solution

0.024 mg/ml DNase, 2% FCS, 1% P/S in 50 ml CBFHH

EDB

25 mM imidazole, pH 7.4, 1 mM DTT, 0.1 mg/ml BSA, 50 mM NaCl, 0.3 mM MnCl₂

Electrophoresis buffer (1x)

25 mM Tris-base, pH 8.8, 0.1% SDS, 192 mM glycine

IonOptix buffer (stock)

135 mM NaCl, 4.7 mM KCl, 0.6 KH₂PO₄, 0.6 mM Na₂HPO₄, 1.2 mM MgSO₄, 10 mM HEPES, pH 7.46

IonOptix buffer (fresh, 1.25 mM Ca²⁺)

IonOptix buffer (stock) plus 1.25 mM CaCl₂, 20 mM glucose

Homogenization buffer (1)

50 mM Tris-HCl, pH 7.4, 0.3 mM sucrose, 0.5 mM EDTA

Homogenization buffer (2)

2 mM Tris-HCl, pH 7.4, 2 mM EGTA, 5 mM EDTA, 1 mM benzamidine, 1 mM Pefabloc®, 0.1% β-mercaptoethanol

Laemmli buffer (1x)

10 mM Tris-HCl, pH 6.8, 2% SDS, 10% glycerol, 100 mM DTT, 0.01% bromophenol blue

Lysis buffer

30 mM Tris-base, pH 8.8, 3% SDS, 5 mM EDTA, 30 mM NaF, 10% glycerol

NEBuffer for PMP (1x)

50 mM HEPES, pH 7.5, 100 mM NaCl, 2 mM DTT, 0.01% Brij 35

P1 buffer

50 mM Tris-HCl, 10 mM EDTA, 100 µg/ml RNase A, pH 8.0

P2 buffer

200 mM NaOH, 1% (w/v) SDS

P3 buffer

M KCO₂CH₃, pH 5.5

PBS

140 mM NaCl, 2.7 mM KCl, 10 mM Na₂HPO₄, and 1.8 mM KH₂PO₄, pH 7.3

Perfusion buffer (stock)

113 mM NaCl, 4.7 mM KCl, 0.6 mM KH₂PO₄, 0.6 mM Na₂HPO₄, 1.2 mM MgSO₄, 12 mM NaHCO₃, 10 mM KHCO₃, 10 mM HEPES, pH 7.4, 30 mM Taurine

Perfusion buffer (fresh)

Perfusion buffer (stock) plus 30 mM ascorbic acid, 5.5 mM glucose, 10 mM BDM

Ponceau red

26 mM Ponceau S in 30 mM TCA

RB

25 mM imidazole, pH 7.4, 1 mM DTT, 0.1 mg/ml BSA, 50 mM NaCl

SPR (Biacore) buffer

10 mM HEPES, 150 mM NaCl, 3 mM EDTA, 0.005% Tween-20, pH 7.4

SPR wash buffer

10 mM NaHCO₃

TAE

40 mM Tris-base, pH 8.3, 40 mM acetic acid, 1 mM EDTA

TBS

100 mM Tris-base, pH 7.5, 150 mM NaCl

TBS-T (0.1%)

100 mM Tris-base, pH 7.5, 150 mM NaCl, 0.1% Tween 20

Trypsin solution

3 mg/ml trypsin, 0.03 mg/ml DNase, 1% P/S in 50 ml CBFHH

2.4 Cell culture media

Dulbecco's Modified Eagle Medium (DMEM), Invitrogen

DMEM + Glutamax™, Invitrogen

LB medium, house-made (0.5% yeast extract, 1% trypton, 171 mM NaCl, pH 7.4)

LB ampicillin agar plate, house-made (15 g agar in 1000 ml LB + 0.1mg/ml ampicillin)

KM medium, house-made (MEM containing 10% FCS and 1% P/S)

Minimum Essential Medium Eagle (MEM), Invitrogen

NKM medium, house-made (DMEM containing 10% FCS, 1% P/S and 1% glutamine)

Opti-Mem®, reduced serum medium, Invitrogen

SOC medium, house-made (0.5% yeast extract, 2% tryptone, 10 mM NaCl, 2.5 mM

KCl, 10 mM MgCl₂, 10 mM MgSO₄, 20 mM Glucose)

2xYT medium, Conda pronadisa

2.5 Compounds with risk phrases (R) and security advices (S)

Acetic acid, Merck, Darmstadt

R: 10-35 S: 23.2-26-45

Acrylamide, 40% solution, Bio-Rad, München	R: 45-46-20/21-23/24/25-43-48 S: 36/37/39-45-60
Adenosine 5'-[γ-thio]triphosphate, tetralithium salt, Sigma-Aldrich, Steinheim	R:36/37/38 S:26-36
Ammonium persulfate (APS), Bio-Rad	R: 8-22-36/37/38-42/43 S: 22-24-26-37
Ampicillin-Trihydrat, Serva, Heidelberg	R: 36/37/38-42/43 S: 22-26-36/37
Aprotinin Sigma-Aldrich, Steinheim	-
Aqua ad injectabilia, Baxter, Unterschleißheim	-
Bacto™ Agar, Becton Dickinson, NJ	-
Bacto™ Tryptone, Becton Dickinson, NJ	-
Bacto™ Yeast extract, Becton Dickinson, NJ	-
Bovine serum albumin (BSA), Roth, Karlsruhe	-
Bradford reagent, Bio-Rad, München	R: 20/21/22-36 S: 26-36/37-45-60
5-Brom-2-desoxyuridin (BrdU), Sigma-Aldrich, Steinheim	R: 40-68 S: 22-24/25-36/37/39-45
Bromophenol Blue, Merck, Darmstadt	S: 22-24/25
2,3-Butanedione monoxime (BDM), Sigma-Aldrich, Steinheim	S: 22-24/25
Calcium chloride dihydrate (CaCl ₂ 2x H ₂ O), Sigma-Aldrich, Steinheim	R: 36 S: 22-24/25
Calyculin A, Enzo Life Science, NY	R23/24/25-38
Cantharadin, Sigma-Aldrich, Steinheim	R36/37/38-28 S45-53
Complete mini-proteases inhibitor cocktail, Roche Diagnostics, Mannheim	-
Coomassie Brilliant Blue, Merck, Darmstadt	R: 20/21/22-34-68 S: 26-36/37/39-45
DiFMUP, Endotherm, Saarbrücken	-
Dinatriumhydrogenphosphat (Na ₂ HPO ₄ 2xH ₂ O), Merck, Darmstadt	S: 22-24/25
Dimethylformamid (DMF), Roth, Karlsruhe	R: 61-20/21-36; S: 53-45
Dimethyl sulfoxide (DMSO), Merck, Darmstadt	R: 36/37/38; S: 23-26-36
DNA loading dye, Fermentas	-
DNA T4-ligase, Fermentas	-
dNTPs, Fermentas, St. Leon-Rot	-

1,4-Dithiothreitol (DTT), Sigma-Aldrich, Steinheim	R: 22-36/37/38; S: 26-36
ECL detection kit, Thermo Scientific, IL	R: 11-19-36/37-40-66
Ethanol (absolut), Merck, Darmstadt	R: 11; S: 7-16
Ethidiumbromid, Fulka	R: 23-68; S: 36/37-45
Ethylene diamintetraacetic acid (EDTA), Sigma-Aldrich, Steinheim	R: 36-52/53; S: 26-61
EZ-Link® Iodoacetyl-LC-Biotin, Thermo scientific	-
Fetal calf serum (FCS), Invitrogen	-
Fibrinogen, Sigma-Aldrich, Steinheim	-
Fluoromount G, Southern Biotech,AL	-
Gene Ruler™ 100 bp DNA Ladder, Fermentas-	-
Glucose, Sigma-Aldrich, Steinheim	-
Glutathione agarose beads, GE Health Care	-
Glycerol, MerckDarmstadt,	-
Glycine, Carl Roth, Karlsruhe	S: 22-24/25
HEPES, Carl Roth, Karlsruhe	-
Hydrochloric acid, 37% solution, Merck, Darmstadt	R: 34-37 S: 26-36/37/39-45
Horse serum, Gibco/Invitrogen	-
Imidazole, Sigma-Aldrich, Steinheim	R:61-22-34 S:36/37/39-26-45-53
Insulin, Sigma-Aldrich, Steinheim	-
IPTG (isopropyl 1-thio-β-D-galactopyranoside)- Carl Roth, Karlsruhe	-
Isoprenaline, Sigma-Aldrich, Steinheim	R: 36/37/38
L-Ascorbic acid, Merck, Darmstadt	-
Liberase Blendzyme 3, Roche Diagnostics, Mannheim	R: 36/37/38-42/43 S: 22-S24/25
Liquemin® N 10 000 (heparin sodium salt 10,000 I.U./mL), Roche Pharma, Grenzach-Wyhlen	-
Liquid nitrogen (LN2), Linde, Hannover	-
L-Glutamin, Invitrogen	-
Magnesium chloride hexahydrate (MgCl ₂ × 6 H ₂ O), Merck, Darmstadt	-

Magnesium sulfate heptahydrate ($\text{MgSO}_4 \times 7 \text{H}_2\text{O}$), Merck, Darmstadt	-
Mangan II-chlorid (MnCl_2), Merck, Darmstadt	R: 22-51/53; S: 61
2-Mercaptoethanol, Sigma-Aldrich, Steinheim	R: 23/24/25; S: 45
Methanol, Merck, Darmstadt	R: 11-23/24/25-39/23/24/25 S: 7-16-36/37-45
Milk powder, Carl Roth, Karlsruhe	-
NEBuffer for PMP, New England Biolabs	-
Okadaic acid, Enzo Life Science, NY	R26/27/28
Paraformaldehyd (PFA), Sigma-Aldrich, Steinheim	R: 20/22-36/37/38-40-43
PBS, Invitrogen	-
Penicillin/Streptomycin, Gibco®/Invitrogen	R: 43; S: 36-38
pNPP (DiTris Salt), Calbiochem, Darmstadt	-
Ponceau S, Sigma-Aldrich, Steinheim	R: 36/37/38 S: 26-36
Potassium chloride (KCl), Merck, Darmstadt	S: 22-24/25
Potassium phosphate monobasic (KH_2PO_4), Merck, Darmstadt	-
Potassium bicarbonate (KHCO_3), Merck, Darmstad	-
Potassium hydroxide (KOH), Merck, Darmstadt	R: 22-35 S: 26-36/37/39-45
Precision Plus Protein Standard, Bio-Rad, München	-
2-Propanol (Isopropanol), Merck, Darmstad	R: 11-36-37 S: 7-16-24/25-26
Sodium azide (NaN_3), Serva, Heidelberg	R: 28-32-50/53 S: 1/2-28-45-60-61
Sodium bicarbonate (NaHCO_3), Merck, Darmstadt	-
Sodium chloride (NaCl), J.T. Baker	-
Sodium chloride, 0.9% solution, Baxter, Unterschleißheim	-
Sodium dodecyl sulfate (SDS), Merck, Darmstadt	R: 11-21/22-36/37/38 S: 26-36/37
Sodium phosphate dibasic dihydrate ($\text{Na}_2\text{HPO}_4 \times 2 \text{H}_2\text{O}$), Merck, Darmstadt	-

Sodium phosphate monobasic (NaH ₂ PO ₄), Merck, Darmstadt	-
Sodium hydroxide (NaOH), Merck, Darmstadt	R: 35; S: 26-37/39-45
Sodium fluoride (NaF), Merck, Darmstadt	R: 25-32-36/38
Sucrose, Merck, Darmstadt	-
TEMED, Bio-Rad, München	R: 11-20/22-34 S: 16-26-36/37/39-45-60
Thrombin, Sigma-Aldrich, Steinheim	R: 22-24/25
Tris-HCl, Merck, Darmstadt	R: 36/37/38; S: 26-36
Trizma® base, Sigma-Aldrich, Steinheim	R: 36/37/38 S: 26-36
Trypan blue, Sigma-Aldrich, Steinheim	R: 45 S: 45, 53
Tween® 20, Sigma-Aldrich, Steinheim	-
Urea, Sigma-Aldrich, Steinheim	-

2.6 Enzymes

Calf Intestinal Phosphatase (CIP), New England Biolabs

Protein kinase A (PKA), purified catalytic subunit, Sigma-Aldrich, Steinheim

Protein Phosphatase 1 (PP1), purified catalytic subunit, Upstate

Protein Phosphatase 1 (PP1), recombinant catalytic subunit, New England Biolabs

Protein Phosphatase Inhibitor-2 (I-2), New England Biolabs

Restriction enzymes (*Acc65I*, *EcoRI*, *KpnI*, *NdeI*, *NotI*, *PacI*, *PmeI*, *SmaI*, *XbaI*) with corresponding buffers (containing 1x BSA), New England Biolabs

2.7 Equipments

Accu jet® pipette controller, Brand, Wertheim, Germany

Amicon® ultra-4, Millipore, MA

Analytical balance (Genius), Sartorius, Göttingen, Germany

Arc lamp power supply, Cairn Research, Faversham, UK

Axiovert 25 inverse microscope, Zeiss, Jena, Germany

BIACORE™ 3000, GE Healthcare, Sweden

Blotting paper (Whatman 3MM), Schleicher & Schuell

Cell MicroControls perfusion chamber, Norfolk, VA, USA

Cell scraper, Sarstedt AG & Co.
Cell strainer, Becton Dickinson
cFlow 8 Channel Flow Controller, Cell MicroControls, Norfolk, VA, USA
ChemieGenius2 Bio Imaging System, Syngene, Cambridge, UK
Cooling centrifuge 5415 R, Eppendorf, Hamburg
Cooling centrifuge Universal 30 RF, Hettich, Tuttlingen
Counting chamber Fuchs-Rosenthal, VWR, Darmstadt
Coverslips (\varnothing 10 mm), Glaswarenfabrik Karl Hecht KG
Culture flasks (T75), Sarstedt AG & Co.
Culture plates (6-well), Greiner Bio-One GmbH
Culture plates (12-well), Nalge Nunc International
Culture plates (24-well), Nalge Nunc International
Culture plates (24-well), Iwaki, Willich
Cuvettes (10 x 4 x 45 mm), Sarstedt AG & Co.
Falcon tubes (15 and 50 ml), Sarstedt AG & Co.
Force transducers, G. Jäckel, Hanau, Germany
Hyperfilm ECL, Amersham Pharmacia Biotech
Laboratory pH meter, Knick, Berlin, Germany
Lab-Tek™ Chamber Slide, Nunc
Magnetic stirrer, Heidolph, Schwalbach, Germany
Metal crucible, in-house production
MENZEL microscope slides, Thermo Fisher Scientific
Microscope slides, Paul Marienfeld GmbH
Micro tubes (1.5, 2.0 ml), Sarstedt AG & Co.
Milli-Q Plus water purification system, Millipore, Schwalbach
Mini protean electrophoresis and Western blotting system, Bio-Rad, München
Minipuls 3 peristaltic pump, Gilson, Middleton, WI, USA
Multiple well plates (96-wells), Sarstedt AG & Co.
Multiple well plates (384-wells), Greiner Bio-One GmbH
MultiScreen punch, Millipore, Schwalbach, Germany
MyoCam, IonOptix Corporation, Milton, MA, USA
MyoPacer field simulator, IonOptix Corporation, Milton, MA, USA
NanoDrop ND-1000, PeqLab, Erlangen, Germany

Neubauer counting chamber, OptikLabor, Bad Homburg, Germany
Nikon Eclipse TS 100 inverse microscope, Nikon, Düsseldorf, Germany
Nitrile gloves, Ansell
Nitrocellulose membrane (Protran® BA 85), Schleicher & Schuell
Nylon membrane (Hybond N+), Amersham Biosciences
Organ baths, in-house production
PCR tubes, Sarstedt AG & Co.
Petri dishes, 10 mm, Sarstedt, Nümbrecht
Peristaltic pump, Gilson Inc., Middleton, WI, USA
Precision balance (Precision Advanced), Ohaus, Pine Brook, NJ, USA
Pipettes, 0.5-10 µL, 10-100 µL, 100-1000 µL, Eppendorf, Hamburg
Pipette tips, Sarstedt AG & Co. (for 10, 100 and 1000 µl pipettes)
Polystyrene cuvettes, Sarstedt, Nümbrecht
Polytron® homogenizer, Kinematica, Littau-Luzern, CH
Power Pac 300, Bio-Rad, München, Germany
Safire² microplate reader, Tecan, Männedorf, CH
Serological pipettes, (2, 5, 10 and 25 ml), Sarstedt AG & Co.
Serological pipettes (10 ml, wide tip), Becton Dickinson
Smart Spec® 3000, Bio-Rad, München, Germany.
Sterile filter (0.22 µm), Sarstedt AG & Co.
Stimulation/Thermistor assay, CellMicroControls, Norfolk, VA, USA
Stimulation chamber for myocytes, CellMicroControls, Norfolk, VA, USA
Stimulation chamber holder with aspirator, CellMicroControls, Norfolk, VA, USA
Streptavidin-coated sensor chip, GE Healthcare, Sweden
Sylgard 184 elastomer, Dow Corning
Temperature controller, CellMicroControls, Norfolk, VA, USA
Thermomixer comfort, Eppendorf, Hamburg
Tissue Lyser, Qiagen, Düsseldorf, Germany
Vacuum filtration units, 500 ml, Sarstedt, Nümbrecht
Videopower, IonOptix Corporation, Milton, MA, USA
VirSonic®,
Vortex-Genie 2, Scientific Industries, Bohemia, NY, USA
Wallac 1409 Liquid Scintillation Counter, PerkinElmer, Waltham, MA, USA

Water bath, GFL, Burgwedel, Germany

Water bath Thermostat, Eppendorf, Hamburg, Germany

2.8 Kits

Plasmid Maxi Kit, Qiagen

NucleoSpin® Extract II, Macherey & Nagel

3 Methods

3.1 Preparation of I-1 protein

3.1.1 Bacterial expression of I-1 protein

I-1 cDNA of mouse heart subcloned in pGEX-2T expression vector, provided by Dr. Katrin Wittköpper, was used to express I-1 as a fusion protein with glutathione-S-transferase (GST). The KpnI-NotI fragment represents the I-1 sequence. An N-terminal thrombin cleavage site was inserted into pGEX-2T (Fig 3.1).

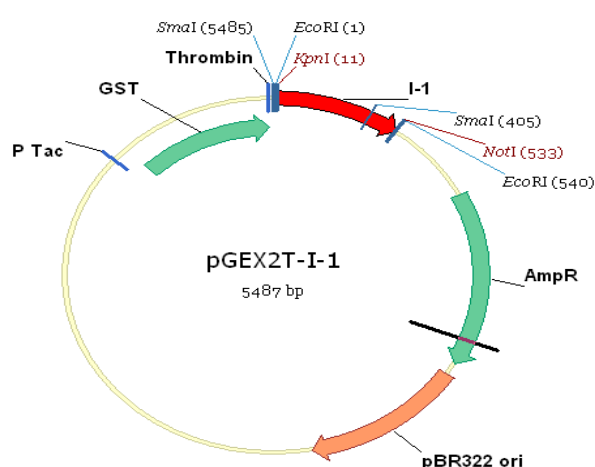


Figure 3.1 Illustration of the pGEX-2T vector containing GST-I-1 and Tac promoter for chemically inducible, high-level expression. GST fusion provides elution condition for proteins from the affinity matrix, and thrombin recognition sites for cleaving the desired protein from the fusion product.

The plasmid was transformed into 100 μ l chemically competent *E. coli* BL21 by heat shock (30 min on ice \rightarrow 30 sec at 42 $^{\circ}$ C \rightarrow 2 min on ice). After incubation in 250 μ l SOC medium for 1 h with shaking, the bacteria were grown overnight on LB ampicillin agarose plates. Ten single colonies from 2 plates were inoculated in 5 ml LB medium containing 25 μ g/ml ampicillin and grown for 4-6 h with vigorous shaking. Then, DNAs were isolated and purified according to the following mini-plasmid preparation protocol: 2 ml of each culture were centrifuged for 1 min at full speed rpm, the pellets were resuspended in 200 μ l P1 buffer and the bacteria were lysed by addition of 200 μ l P2 buffer. The lysis was subsequently stopped with 200 μ l P3 buffer, then centrifuged 10 min (full speed, 4 $^{\circ}$ C). The supernatants were precipitated with 500 μ l isopropanol and centrifuged for 20 min (full speed, 4 $^{\circ}$ C). The DNA pellets were washed with 70% ethanol and centrifuged again for 10 min. The dried pellets were resuspended in 30 μ l H₂O. The concentration of DNA was determined by the NanoDrop[®] spectrophotometer at 260 nm. Absorbance was also determined at 280

nm and the ratio A260/A280 was calculated to check for protein contamination. A ratio of 1.7-1.9 was considered as optimal ratio for DNA.

Positive colonies were first verified by restriction digestions with *SmaI* and *EcoRI* and checked after electrophoresis on a 1% agarose gel (0.5 g agarose in 50 ml TAE plus 0.4 µg/ml ethidium bromide for DNA staining). The electrophoresis was performed after loading the DNA, supplemented with 1x loading dye and Gene Ruler™ 100 bp DNA Ladder as molecular weight marker. Gel images were recorded with the Chemie Genius2 Bio Imaging System.

The DNAs of three positive colonies were sequenced by Eurofins MWG Operon (Munich, Germany), after PCR amplification using *KpnI* forward and *NotI* reverse primers (Tab 3.1 A-C).

Table 3.1 PCR amplification of I-1 for sequencing. A) The sequences of I-1 forward and reverse primers.

Primer	Sequence	T _m (°C)
KpnI for	5'-GGTACCGCCATGGAGCCCGACAACGTT-3'	70
NotI rev	5'-GCGGCCGCTCAATTCAGATCTTCGCTA ATAAGCTTTTGCTCTGACAGTGGACTTGAG-3'	75

B) PCR reaction for I-1 sequencing

Component	Final concentration
10x PCR buffer	1x
dNTPs	0.2 mM/nucleotide
MgCl ₂	3 mM
<i>Taq</i> -DNA Polymerase	0.1 U/µl
KpnI for primer	0.1 µM
NotI rev primer	0.1 µM
Template (DNA)	5-500 ng
H ₂ O	ad 50 µl

C) PCR program for I-1 sequencing

Step	Temperature	Time	Cycles
Denaturation	94 °C	10 min	1
Denaturation	94 °C	30 sec	30
Hybridization	64 °C	1 min	
Elongation	72 °C	1.5 min	
Elongation	72 °C	10 min	1

From one positive culture 100 µl was transferred into 30 ml LB medium and incubated overnight with shaking. Several freeze cultures were prepared from this overnight culture (200 µl bacterial culture plus 800 µl glycerol) and stored at -80 °C. Finally, 10 ml of overnight culture were inserted into 500 ml LB medium plus ampicillin. The bacteria were grown until $OD_{600}=0.5-0.6$, and then cooled to 30 °C. The GST-I-1 expression was induced with 1 mM IPTG (isopropyl 1-thio- β -D-galactopyranoside) for 4 h. 1 ml of bacterial culture before (T0) and after 4 h IPTG induction (T4) was centrifuged with full speed rpm for 10 min at RT. The pellet was resuspended in 100 µl PBS and analyzed by SDS-PAGE to control the expression of target protein. Then, the whole culture was sedimented by centrifugation at 4000 g for 10 min and resuspended in 10 ml ice-cold PBS. The resuspended culture was lysed by sonication and cell debris was removed by centrifugation (5000 g, 10 min and 4 °C). GST-I-1 protein was purified from clarified bacterial lysate by affinity purification with glutathione agarose beads. 500 µl PBS-equilibrated beads were incubated with bacterial lysate (45 min, RT) and after, washed three times with PBS and eluted after 2x incubations (2 h, RT and overnight 4 °C) with 1 ml PBS containing 25 units thrombin. Thrombin released I-1 by cleaving it from GST. Finally, protein concentrations were determined using the Bradford method (1976) and the quality of protein was verified by coomassie-stained SDS-PAGE and Western blot analysis using antibody against I-1 (see 3.7)

3.1.2 Site-directed mutagenesis of I-1

The methods in this part were carried out with the kind support of Dr. Uwe Borgmeyer and Ute Süsens (ZMNH, Hamburg, Germany).

The *NotI* linearized cDNA plasmid pGex-ml-1 was used as template. Site-directed mutagenesis was performed by PCR with forward and reverse primers (Metabion), as shown in Tab 3.2 A. To replace amino acids R³⁰⁻³³ by alanines, a 5'-fragment (Kpn for/Start rev) and a 3'-fragment (I-1^{R/A} for/ *NotI* rev) were generated. Deletion of the “KIQF” and mutagenesis of amino acids “KIQ” to “RLN” was achieved with mutated 5'-primers (Tab 3.2 B-C). PCR products were analyzed by agarose gel electrophoresis, purified with NucleoSpin® Extract II and digested with *Acc65I* (*KpnI*) and *NotI*, respectively.

Ligation of PCR fragments into pBluescript II SK (*Acc65I/NotI*) was carried out in a final volume of 20 µl containing T4-DNA-ligase, 1x T4 buffer, 30 ng vector and 5-10 ng of the respective PCR fragments for 30 min at RT. 5 µl of the ligation reactions were transformed into 50 µl of competent *E. coli* XL-1 Blue MRF' by incubation for 30 min on ice followed by a 5 min incubation at 37 °C. After incubation in 500 µl SOC medium at 37 °C with shaking, cells were plated on LB agar plates plus ampicillin supplemented with XGal and IPTG. For DNA preparation, 2 ml of 2xYT medium supplemented with ampicillin were inoculated with single white bacterial colonies and grown overnight at 37 °C with vigorous shaking and mini- plasmid preparation was performed as described in 3.1.1.

Successful cloning was verified by restriction enzyme digestion with *NotI* and *Acc65I*. Mutations were verified by DNA sequencing with T3 (5'-AATTAACCCTCACTAAAG-3') and T7 (5'-TAATACGACTCACTATAG-3') primers. The sequencing service was provided by Dr. Sabine Hoffmeister-Ullerich (Bioanalytics Facility, ZMNH).

Acc65I/NotI inserts of the mutants were isolated by agarose gel electrophoresis and ligated into the bacterial expression vector pGEX-2T. The analyses of three mutant plasmids, pGEX-ml-1R/A, pGEX-ml-1KIQ/RLN and pGEX-ml-1ΔKIQF and protein expression were performed as described in 3.1.1.

Table 3.2 Site-directed mutagenesis of I-1. A) Primers for I-1 mutagenesis. Restriction enzyme sites are in italics, the start ATG codons and the translational stop codons are underlined. The location of the 12 nucleotide deletions is indicated, triplets coding for newly introduced amino acids alanine, arginine, leucine and asparagine are shown in bold.

Primer	Sequence
Kpn for	5'-ata <i>GGTACC</i> GCC <u>ATG</u> GACCCCGACA-3'
Not rev	5'-ata <i>GCGGCCGC</i> <u>TCAGACCAAGCTGGCTCCCTG</u> -3
Start rev	5'-p-AATCTGCTCCGCCGCCTCCGGGT-3'
I-1 _{R/A} for	5'- GCT GCC GCA GCC CCCACCCCTGCCACACTTGTG -3'
I-1 _{KIQ/RLN} for	5'-ata <i>GGTACCGCC</i> <u>ATG</u> GAGCCCGACAACAGCCACGG AGA CTG AAT TTTACGGTCCCGCTGCTGGAGCCT-3'
I-1 _{ΔKIQF} for	5'-ata. <i>GGTACCGCC</i> <u>ATG</u> GAGCCCGACAACAGCCACGG -Δ12 ACGGTCCCGCTGCTGGAGCCT-3'

B) PCR reactions for I-1 mutagenesis

	Primer	Fragment size (bp)
Start	{ Kpn for Start rev	80
Mutant	{ I-1 _{R/A} for Not rev	400
Mutant	{ I-1 _{KIQ/RLN} for NotI rev	400
Mutant	{ I-1 _{ΔKIQF} for Not rev	388

C) PCR program for I-1 mutagenesis

Step	Temperature	Time	Cycles
Denaturation	95 °C	2 min	1
Denaturation	95 °C	30 sec	25
Annealing	65 °C	30 sec	
Elongation	72 °C	30 sec	
Elongation	72 °C	5 min	1

3.1.3 PKA phosphorylation/thiophosphorylation of I-1

The recombinant I-1 protein was *in vitro* phosphorylated at Thr³⁵ using purified catalytic subunit of PKA (specific activity ~10 U/μg protein) to become activated. A reducing agent such as dithiothreitol (DTT) is essential for enzyme activity; therefore PKA was reconstituted in water containing 6 mg/ml DTT. The phosphorylation reaction was carried out in PBS at pH 7.4, containing 6 mM MgCl₂, 0.3 mM ATP and 1 U PKA per 1 μg I-1 protein, for 90 min at 30 °C (Fig 3.2). A control reaction was performed in parallel, containing I-1 and PKA, without ATP and MgCl₂. The reactions were terminated by incubating at 95 °C for 5-10 min and desalted in EDB using Amicon®, 10K devices, according to manufacturer's guideline. The extent of I-1 phosphorylation was monitored by Western blot analysis with an antibody against phospho-DARPP-32, which also detects phospho-Thr³⁵ (1:1000) in I-1.

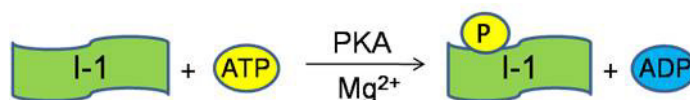


Figure 3.2 The scheme of PKA mediated phosphorylation of I-1 protein.

Thiophosphorylation of I-1 protein was performed essentially as described above except that ATP was substituted with 0.3 mM ATP-γ-S, which is a non-hydrolyzable ATP analog (Fig 3.3). Instead of 6 mM, 2 mM MgCl₂ was used and the reaction was incubated at 30 °C for 24 h. The incubation mixture was deactivated at 95 °C for 10 min and desalted in the assay buffer. Estimation of thiophosphorylation rate was performed by Western blot analysis using the same antibody against phospho-I-1.

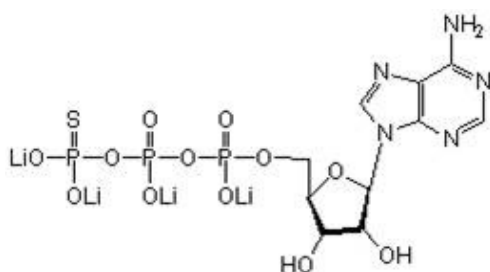


Figure 3.3 The structure of Adenosine 5'-[γ-thio] triphosphate tetra lithium salt (ATP-γ-S).

3.1.4 Biotinylation of I-1

Biotinylation is a process of covalently attaching biotin to a protein. Biotin binds to avidin or streptavidin proteins with an extremely high affinity (K_d 10⁻¹⁵) and specificity,

which facilitates protein purification, detection and in our case protein-protein interaction investigations.

Several reactive moieties of amino acids are available for biotinylation without interrupting biological functions of proteins, including primary amines (-NH₂), sulfhydryls (-SH) and carboxyls (-COOH) groups. In this regard, we applied EZ-Link® Iodoacetyl-LC-Biotin reagent that reacts by substitution of iodine with sulfhydryl (-SH) group located in the side chain of cysteine (Fig 3.4). The WT and mutant I-1 proteins contain two cysteines at residue 114 and 147, which could provide free sulfhydryl groups. The Iodoacetyl-LC-Biotin reagent was dissolved in dimethylformamide (DMF) fresh before the reaction in a 4 mM stock concentration. The reactions were carried out in PBS, pH 8-9, containing 5-6 µM WT or mutant I-1 proteins, 10 mM Tris [2-carboxyethyl] phosphine (TCEP), 6 M guanidine hydrochloride, 0.2 mM EDTA, and initiated by addition of 50 µM biotin reagent. After 20 min incubation at RT, the reactions were stopped by desalting in PBS through Amicon® devices. The biotinylated proteins were phosphorylated by PKA as described in 3.1.3.

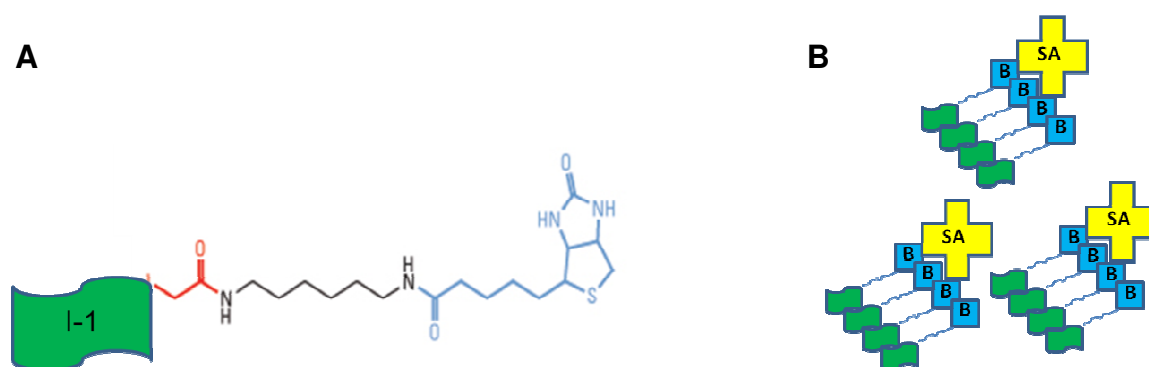


Figure 3.4 Biotinylation of I-1 protein by Iodoacetyl-LC-Biotin™ reagent. **A)** Iodoacetyl group (red) as a sulfhydryl-reactive group used to label proteins with biotin (blue) and an additional spacer arm (black). **B)** Streptavidin (SA) can bind to four biotin complexes.

3.2 Surface plasmon resonance (SPR) measurements

SPR measurements were performed on a BIACORE™ 3000 system with the kind supports of Dr. Christian Schulze (ZMNH, Hamburg, Germany). SPR-based measurement is an optical method to measure the refractive index near (within ~300 nm) a metallic sensor surface (gold or silver). A protein can be immobilized on the backside of sensor. If a protein or ligand in mobile phase interacts with the

immobilized protein, the reflective index of sensor will change. This change can be measured in real time and demonstrated in a sensorgram (Fig 3.5).

The biotin-conjugated I-1, I-1_{R/A}, I-1_{KIQ/RLN} and I-1_{ΔKIQF} were phosphorylated as described above and prepared in SPR buffer (filtered through 0.45 μm mesh). Then, the proteins were immobilized on a streptavidin-coated sensor chip at a concentration of 1.4 μM, with 2 μl/min flow-rate until the resonance unit reached a steady state. The unbound proteins were washed by injecting wash buffer, until the curves reached steady state. Then, recombinant PP1 was injected at concentrations ranging from 1.87 nM to 30 nM to induce the binding. Further washings were performed for dissociation. The equilibrium dissociation constant, K_D , was calculated using BIAevaluation 3.0 software (GE Healthcare, Sweden).

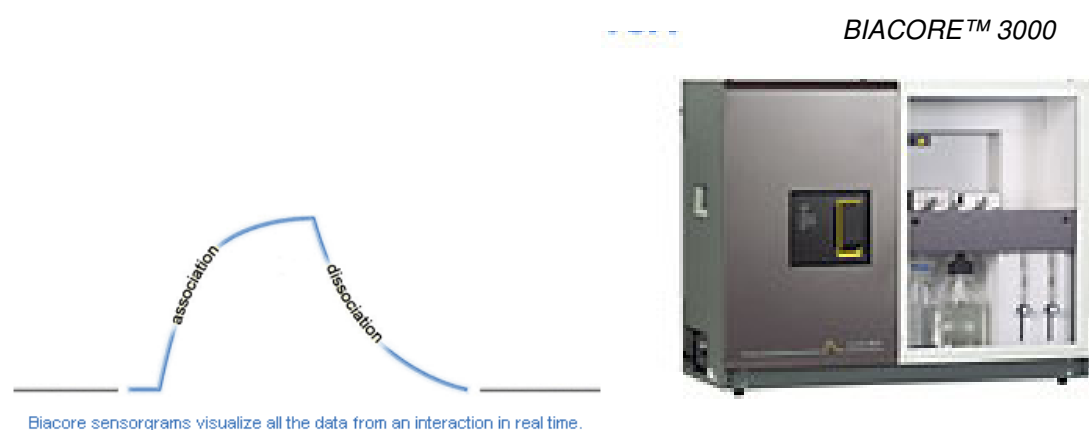


Figure 3.5 The kinetics of an interaction. The rates of complex formation (K_a) and dissociation (K_d), can be determined from the information in a sensorgram.

3.3 Phosphatase assay development

3.3.1 pNPP as a chromogenic substrate

Para-nitrophenyl phosphate (pNPP) is a chromogenic substrate that is catalysed by phosphatases (pH>7) forming a yellow compound (pNP). The absorption of pNP can be measured at 405 nm, which is correlated to enzyme activity (Fig 3.6). The catalytic subunit of recombinant PP1 from rabbit skeletal muscle (specific activity 8.151 U/μg protein) was applied in the assay. The reactions were performed in transparent flat bottom 96-well plates with 220 μl total volume. Various amounts of recombinant PP1 (0.1, 0.3, 1, 3, 10 U) were prepared in 40 μl enzyme dilution buffer (EDB) in the wells. Then, 160 μl reaction buffer (RB) was added into the wells and mixed well. The

reactions were initiated by addition of 20 μ l RB containing 50 mM pNPP yielding a final concentration of 4.5 mM, and the absorptions were measured immediately. The substrate saturation curve was obtained with 1 U (15 nM) PP1 at different substrate concentrations (1 to 300 mM). The absorbance was measured at 405 nm using multiplate reader TECAN® Safire² and the Magellan software 5.03 up to 60 min at 30 °C. The gradient of optical density (Δ OD/min) was considered as PP1 activity for each sample.

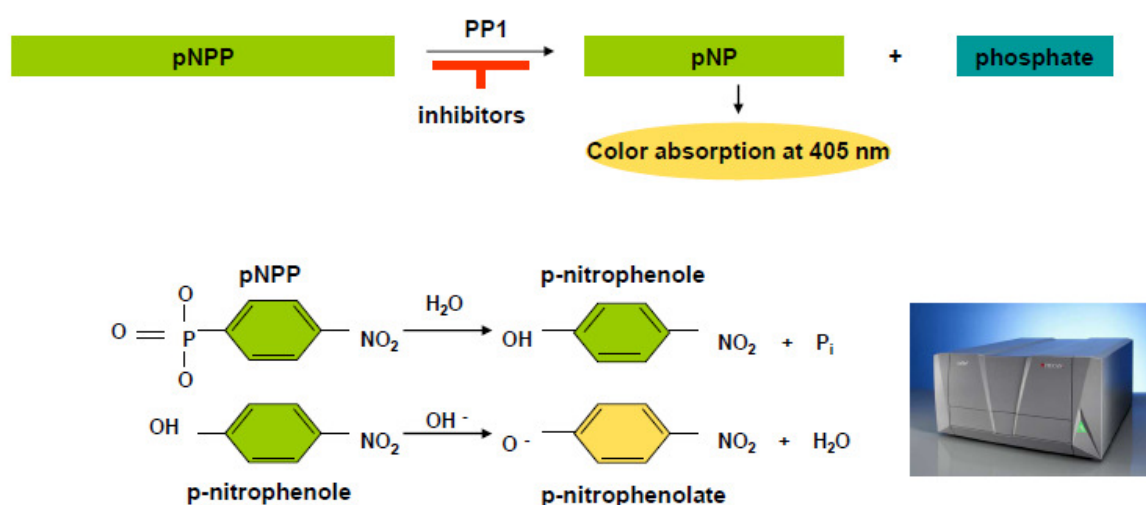


Figure 3.6 PP1-mediated dephosphorylation of the chromogenic substrate (p-NPP). In a first step, the enzyme dephosphorylates its substrate pNPP. In a second step, the phenolic OH-group is deprotonated resulting in p-nitrophenolate with absorption at 405 nm (yellow). PP1 inhibitors lead to decreased absorption.

3.3.2 DiFMUP as a fluorogenic substrate

Fluorogenic substrates based on 4-methylumbelliferone (4-MU) have been widely used for the detection of glycosidase and phosphatase activities, especially alkaline phosphatases (Gee et al. 1999). 6, 8-difluoro-4-methylumbelliferyl phosphate (DiFMUP) is a fluorinated derivative of 4-MU with lower pK_a value suitable to detect acid phosphatases. DiFMUP was also used for the detection of PP1 and PP2A activities (Fontal et al. 1999).

A 10 mM stock solution of DiFMUP was prepared in 50 mM Tris-HCl, pH 7.0 and aliquots were stored at -20 °C. The assay was carried out in black flat bottom 384-well plates using the same buffer system as described for the colorimetric assay in a total reaction volume of 100 μ l. Different amounts of PP1 catalytic subunit (0.001-

0.016 U; specific activity 25 U/ μ g protein) were prepared in 20 μ l EDB. After addition of 70 μ l RB, dephosphorylation reactions were started by addition of 10 μ l RB containing 500 μ M DiFMUP (final concentration 50 μ M). For kinetic analysis a constant concentration of recombinant PP1 (0.002 U = 21.6 pM) was added to different concentrations of DiFMUP (5, 10, 20, 40, 80 and 160 μ M). The fluorescence intensities of hydrolyzed DiFMU, as fluorogenic product (excitation/emission = 385/490 nm), were monitored by TECAN® Safire² reader at 30 °C (Fig 3.7). The gradient of relative fluorescence unit during 30 min (Δ RFU/min) was considered as phosphatase activity.

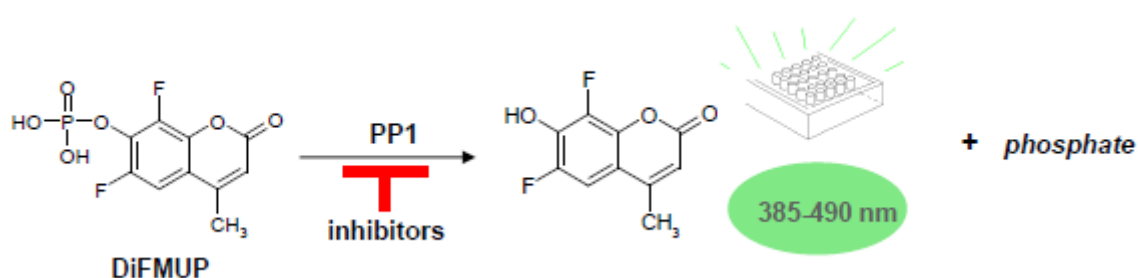


Figure 3.7 PP1-mediated dephosphorylation of DiFMUP.

Using DiFMUP as substrate, the activities and inhibitions of native PP1, purified from rabbit skeletal muscle were compared with recombinant PP1. The hydrolysis rates of DiFMUP were measured in the presences of 0.001-0.016 U native PP1, as described for recombinant PP1.

3.3.3 Phosphatase inhibitors in the colorimetric and fluorescence assays

A general characterization of both colorimetric and fluorescence assays was performed using protein and chemical inhibitors of PP1. Fig 3.8 demonstrated the structures of small toxins with potent PP1 and PP2A inhibitory effects. The reported IC₅₀ values are, 1-2 nM of inhibitor-2 (I-2) for PP1, 1-2 nM of OA for PP2A and ~50 nM for PP1, 100-500 nM and 40 nM of cantharidin for PP1 and PP2A, respectively, and 0.4-1 nM of calyculin A for both PP1 and PP2A (Herzig & Neumann 2000; Swingle et al. 2007).

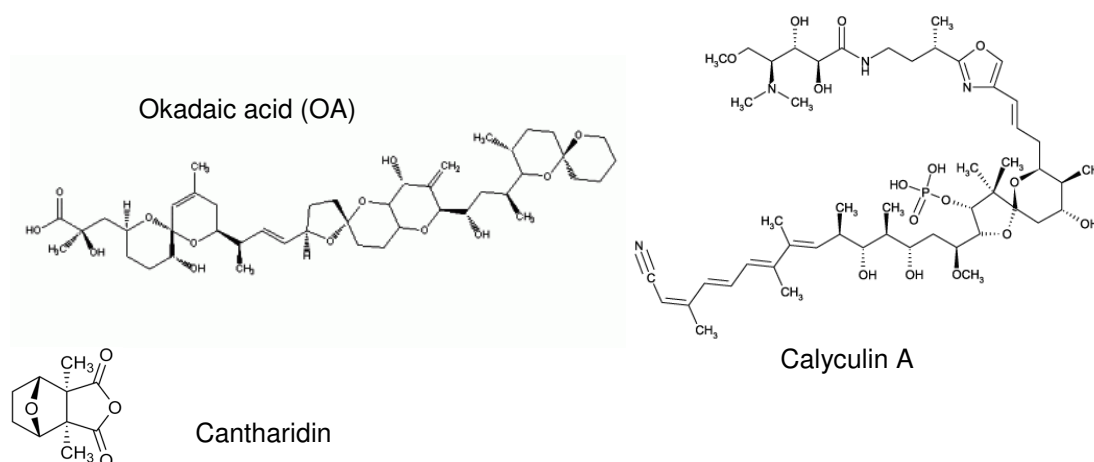


Figure 3.8 Structures of small molecule phosphatase inhibitors. OA, a cytotoxin from shellfish causing diarrhoea, is a fatty acid isolated from dinoflagellates. Cantharidin, as a terpenoid, is derived from many species of blister beetle. Calyculin A is secreted by a marine sponge *Discodermia calyx*.

The effects of PKA-phosphorylated/thiophosphorylated I-1, I-2, OA cantharidin and calyculin A were compared using pNPP or DiFMUP as substrate.

OA, cantharidin and calyculin A were dissolved in DMSO as a 10 mM stock concentration and stored at -20 °C. All the proteins and inhibitors were diluted with EDB to the appropriate concentrations, freshly before the assay. Various concentrations of inhibitors ranging from 0.1 to 1000 nM were preincubated with 1 U or 0.002 U PP1, in the colorimetric or fluorescence assay, respectively. Tab 3.3 showed the procedure of both phosphatase assays with PP1 inhibitors.

Table 3.3 The phosphatase assay in the presence of inhibitors. A) The pipeting protocol of the colorimetric assay.

Addition of 20 µl of several concentrations (0.1-1000 nM) of inhibitors to the assay plate
Addition of 20 µl EDB to the control wells
Addition of 20 µl PP1 (0.05 U/µl) to all wells
Addition of 160 µl RB to all wells
Incubation for 10 min at RT
Addition of 20 µl pNPP to all wells
Measurement of OD (405 nm) for every 1 min 30 min at 30 °C

B) The pipeting protocol of the fluorescence assay

Addition of 18 μ l of several concentrations (0.1-1000 nM) of inhibitors to the assay plate

Addition of 18 μ l EDB to the control wells

Addition of 2 μ l PP1 (0.001 U/ μ l) to all wells

Addition of 70 μ l RB to all wells

Incubation for 10 min at RT

Addition of 10 μ l DiFMUP (500 μ M in RB) to all wells

Measurement of RFU (385/490 nm), every 1 min for 30 min, at 30 $^{\circ}$ C

In addition, the inhibitory activity of I-1^P at various concentrations was compared in the presence of 0.002 U native and recombinant PP1, using DiFMUP as substrate.

3.3.4 The synthetic peptides of I-1

Based on the available data from crystal structures of PP1 with microcystin (Goldberg et al. 1995) and myosin phosphatase targeting 1 (MYPT1; Terrak et al. 2004), I-1-peptides were synthesized consisting of sequences likely involved in PP1 binding. The peptides, with the sequences ⁶SPRKIQFTV¹⁴, ¹⁹PHLDPEAAEQI²⁹ and ²⁵AAEQIRRRR³³ were commercially synthesized by PEPTIDE 2.0 (USA) or PANATEcs® (Germany) as lyophilized acetate salt with >90% purity from HPLC analysis and then dissolved in DMSO or slightly acidic distilled water (pH 5-6) in a stock concentration of 10 mM and the aliquots were stored at -80 $^{\circ}$ C.

The effects of these peptides were investigated in both colorimetric and fluorescence phosphatase-inhibitor assay systems. The PP1-I-1 master mixtures (MM) were prepared freshly. The final amounts of PP1 were 1 U in the calorimetric assay and 0.002 U in the fluorescence assay. The final concentrations of I-1^{SP} and I-1^P were 500 nM and 50 nM, respectively. Followingly, various concentrations of the peptides were preincubated with either PP1 or PP1-I-1 MM according to the protocols demonstrated in Tab 3.4 A-B.

In addition, the effects of these peptides were investigated in the presences of 10 nM I-2 and 10 nM calyculin A in the pNPP-based assay. Preparation of the master mixtures and assay procedures were similar to I-1^{SP}, as described above.

Table 3.4 The assay procedure of the peptides. A) The pipetting protocol for the colorimetric assay.

Addition of 20 μ l of different concentrations of the peptides (1-300 μ M) to the assay plate
 Addition of 20 μ l EDB to the control wells
 Addition of 20 μ l PP1 or PP1-I-1^{SP} MM to all wells
 Addition of 160 μ l RB to all wells
 Incubation for 10 min at RT
 Addition of 20 μ l pNPP (50 mM in RB)
 Measurement of OD, every 1 min for 30 min, at 30 °C

B) The pipetting protocol for the fluorescence assay

Addition of 18 μ l of different concentrations of the peptides (1-300 μ M) to the assay plate
 Addition of 18 μ l EDB to the control wells
 Addition of 2 μ l PP1 or PP1-I-1^P MM to all wells
 Addition of 70 μ l RB to all wells
 Incubation for 10 min at RT
 Addition of 10 μ l DiFMUP (500 μ M in RB)
 Measurement of RFU, every 1 min for 30 min, at 30 °C

According to the obtained results from phosphatase assay (see 4.3), the possible functional consequences of disturbing the interaction of PP1 and I-1 in living cells were examined by modification of the I-1 peptide, ⁶SPRKIQFTV¹⁴ by attaching an 11-arginine chain. Poly-Arg I-1^{SPRKIQFTV}, FITC-labeled poly-Arg I-1^{SPRKIQFTV} and poly-Arg scrambled I-1^{KSIPRQTFV} were provided by PANATecs® as lyophilized powder with >80-90% purity dissolved in DMSO as a 10 mM stock and stored at -80 °C.

3.4 Cell culture

3.4.1 Preparation of HEK 293 cells

HEK 293 cells are human embryonic kidney cells that are easy to grow and transfect (Fig 3.9). The culturing of HEK 293 cells was carried out in DMEM + Glutamax™ supplemented with 10% inactive fetal calf serum (FCS), and 1% penicillin/streptomycin (P/S) in 10 cm tissue culture dish, incubating at 37 °C and 5%

CO₂. The medium was refreshed every two days. At ~80% density, the cells were split in a desired dilution (1:5, 1:10 or 1:20) after washing with 10 ml PBS and incubating with 2 ml trypsin-EDTA for 3-5 min at 37 °C. Trypsin digestion was stopped by addition of 10 ml medium containing serum.

The freezing cultures were prepared from 10⁷ cells long time storage. After trypsin treatment, the cells were spun (3 min, 1000 rpm, RT) and resuspended in 2 ml medium containing 50% active FCS, 40% DMEM and 10% DMSO and transferred into cryotubes. The cryotubes were frozen slowly overnight at -80 °C and then stored in liquid nitrogen.

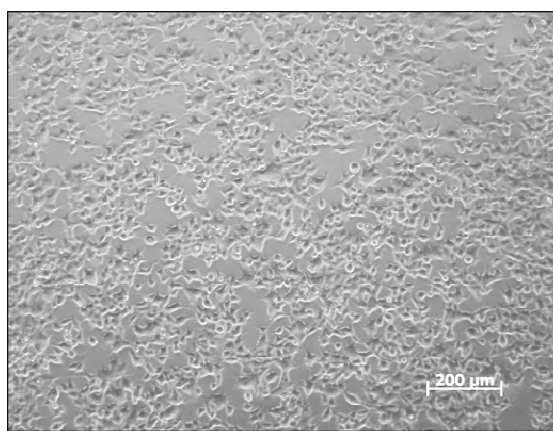


Figure 3.9 Monolayer culture of HEK 293 cells.

3.4.2 Preparation and treatment of NRCMs

Preparation of neonatal rat cardiomyocytes (NRCM) has been kindly done by technical assistants of our institute, June Uebeler and Thomas Schulze. The whole process took place aseptically and the applied materials and tools were autoclaved.

Organ extraction from neonatal rat was authorized by the Behörde für Soziales, Familie, Gesundheit und Verbraucherschutz der Freien und Hansestadt Hamburg (Org 366). Neonatal rats, 1-4 day old, were sacrificed by cervical dislocation. Rat hearts were removed, kept in ice-cold Ca²⁺/Mg²⁺-free Hanks buffer (CBFHH) and then ventricles were separated, washed, minced into small fragments and subjected to serial enzymatic digestion by trypsin/DNase according to a modified protocol from Webster et al. (1993). The small ventricle pieces (max. 1 mm) were incubated with trypsin solution for 10 min at room temperature with rotation. Then, after sedimentation the supernatant was removed and the pellet was incubated again with trypsin solution until getting turbid. After sedimentation, the supernatant was collected

in a new falcon device and the pellet was resuspended and triturated with DNase solution, then sedimented and supernatant was added into the latter one. This cycle was repeated several times to isolate cardiomyocytes from other parts of ventricles. The collected suspension was centrifuged (60 g, 4 °C, 20 min), the cell pellet was resuspended and triturated in Nicht-Kardiomyozyten-Medium (NKM) plus 0.8% DNase, again centrifuged, resuspended in 5 ml NKM medium and finally filtered through a 100 µm mesh filter. The concentration of cell suspension was estimated by counting the cells using trypan blue and a Neubauer chamber.

After trypsin digestion, cells were preplated in 10 cm cell culture dishes for 90 min at 37 °C to reduce the number of non-cardiomyocyte cells like fibroblasts. Unattached cells, which were mainly cardiomyocytes, were transferred to a Falcon tube, centrifuged (60 g, 4 °C, 15 min), and the pellet resuspended in 5 ml Kardiomyozyten-Medium (KM) and the cells were counted again. NRCMs were plated on gelatin-coated (0.01 mg/ml; in 1x PBS) 12-well dishes at a density of $3.5\text{--}4 \times 10^5$ cells/well and incubated at 37 °C and 7% CO₂. The KM medium was supplemented with 0.1 mM 5'-bromo-2'-deoxyuridine (BrdU) to prevent overgrowth of fibroblasts. After 24-48 h, the cardiomyocytes adhered to the bottom and established cell-cell contacts forming two-dimensional synchronously beating cells (Fig 3.10 A).

For immunohistological purposes, NRCMs were cultured in a 2-well Chamber Slide. The upper structure of this slide is removable providing a direct microscopic analysis of the cells after culturing and staining (Fig 3.10 B).

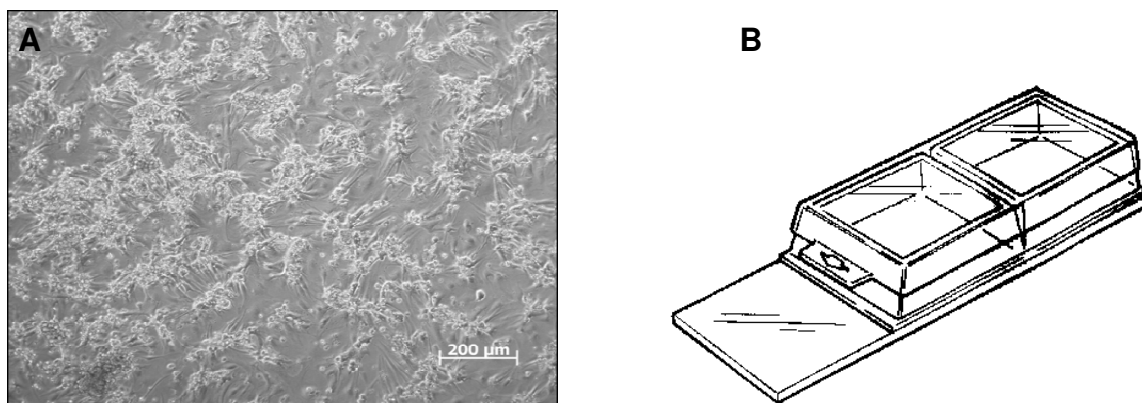


Figure 3.10 The culturing of NRCMs **A)** NRCMs (stretched form) after 48 h culturing. **B)** Removable, polystyrene media chamber with cover. The NRCMs ($\sim 3 \times 10^5$ /well) grow on a sterile, non-fluorescent glass microscope slide treated for attachment and growth of cells.

After 3 days of culturing, the medium was removed and NRCMs were treated with vehicle (DMSO 0.1%) or 10 μ M poly-Arg modified peptides in 1 ml serum free medium. Following 60 min incubation at 37 °C, 10 nM isoprenaline was added to stimulate the β -adrenergic signaling cascade. After 5 min incubation, the cells were washed with ice-cold PBS and prepared for immunohistological staining and Western blot analysis (see 3.5 and 3.7).

3.4.3 Preparation and treatment of EHTs

Generation of fibrin-based mini EHTs was performed using the protocol of Hansen et al. (2010). The whole process was performed aseptically.

A reconstitution mixture was prepared on ice as follows: 4.1×10^5 NRCM cells/ml, 5 mg/ml bovine fibrinogen (stock 200 mg/ml plus 0.5 μ g/mg fibrinogen in 0.9% NaCl sterile). 2x DMEM containing 1% P/S was added to match the volumes of fibrinogen and thrombin stock to ensure isotonic conditions.

The preparation of a 24-well plate was carried out by addition of 1.5 ml/well 2% agarose (hot, in PBS) and placing Teflon spacers (Fig 3.11 A) into the wells to produce casting molds. After hardening of the agarose (~10 min), Teflon spacer were removed carefully and replaced with silicon post racks that are composed of a 2-component Sylgard 184 elastomer (Fig 3.11 B). The pairs of posts should extend into each casting mold. Then, for each mini-EHT 100 μ l reconstitution mix was mixed rapidly with 3 μ l thrombin and pipetted into the agarose slots. The constructs were incubated at 37 °C, 7% CO₂ for 2 h to fibrinogen polymerization. Another 24-well-plate was prepared by 1.5 ml/well DMEM culture medium consisting of 10% inactive horse serum, 2% chick embryo extract (CEE), 1% P/S, 0.1% insulin and 0.1% aprotinin. The completed constructs were removed from agarose casting molds after addition of 200-300 μ l culture medium and transferred into the prepared culture plate (Fig 3.11 C). Constructs were incubated at 37 °C, 7% CO₂ and fed every 2 days with fresh culture medium as described above.

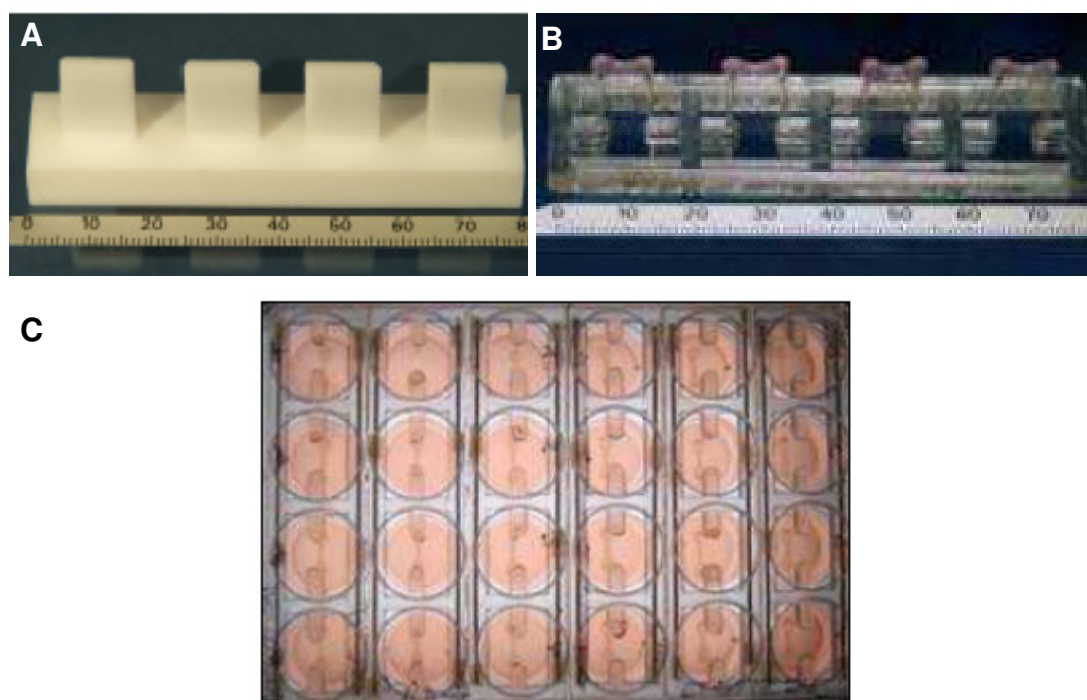


Figure 3.11 Generation of 24 mini EHTs. **A)** Teflon spacer with 12 mm length, 3 mm width and 13.5 mm height. **B)** Silicon post rack with 4 EHTs, length/width of rack: 79 x 18.5 mm, length of posts 12 mm, diameter 1 mm, plate diameter 2 mm, distance 8.5 mm. **C)** The scheme of EHT generation in a 24-well plate (Hansen et al. 2010).

At day 14 after generation, the EHTs were treated with either 0.1% DMSO or 10 μ M poly-Arg modified peptides for 60 min at 37 °C in culture medium without serum plus 30 mM BDM.

3.4.4 Preparation and treatment of AMCMs

Adult mouse cardiomyocytes (AMCM) were kindly prepared by Lisa Krämer, our technical assistant, following a modified method of O'Connell et al. (2003). Organ extraction for adult mice was authorized by the Behörde für Soziales, Familie, Gesundheit und Verbraucherschutz der Freien und Hansestadt Hamburg (Org 370).

A 3-4 month-old mouse was heparinised (20000 U/kg) to avoid blood clotting in the coronary vessels during the following procedure. After 10 min, the mouse was sacrificed by cervical dislocation in light CO₂ anesthesia. After median thoracotomy, hearts were excised, mounted on a temperature-controlled modified Langendorff perfusion apparatus and retrogradely perfused through the aorta with a Ca²⁺-free modified Perfusion buffer at 37 °C for 4 min at 3 ml/min (Fig 3.12 A). This perfusion

buffer was then switched to a digestion buffer at 37 °C for 8-9 min. The ventricles were excised, minced with forceps and dissociated by gentle pipetting. The enzyme activity was stopped by addition of 10% and 5% fetal bovine serum (FBS), and CaCl_2 was stepwise reintroduced up to a concentration of 1 mM. The rod-shaped cells (Fig 3.12 B), as intact AMCMs, were counted under the microscope, using a Neubauer chamber.

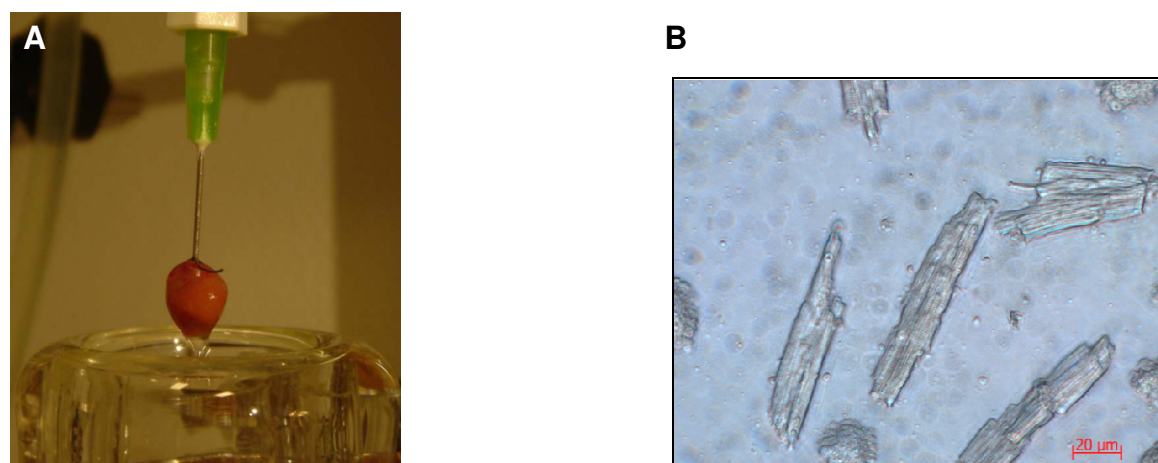


Figure 3.12 Preparation of isolated adult mouse cardiomyocytes. A) Adult mouse heart during perfusion **B)** An isolated ventricular myocytes from adult mouse heart.

The cells were sedimented by light centrifugation at 40 g for 1 min and subsequently transferred into the IonOptix buffer containing 1.8 mM CaCl_2 . 500 μl of cell suspension were preincubated with either 1% DMSO or 3 μM and 10 μM poly-Arg modified peptides for 1h at 37 °C, 2% CO_2 .

3.5 Immunohistological staining and confocal microscopy

3.5.1 Immunohistological staining of NRCMs

Cells were washed with ice-cold PBS and fixed in 4% paraformaldehyde (PFA) for 10 min. Then, the cells were washed 3x with PBS and blocked with block buffer for 60 min to permeabilize the cells for antibodies. Subsequently, antibody labeling against sarcomeric α -actinin was performed with a 1:800 dilution of anti- α -actinin in antibody solution for 60 min. Following washing with PBS, the secondary antibody, goat anti-rabbit IgG Alexa 546 (1:800) and DRAQ5™ (1:800) were applied for 60 min to visualize the sarcomeric structure of cardiomyocytes and nuclei, respectively. After

washing with PBS, the slides were mounted with Fluoromount™ G to reduce fluorochrome quenching during fluorescence microscopy and seal the slides during storage.

3.5.2 Immunofluorescence staining of EHTs

EHTs were gently separated from their silicone racks and transferred into 2 ml tubes. The EHTs were fixed by Roti®-Histofix (Roth) overnight, washed 3x 15 min with TBS, incubated with blocking buffer and after short washing, incubated with primary antibody against cardiac MyBP-C protein (1:200, COC2) in 500 µl antibody solution overnight at 4 °C then washed overnight at 4 °C and incubated with goat anti-rabbit Alexa 546, as a secondary antibody and DRAQ5™ (1:800) overnight at 4 °C. After washing at 4 °C, overnight, the EHTs were transferred on the MENZEL microscope slides with slots and mounted with Fluoromount™ for microscopic analysis.

3.5.3 Confocal laser scanning microscopy

Confocal laser scanning microscopy provides high-resolution images with depth selectivity for optical analysis, whereby samples with higher thickness can be analyzed than in standard microscopy. A point laser source is responsible for illuminating the specimen with discrete fluorescent intensities. The confocal images were recorded with a LSM Zeiss microscope (Carl Zeiss) using Axiovert 200 M software (Carl Zeiss MicroImaging GmbH). Argon 488 nm, HeNe-1 543 nm and HeNe-2 633 nm laser settings were applied for analysis of FITC, Alexa and DRAQ5™, respectively.

3.6 Video-optical measurements of AMCMs

Contractile properties of isolated adult mouse cardiomyocytes were determined with an IonOptix system (IonOptix Corporation, MA, USA), following the protocol of Pohlmann et al. (2007) and with the kind supports of Prof. Lucie Carrier (Institute of Experimental Pharmacology and Toxicology, University Medical Center Hamburg-Eppendorf, Hamburg) . In skeletal and heart muscle, the thin and thick filaments show a characteristic organization, which due to their different optical properties, is

observed under the light microscope as a cross-striated pattern of alternating dark and light bands. When analyzing the optical density in a series of sarcomeres, this results in a sinusoidal curve with the wavelength of the sine representing the sarcomere length. This density trace was recorded by the IonOptix MyoCam™ (IonOptix Corporation, MA, USA) and then transformed by the IonWizard sarcomere length acquisition software into a signal of sarcomere length by applying a Fast Fourier Transform (FFT). The program recorded and saved sarcomere length as a function of time including also the stimulation marks which were necessary for the analysis (Fig 3.13 A). The camera sampled images with a frequency of 240 Hz which was quick enough to monitor cell contraction. The analysis was performed with the IonWizard 6.0 software (Fig 3.13 B).

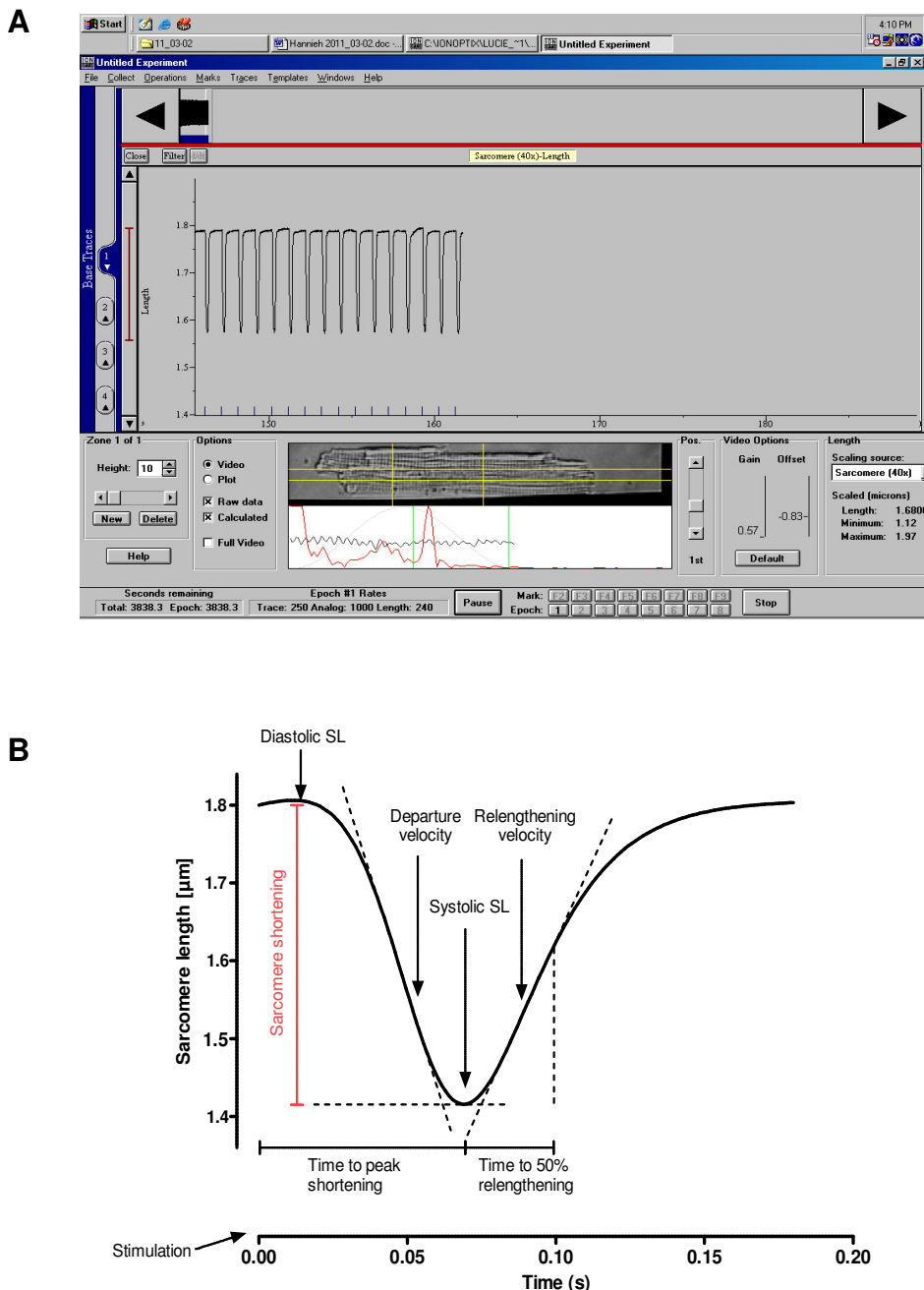


Figure 3.13 Video-optical measurements of single adult mouse cardiomyocytes. A) Sarcomere length measurements from a single myocyte paced with a frequency of 1 Hz. **B)** Analysis of an averaged sarcomere length (Pohlmann 2008). The definitions of the contractile parameters are:

Diastolic sarcomere length = the pre-stimulation baseline value of sarcomere length.

Systolic sarcomere length = the value of the sarcomere length transient at its maximal deflection from baseline.

% Sarcomere shortening = shortening amplitude expressed as % of diastolic sarcomere length.

Shortening velocity = the minimum of the first derivative of the sarcomere length transient i.e. the steepest slope of the deflection phase of the sarcomere length recording.

Time to peak shortening = time for the transient to reach peak sarcomere length during the deflection phase of the transient.

Relengthening velocity = the maximum of the first derivative of the sarcomere length transient i.e. the steepest slope of the recovery phase of the sarcomere length recording.

Time to 50% relengthening = time for the transient to return 50% of the peak sarcomere length during the recovery phase of the transient.

The treated AMCMs with DMSO or poly-Arg I-1^{SPRKIQFTV} were diluted in IonOptix buffer to a final concentration of about 15,000 –20,000 rod-shaped myocytes per ml. About 400 µl of the myocytes suspension was pipetted into a cell perfusion chamber (Cell MicroControls) and mounted on the stage of an inverted microscope (Nikon Eclipse TS 100). A stimulation assay consisting of two platinum iridium electrodes allowed electric stimulation of the myocytes with a field stimulator (MyoPacer). Myocytes were paced with a frequency of 1 Hz at 10 V and with 4 ms impulse duration. The cell chamber was perfused using a drop-sensor controlled flow controller (cFlow 8 Channel) to fill the chamber and a peristaltic pump to aspirate the solution. The flow rate was set to 0.5 ml/min.

3.7 Protein preparations and analysis

3.7.1 Preparation of cell and tissue homogenates

For Western blot purposes, NRCMs or HEK cells were homogenized in 120-150 µl lysis buffer. Samples were stored at -20 °C until utilization. Tissue homogenates for phosphatase assay were prepared from ventricle and skeletal muscles of 17-week old mouse and human left ventricles. The available tissues of non-failing, ischemic cardiomyopathy (ICM) and dilated cardiomyopathy (DCM) heart tissues were obtained from patients after heart transplantation.

By an authorized organ extraction in mouse as mentioned before (3.4.4), the heart was extracted, rinsed in isotonic 0.9% NaCl solution and the atria were removed. The other organs like lung, liver and kidney were also excised and their weights noted. After weighing, tissues were frozen in liquid nitrogen, powdered with a steel mortar in liquid nitrogen and stored at -80 °C until utilization.

For application in the phosphatase assays, various preparations were examined to find the optimal procedure for keeping PP1 activity. I) 50-100 mg frozen powder of mouse organs or HEK 293 cells from 10 cm culture dish were mixed in 2 ml ice-cold homogenization buffer (1), and after homogenization by Tissue Lyser™ for 60 s, 30 Hz, centrifuged at 500 g, 5-10 min, at 4 °C. The supernatant was considered as

homogenate. 1 ml of homogenate was further spun by ultracentrifuge (TF 90,000 rotor) at 35000 rpm for 30 min, at 4 °C. The collected supernatant was considered as cytosolic fraction. II) 20-30 mg frozen human heart powder was mixed with 100-150 µl 1x NEBuffer for PMP, supplemented by complete mini-proteases inhibitor cocktail (1 tablet for 10 ml buffer). Then the mixture was homogenized with the Tissue Lyser™ twice for 60 s, after 3x freeze-thaw cycles, and centrifuged at 1000 g, 5 min, and 4 °C. The supernatant as homogenate was collected and after protein measurement (Bradford's method) stored at -80 °C until utilization.

3.7.2 Quantification of protein using Bradford's method

Bradford's method is a protein determination method based on the binding of Coomassie Brilliant Blue G-250 to proteins (Bradford 1976). The binding of dye to proteins causes a shift in the absorption maximum of the dye from 465 to 595 nm. The absorption at 595 nm is correlated to the concentration of protein. The standard curve was created using 0.1 mg/ml bovine serum albumin (BSA) as a standard protein (Tab 3.5). The Bradford reagent, Roti®-Quant, was diluted 1:4 with 0.1 N NaOH prior to the assay. The samples were diluted 1:100 or 1:50 with H₂O in the cuvettes (10 x 4 x 45 mm) and incubated with 400 µl diluted reagent for 10 min at RT. The absorptions were measured by a spectrophotometer.

Table 3.5 Preparation of standard curve using BSA as standard protein.

Standard (µl)	H ₂ O (µl)	End concentration (µg/ml)
0	100	0
20	80	20
40	60	40
60	40	60
80	20	80
100	0	100

3.7.3 SDS-PAGE and Western blot

Sodium dodecyl sulfate polyacrylamide gel electrophoresis (SDS-PAGE) is a technique to separate proteins according to their molecular weight. Separation of the proteins was performed by gel electrophoresis under reducing and denaturing conditions. Therefore, indicated amounts of recombinant or isolated proteins were prepared with Laemmli buffer, heated at 95 °C for 5 min to achieve more denaturation of secondary and tertiary structures and loaded on a SDS containing polyacrylamide gel. The stacking gel consisted of 5% acrylamide/N,N'-methylene-bis-acrylamide, 125 mM Tris-base, pH 6.8, 0.1% SDS, with 0.1% ammonium persulfate (APS) and 0.1% N,N,N',N'-tetramethylethylenediamine (TEMED) to start polymerization, and the separating gel consisted of 10-15% acrylamide/bisacrylamide, depending on the size of the analyzed proteins, 375 mM Tris-base, pH 8.8, 0.1% SDS, with 0.1% APS and 0.04% TEMED to start polymerization. The electrophoresis was run for one to two hours in an electrophoresis module at a constant voltage of 120 V with the electrophoresis buffer. After the electrophoresis, the proteins were either stained by Coomassie or transferred on a blot membrane for further immunostaining. The transfer was carried out using either nitrocellulose or polyvinylidene fluoride (PVDF) membranes depending on the indicated antibody for 90 min with a constant current of 300 mA in transfer buffer. The efficiency of the transfer was controlled afterwards by staining the membranes with Ponceau red.

After rinsing with TBS-T, the membranes were saturated with 5% milk powder dissolved in TBS-T and then incubated overnight with different primary antibodies in TBS-T at 4 °C (Tab 3.6). The membranes were incubated with the secondary antibodies for 1 h at room temperature. Then the membranes were incubated with the Western blot detection kit ECL or ECL-Dura for 5 min, which contain a substrate for the peroxidase, creating a chemoluminescence. For visualization, the films (Hyperfilm ECL) were illuminated for 1-30 min and subsequently developed. The intensities of the bands were analyzed by densitometry with the GeneTools software (Syngene).

Table 3.6 The list of antibodies for Western blot analysis.

Primary antibody	Size of protein (kDa)	Secondary antibody
α -actinin (1:1000)	100	mouse 1:20000
Calsequestrin (CSQ; 1:2500)	53	rabbit 1:10000
DARPP-32-PThr ³⁴ (1:1000)	28	rabbit 1:5000
I-1 total (1:1000)	28	rabbit 1:5000
PLB total (1:5000)	7	mouse 1:5000
PLB-PSer ¹⁶ (1:5000)	7	rabbit 1:5000
PLB-PThr ¹⁷ (1:5000)	7	rabbit 1:5000
PP1 α (1:1000)	37	rabbit 1:5000

3.8 Screening of compounds in the PP1-I-1 assay

Screening of different groups of compounds was performed by our colorimetric or fluorescence assay to identify compounds with inhibitory effect on the active form of I-1 (Thr³⁵-phosphorylated). A set of synthetic or natural compounds was randomly selected and delivered by either Endotherm Life Science Molecules (Saarbrücken, Germany) or Greenpharma (Orleans, France). The solid powders were dissolved in DMSO with a stock concentration of 10 mM and stored at -20°C until utilization in the assay as described above.

The screenings were done in 96-well and 384-well formats with 220 μ l or 100 μ l final volumes using colorimetric or fluorescence assays, respectively. The reagents including PP1, I-1 and compounds were diluted in EDB, while the substrates were prepared in RB. First, a single concentration of the compounds (10-20 μ M) was tested in the presence of PP1-I-1 complex (Tab 3.7 A-B). The master mixtures were prepared containing PP1 and I-1^{SP} for colorimetric assay, and PP1 plus for fluorescence assay, freshly prior to the assay, as described in 3.3.4. All the compounds with any noticeable effect on PP1-I-1^P complex or PP1c were further analyzed applying various concentrations (1-300 μ M) in the assay. The indicated compounds were also tested for their effects on the PP1 free catalytic subunit (PP1c) after incubation with 1 U or 0.002-0.004 U PP1 in the colorimetric or fluorescence assay, respectively.

Tab 3.7 The assay procedure of the compounds for I-1 inhibitory effect A) The pipetting protocol of compound screening in the pNPP-based assay.

Addition of 2 μ l of a single concentration of a compound (10-20 μ M) to the indicated wells
Addition of 2 μ l DMSO to the control wells
Addition of 38 μ l PP1-I-1^{SP} MM to all wells
Addition of 160 μ l RB to all wells
Incubation for 10 min at RT
Addition of 20 μ l pNPP (50 mM in RB)
Measurement of OD, every 1 min for 30 min, at 30 °C

B) The pipetting protocol of compound screening in the DiFMUP-based assay.

Addition of 2 μ l of a single concentration of a compound (10-20 μ M) to the indicated wells
Addition of 2 μ l DMSO to the control wells
Addition of 18 μ l PP1-I-1^P MM to all wells
Addition of 70 μ l RB to all wells
Incubation for 10 min at RT
Addition of 10 μ l DiFMUP (500 μ M in RB)
Measurement of RFU, every 1 min for 30 min, at 30 °C

3.8.1 *In silico* selected compounds

The idea to identify chemical interactors of PP1 that potentially block the interaction of PP1 and I-1 prompted us to screen a library of compounds by bioinformatics tools, which was provided by Dr. Björn Windshügel in the Center for Bioinformatics of Hamburg University. For virtual screening, ZINC as a database of commercially-available compounds was employed. From 14 million compounds with ready-to-dock 3D structures, 3.4 million lead-like compounds were further filtered to perform a PP1-focused library. Subsequently, the affinities of 100,000 selected compounds to PP1 acidic groove were computationally examined by AutoDock program. After a final scoring, the selected compounds were kindly supplied by Dr. Lars Kattner (Endotherm GmbH, Saarbrücken, Germany). Because of synthesis and delivery problems, among 23 selected compounds just 13 compounds were investigated in the phosphatase assay. All the compounds were dissolved in DMSO as a 10 mM

stock and stored at -20 °C. Screening of these compounds in was performed in both colorimetric and fluorescence assays, as described in Tab 3.7.

3.8.2 Determination of Z'-factor for the fluorescence assay

A screening coefficient, called “Z'-factor”, provides a useful tool for comparing the quality of assays for high-throughput screenings (HTS). This coefficient reflects both the assay signal dynamic range and the data variation (Fig 3.14 A). The Z'-factor was determined for the DiFMUP-based PP1 assay using a formula published by Zhang et al. (1999; Fig 3.14 B). The hydrolysis rates of DiFMUP per min and standard deviations of 64 wells blank, 64 wells PP1 and 64 wells PP1-I-1^P were applied for the calculations. The blank contained 20 µl EDB and 70 µl RB without enzyme, PP1 sample contained 0.004 U PP1 in 20 µl EDB and 70 µl RB, and PP1-I-1^P samples contained 0.004 U PP1 plus 50 nM I-1^P in 20 µl EDB and 70 µl RB. The reactions were initiated by addition of 10 µl DiFMUP resulting in 50 µM final concentration and the fluorescence intensities were monitored for 60 min.

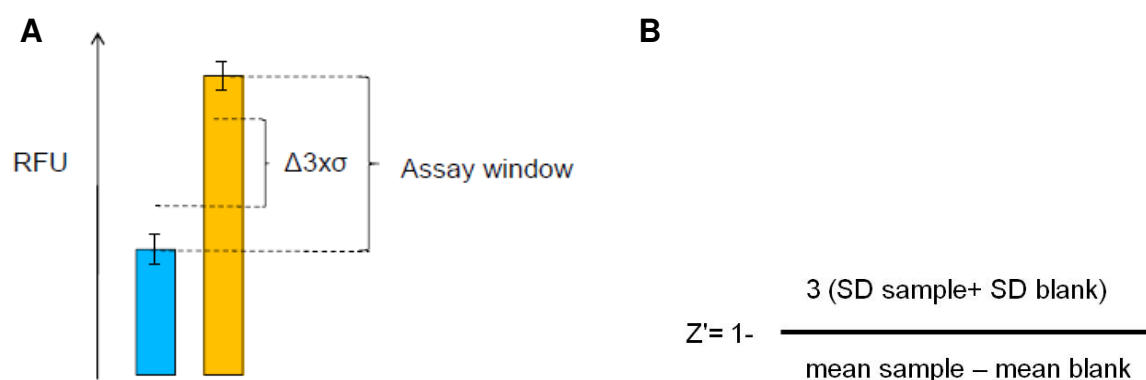


Figure 3.14 Determination of Z'-factor. **A)** Illustration of signal dynamic range and variation between low and high controls in the fluorescence assay. **B)** Definition of Z'-factor in terms of mean and standard deviations of blank and sample.

3.8.3 High-throughput screening

We applied our fluorescence phosphatase assay for high throughput screening (HTS) by cooperation with European ScreeningPort (ESP), which is an organization offering small molecule screening services to academic institutions (Fig 3.15 A).



Figure 3.15 High-throughput screening using the facilities of ESP **A)** Robotic systems are used to simultaneously assay the biological or biochemical activity of a large number of drug-like compounds in pharmacologically relevant systems. **B)** The compound library for the endpoint assay.

In the first run, 3560 compounds including, ChemBioNet and KiWiZ libraries and FDA approved drugs (Fig 3.15 B) were subjected to a single-point HTS using the DiFMUP-based fluorescence assay. The screenings consisted of a counter assay for identification of interfering compounds, PP1-I-1^P assay for I-1 antagonists and PP1 assay for compounds affecting PP1 activity, directly. Preparation of the reagents and the assay protocols have been shown in Tab 3.8.

Tab 3.8 The single-point assay of HTS. A) Preparation of the reagents for single-point HTS.

<u>PP1 Dilution</u>		(Multidrop LW)					
<u>Predilute PP1 1:100 in EDB (Stock: 2.7 μM --> 27 nM)</u>							
				1 plate			
Reagent		working		final		Volume	Volume
27 nM	PP1	108 pM		21.6 pM		3.1 μL	201.5 μL
	EDB					764.9 μL	49.7 mL
						768 μL	50 mL
<u>I-1^P Dilution</u>		(FlexDrop)					
				1 plate			
Reagent		working		final		Volume	Volume
26.6 μM	I-1 ^P	100 nM		30 nM		4.3 μL	300.7 μL
	EDB					1147.7 μL	79.7 mL
						1152 μL	80 mL
<u>DiFMUP Dilution</u>		(Multidrop HW)					
				1 plate			
Reagent		working		final		Volume	Volume
10 mM	DiFMUP	100 μM		50 μM		19.2 μL	1200 μL
	RB					1900.8 μL	121.2 mL
						1920 μL	120 mL

B) The assay procedure of the counter screen

Addition of 3 μ L I-1^P (100 nM) to column 24 (low signal control)

Addition of 3 μ L EDB to all wells except column 23

Column 23 is PP1 control (high signal control)

Addition of 2 μ L PP1 (108 pM) to all wells incubation 10 min 30 °C

Addition of 5 μ L DiFMUP (10 μ M) to all wells incubation 30 min 30 °C

Addition of compounds to columns 1–22 of assay plates (20 nl of 10 mM Stock)

Measurement of fluorescence Intensities

C) The assay procedure of PP1-I-1^P screen

Addition of compounds to assay plates, columns 1–22 (20 nl of 10mM Stock)

Addition of 3 μ L I-1^P (100 nM) to all wells except column 23 (high signal control)

Addition of 3 μ L EDB to column 23

Column 24 represents PP1-I-1^P control (low signal control)

Addition of 2 μ L PP1 (108 pM) to all wells incubation 10 min 30 °C

Addition of 5 μ L DiFMUP (10 μ M) to all wells incubation 30 min 30 °C

Measurement of fluorescence Intensities

D) The assay procedure of PP1 screen

Addition of compounds to columns 1–22 of assay plates (20 nl of 10 mM Stock)

Addition of 3 μL I-1^P (100 nM) to column 24 (low signal control)

Addition of 3 μL EDB to all wells except column 24

Column 23 is PP1 control (high signal control)

Addition of 2 μL PP1 (108 pM) to all wells incubation 10 min 30 °C

Addition of 5 μL DiFMUP (10 μM) to all wells incubation 30min 30 °C

Centrifuge plates

Measurement of fluorescence Intensities

In the second run, screening of nearly 5280 compounds was carried out in a kinetic measurement format, using PP1-I-1^P fluorescence assay. The compounds and reagents were prepared as described in Tab 3.9 A, and the reactions were performed according to the procedure showed in Tab 3.9 B.

Tab 3.9 The kinetic assay of HTS A) Preparation of the reagents

<u>PP1-I-1^P Dilution</u>					
<u>Predilute PP1 1:100 in EDB (Stock: 2.7 μM --> 27 nM)</u>					
				1 plate	
Reagents		working	final	Volume	Volume
27 nM	PP1	43.2 pM	21.6 pM	2.9 μL	80 μL
27 μM	I-1 ^P	60 nM	30 nM	4.1 μL	112.8 μl
		EDB		1833 μL	49.8 mL
				1840 μL	50 mL
<u>PP1 Dilution</u>					
<u>Predilute PP1 1:100 in EDB (Stock: 2.7 μM --> 27 nM)</u>					
				1 plate	
Reagent		working	final	Volume	Volume
27 nM	PP1	43.2 pM	21.6 pM	0.1 μL	40 μL
		EDB		79.9 μL	25 mL
				80 μL	25 mL
<u>DiFMUP Dilution</u>					
				1 plate	
Reagent		working	final	Volume	Volume
10 mM	DiFMUP	10 μM	5 μM	1.9 μL	120 μL
		RB		1918.1 μL	119.9 mL
				1920 μL	120 mL

B) The assay procedure

Addition of compounds to columns 1–22 of assay plates (20 nL of 10 mM Stock)

Addition of 5 μ L of PP1 to column 23 (high signal control)

Addition of 5 μ L PP1-I-1^P to all wells except column 23

Column 23 is PP1 control (high signal control)

Incubation for 30 min at 30 °C

Addition of 5 μ L DiFMUP to all wells

Incubation for 30 min at 30 °C

Measurement of fluorescence intensities: every 3 min for 30 min, at 30 °C

Identification of the potential hits was carried out by analysis of the recorded data during measurement time (Fig 3.16).

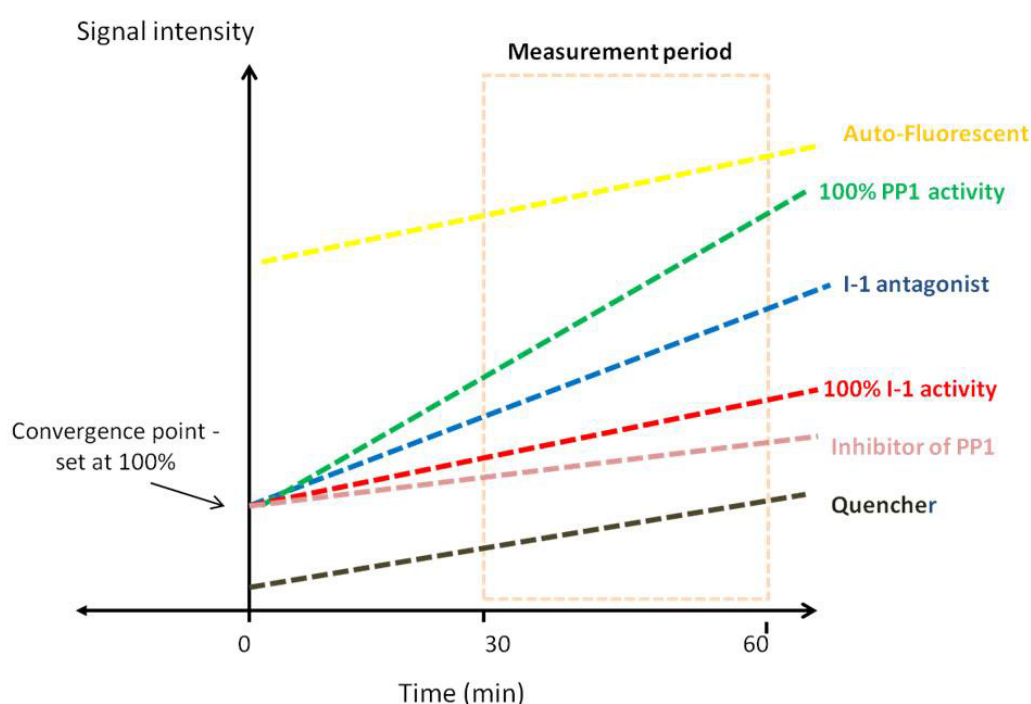


Figure 3.16 Data analysis in the kinetic measurements. The linear regressions were applied to obtain the signal intensities at T=0. Subsequently, the intensities were normalized to DMSO controls to compare the percentage of convergence. Auto-fluorescent compounds show a higher baseline and will not converge. Compounds with I-1 inhibitory effect have the same signal intensity as PP1 (high control) and PP1-I-1^P (low control) at T=0, but increased gradient during measurement period compared to low control. PP1 inhibitors show additional inhibition of I-1 effect with a converged intercept towards the controls at T=0.

Hit confirmation from both endpoint and kinetic screenings was performed according to Tab 3.10 using different concentrations of the selected hits compounds.

Table 3.10 The assay protocol for hit validation

Addition of 2 µl of different concentrations of the compounds (1-300 µM) to the indicated wells
Addition of 2 µl DMSO to the control wells
Addition of 48 µl PP1-I-1 ^P or PP1 MM to all wells
Incubation for 10 min at RT
Addition of 50 µl DiFMUP (100 µM in RB)
Incubation for 10 min at RT
Measurement of RFU, every 1 min for 30 min, at 30 °C

3.9 Determination of endogenous phosphatase activity

3.9.1 Measurement of phosphatase activities in the radioactive assay

The measurement of phosphatase activities using radioactive assay was done by Dr. Peter Boknik in the Institute of Pharmacology and Toxicology of Wilhelms-University, Münster, Germany. The radioactive assay is based on dephosphorylation of [³²P]-labeled phosphorylase a, which is a specific substrate for PP1 and PP2A (Neumann et al. 1999). Preparation of substrate is carried out by phosphorylation of isolated phosphorylase b from rabbit skeletal muscle with phosphorylase kinase using γ-[P³²]-ATP to generate [³²P]-labeled phosphorylase a. HEK 293, mouse heart and skeletal muscle were prepared in homogenization buffer (2) and treated with DMSO, OA (3 nM) or I-2 (1 µM) for 10 min at RT. Following preincubation with substrate for 30 min at 30 °C, the samples were diluted in a way that not more than 20% of substrate was hydrolyzed. Finally, the reactions were stopped by addition of 50% trichloroacetic acid (TCA) containing 20 g/l BSA. After 10 min incubation on ice, the reactions were centrifuged at 13,000 g for 5 min at 4 °C to sediment the precipitated proteins and supernatants were transferred into scintillation counter to quantify the released ³²PO₄, which is correlated to the phosphatase activity.

3.9.2 Measurement of phosphatase activities in the fluorescence assay

The endogenous phosphatase activities of HEK 293 cells, as well as human and mouse heart homogenates were measured in the fluorescence assay. In order to identify and quantify the different type of phosphatases, particularly PP1, various phosphatase inhibitors including OA and tautomycin (TTM) as Ser/Thr phosphatase inhibitors and I-2 as PP1 specific inhibitor, were applied in the assay.

The inhibitors were diluted in EDB to the desired concentrations and the homogenates were prepared as described in 3.7.1. Then, total phosphatase activities of 5 µg protein were monitored after treatment with inhibitors (Tab 3.11). The fluorescence signals were measured at 300 nm excitation and 490 nm emission wavelengths.

Tab 3.11 The assay procedure of phosphatase activities in cell/tissue lysate

Addition of 5 µl inhibitors to the assay plate (except control wells)

Addition of 40 µl EDB to all wells

Addition of 5 µl tissue/cell homogenate (1 µg/µl) to all wells

Incubation for 10 min at RT

Addition of 50 µl DiFMUP (100 µM)

Incubation for 10 min at RT

Measurement of RFU, every 3 min for 30 min, at 30 °C

3.10 Statistical analysis

Data are reported as mean of n=2 or mean ± SEM of n>3. Statistical analyses were performed with the GraphPad Prism 5.02. The differences between the groups were calculated by either one-way ANOVA or Two-way ANOVA. The significance definitions are *P<0.05, **P<0.01 and ***P<0.001. Curve fit and comparison of fitting, and enzyme kinetics including Michaelis-Menten constant (K_m) and maximum enzyme velocity (V_{max}) were performed with the GraphPad Prism 5.02 software.

4 Results

The work aimed at developing a non-radioactive phosphatase assay for screening of small molecules that interfere with protein-protein interaction in a multi-well format. For this purpose the phosphatase activities of recombinant proteins were monitored using colorimetric or fluorogenic substrates. Both assays were validated using several chemical and non-chemical protein PP1 inhibitors. Recombinant I-1 protein was bacterially expressed and purified. Activation of I-1 was carried out by PKA phosphorylation/thiophosphorylation. Finally, the assay was established for screening approaches, using single concentrations of PP1 and I-1, resulting in 50-60% inhibition of phosphatase activity.

Mutant I-1 proteins were generated by site direct mutagenesis to investigate PP1/I-1 interaction. The effects of small inhibitory or competitive I-1 peptides to I-1 activity were compared in the phosphatase assays. The biological activities of an identified effective peptide was further investigated *in vitro*.

After assay optimization as confirmed by an excellent Z'-factor, the fluorescence assay was miniaturized and automated for high-throughput screening (HTS). We evaluated the potential hits with repeated single-point measurement and detailed kinetic measurements.

The feasibility of the fluorescence-based assay was examined using several phosphatase inhibitors, in myocardial tissue and/or a variety of cell lysates.

4.1 Development of PP1-I-1 assay systems

4.1.1 Preparation of I-1 recombinant protein

Recombinant I-1 protein for utilization in the assay was generated by *E.coli* BL21 bacteria containing cDNA of mouse heart I-1. Thus, pGEX-2T expression vector enabled the expression of GST-tagged protein after IPTG induction, which promoted I-1 generation by bacteria. Restriction digestions of the plasmid with *Sma*I and *Eco*RI enzymes yielded a 0.47 kb and a 0.58 kb fragment, respectively, indicating of presence of the insert (Fig 4.1 A). Sequencing of the entire open reading frame in both directions using primers that described in Tab 3.1.1, verified the insert.

GST-tagged expressed protein was purified from bacterial lysate by glutathione agarose beads and finally I-1 was eluted by thrombin cleavage from GST. The recombinant protein was characterized via SDS-PAGE with an apparent molecular mass of 28 kDa by coomassie-staining and Western blot using polyclonal antibodies against I-1 (Fig 4.1B).

Since I-1 phosphorylation on Thr³⁵ is necessary for its activity against PP1, PKA phosphorylation *in vitro* was carried out to activate I-1. Western blot analysis characterized phosphorylation extent of the protein using phospho-specific antibodies (Fig 4.1 C left). In contrast to isolated PP1 from tissue (native PP1), recombinant PP1 expressed in *E.coli* exhibits almost no sensitivity against I-1^P and is even able to dephosphorylate it (Alessi et al. 1993; Huang et al. 1997). Western blot analysis showed that I-1 phosphorylation state is completely disappearing after 5 min incubation with 1 U recombinant PP1 (Fig 4.1 C right). Thiophosphorylation was carried out to protect phosphorylation state of I-1 using a non-hydrolysable ATP analogue, ATP-γ-S. Although thiophosphorylation renders I-1 fully resistant to dephosphorylation, the thiophosphorylated I-1 (I-1^{SP}) was partially protected against recombinant PP1 enzymatic activity (Fig 4.1 C right).

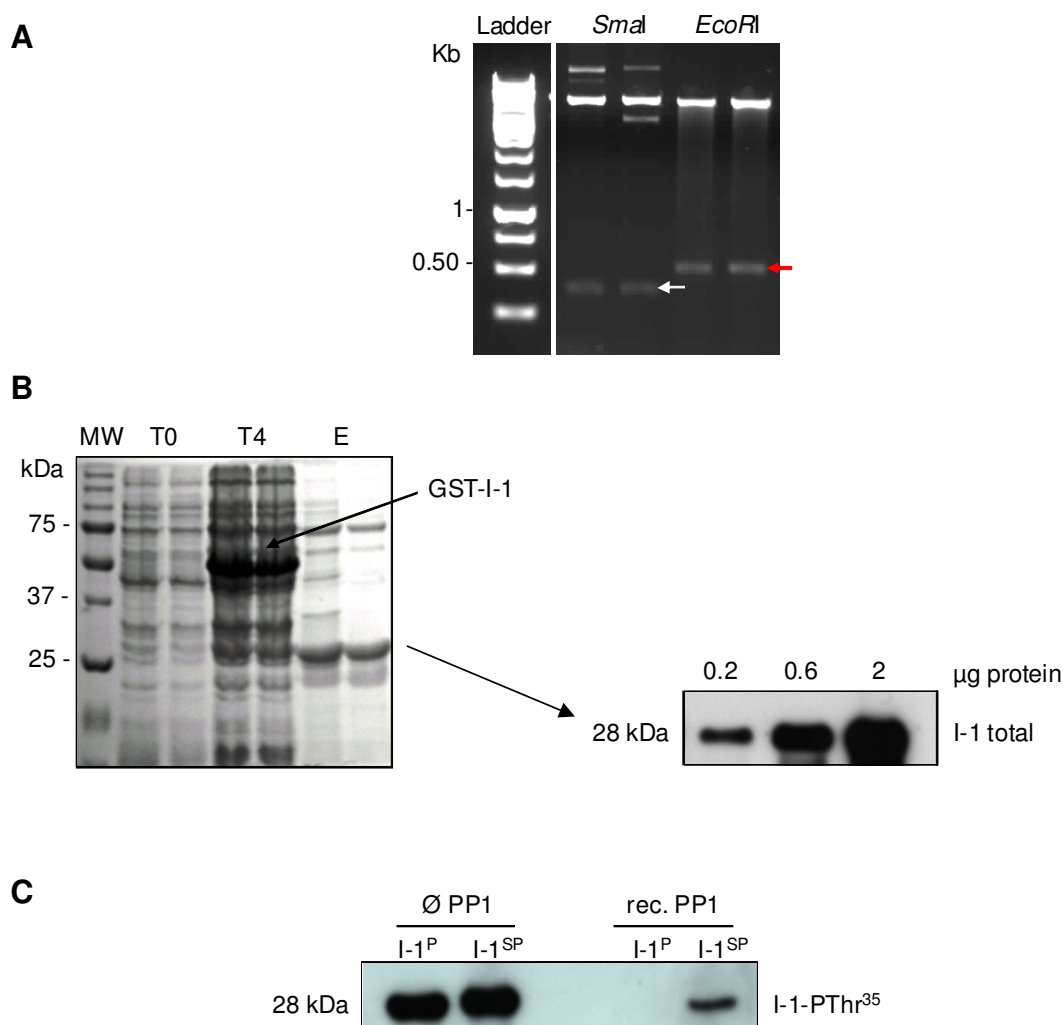


Figure 4.1 Generation, phosphorylation and thiophosphorylation of recombinant I-1 protein. A) Gel analysis of two pGEX-2T plasmids after restriction digestion with *SmaI* and *EcoRI*. The expected bands are marked with white and red arrows, respectively. **B)** Detection of recombinant protein. Coomassie-staining (left panel) and Western blot analysis (right panel) show the recombinant I-1 protein. MW; represents the molecular weight of standard protein. T0 and T4 indicate the time before and 4 h after IPTG induction, respectively, leading to produce GST-tagged I-1 (57 kDa). The final elute (E) from thrombin cleavage contains a 28 kDa I-1 protein. In Western blot analysis (right panel) I-1 protein was detected using I-1 antibodies. **C)** PKA phosphorylation and thiophosphorylation of I-1. Western blot analysis demonstrates the phosphorylation (I-1^P) and thiophosphorylation (I-1^{SP}) levels of I-1 before and after incubation with 1 U recombinant PP1.

4.1.2 development and characterization of the colorimetric assay

The chromogenic substrate, pNPP was utilized to determine PP1 activity. The dephosphorylation reaction yields pNP, which is a yellow product that can be measured at 405 nm with a spectrophotometer. The activities of various

concentrations of recombinant catalytic subunit of PP1 (PP1c) were monitored using 4.5 mM pNPP. The increase in optical density (OD) showed a linear regression between arbitrary units and PP1 concentration (Fig 4.2 A). We have chosen 1 U/well PP1 for further assays based on the achieved ODs. The gradient of OD was measured at a time period of 30 min with 5 min intervals. At this time the increase of absorption was linear (Fig 4.2 B). Therefore, we applied a fixed-time mode for 30 min. The saturation concentration of the substrate was studied using 1 U PP1 and different concentrations of pNPP. The kinetic data were calculated by Michaelis-Menten saturation curve, where the K_m and V_{max} values were 4.2 mM and 0.008 $\Delta OD/min$, respectively (Fig 4.2 C).

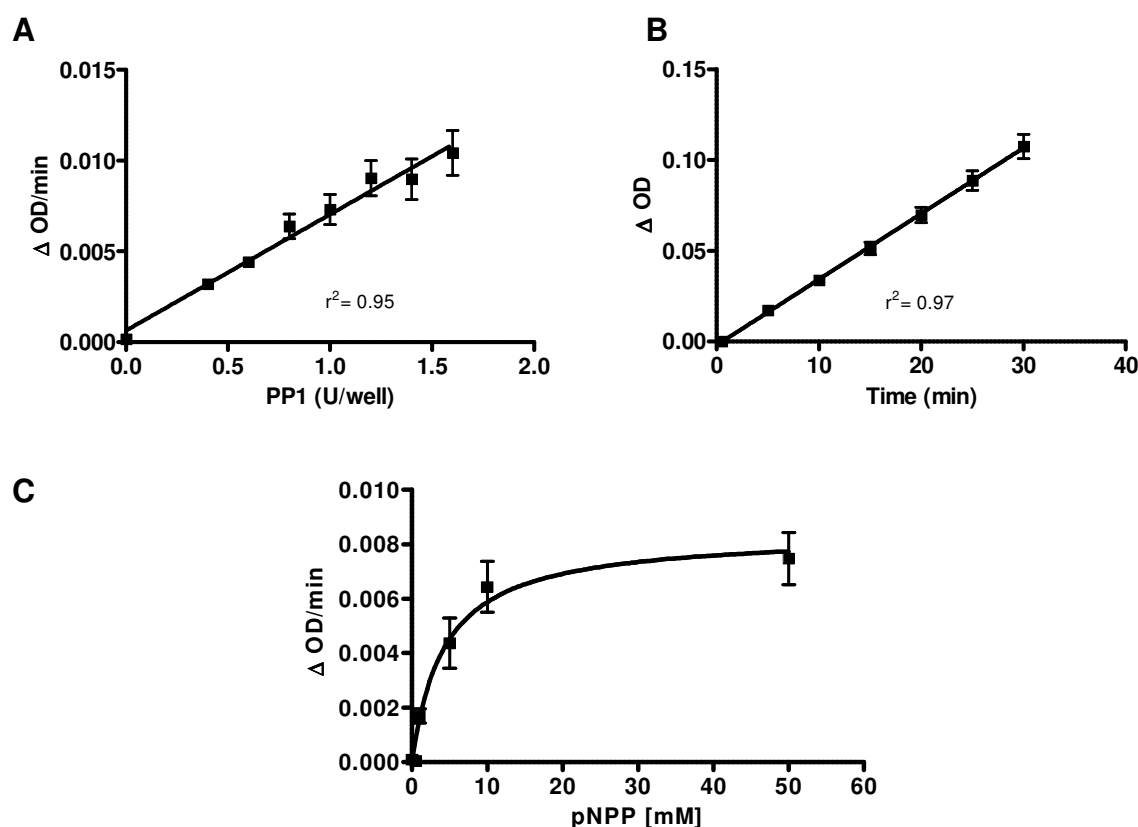


Figure 4.2 pNPP as a substrate for PP1. **A)** The increase of absorption versus the amount of PP1 in the presence of 4.5 mM pNPP. **B)** OD gradient versus time during 30 min measurement. **C)** Saturation curve of pNPP for 1 U PP1. The data presented are the means \pm SD of n=6-9 from two or three independent experiments.

We compared the inhibitory effects of various PP1 inhibitors to test the accuracy of our assay condition. I-2, as a selective inhibitor of PP1, cantharidin, okadaic acid (OA) and calyculin A, as chemical non-selective inhibitors of PP1 were applied to the

assay. Concentration-inhibition curves in the presence of 1 U PP1 are shown in figure 4.3 A. The obtained IC_{50} values were consistent with earlier reports (Peti et al. 2012). This data indicated the principal feasibility of our colorimetric assay system. For establishing PP1-I-1 assay, we compared the inhibitory effects of non-phosphorylated I-1 (I-1) and thiophosphorylated I-1 (I-1^{SP}). I-1^{SP} inhibited PP1 activity with an IC_{50} value of ~300 nM (Fig 4.3 B). The obtained IC_{50} value indicated still lower sensitivity of recombinant PP1 against I-1^{SP} than native PP1 (1-2 nM; Nimmo & Cohen 1978).

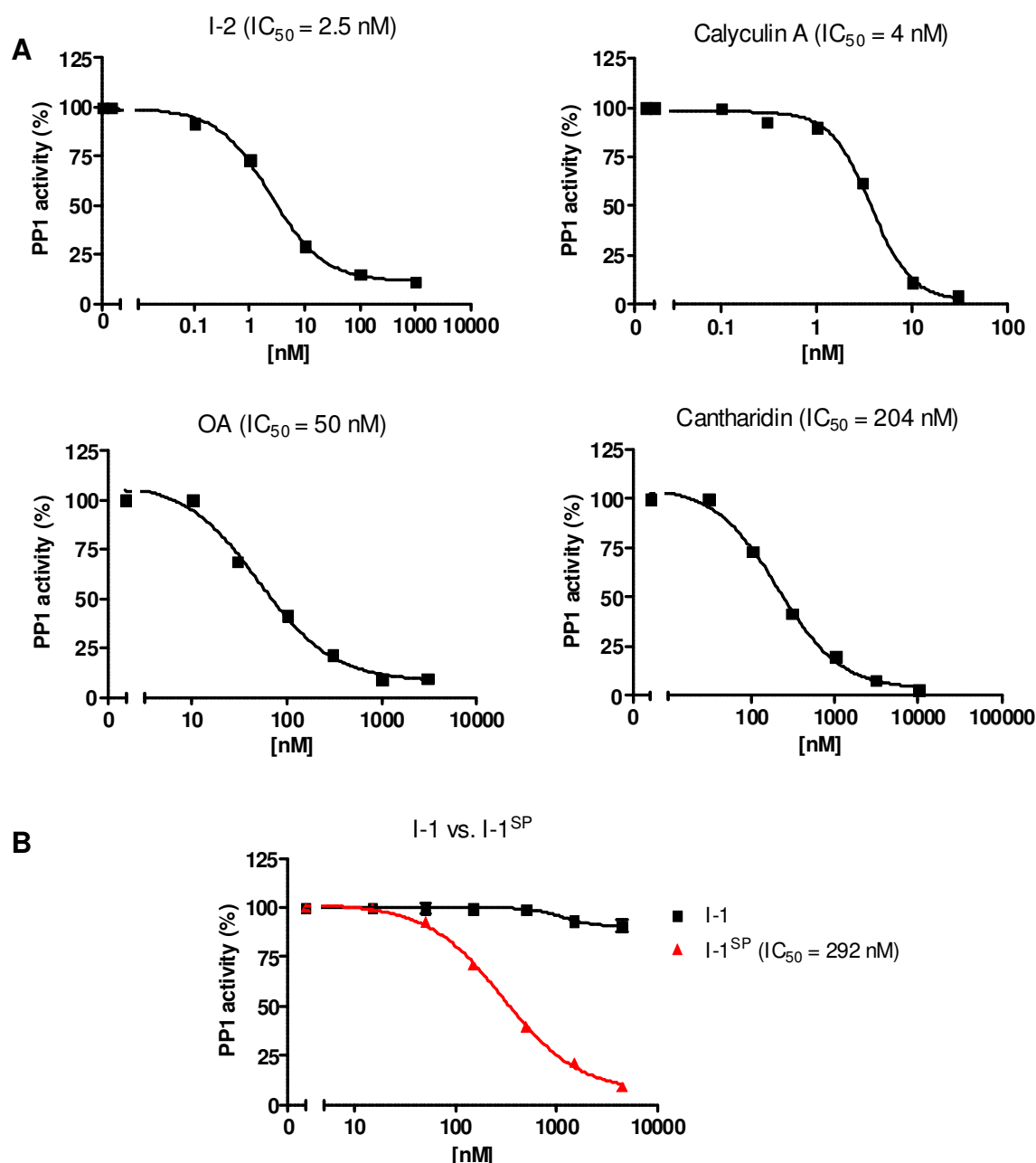


Figure 4.3 PP1 inhibitors in the colorimetric assay. Concentration-inhibition curves of **A)** I-2, calyculin A, OA, cantharidin and **B)** I-1 versus I-1^{SP} were plotted after preincubation with 1 U PP1. The control without inhibitor was considered as 100%. The values are expressed as the mean of $n=2$.

4.1.3 Development and characterization of the fluorescence assay

Although the chromogenic pNPP seemed to be appropriate, it required a rather high amount of enzyme. Moreover, the absorbance measurements of natural colored compounds were complicated in this assay.

In order to circumvent these limitations, we developed a fluorescence phosphatase assay using DiFMUP as a fluorogenic substrate. In order to determine appropriate concentrations of enzyme and substrate, reaction progress curves were measured for different enzyme concentrations at fixed 50 μM DiFMUP (Fig 4.4 A). A linear relationship between signal enhancement and time was obtained using 50 μM DiFMUP and 0.002 U PP1 (Fig 4.4 B). The kinetic curve for DiFMUP saturation was plotted against different concentration of substrate at a constant concentration of PP1 (0.002 U). Although saturation of the substrate was still not achieved, the Michaelis-Menten equation resulted in K_m and V_{\max} values of 194 μM and 1672 $\Delta\text{RFU}/\text{min}$, respectively (Fig 4.4 C).

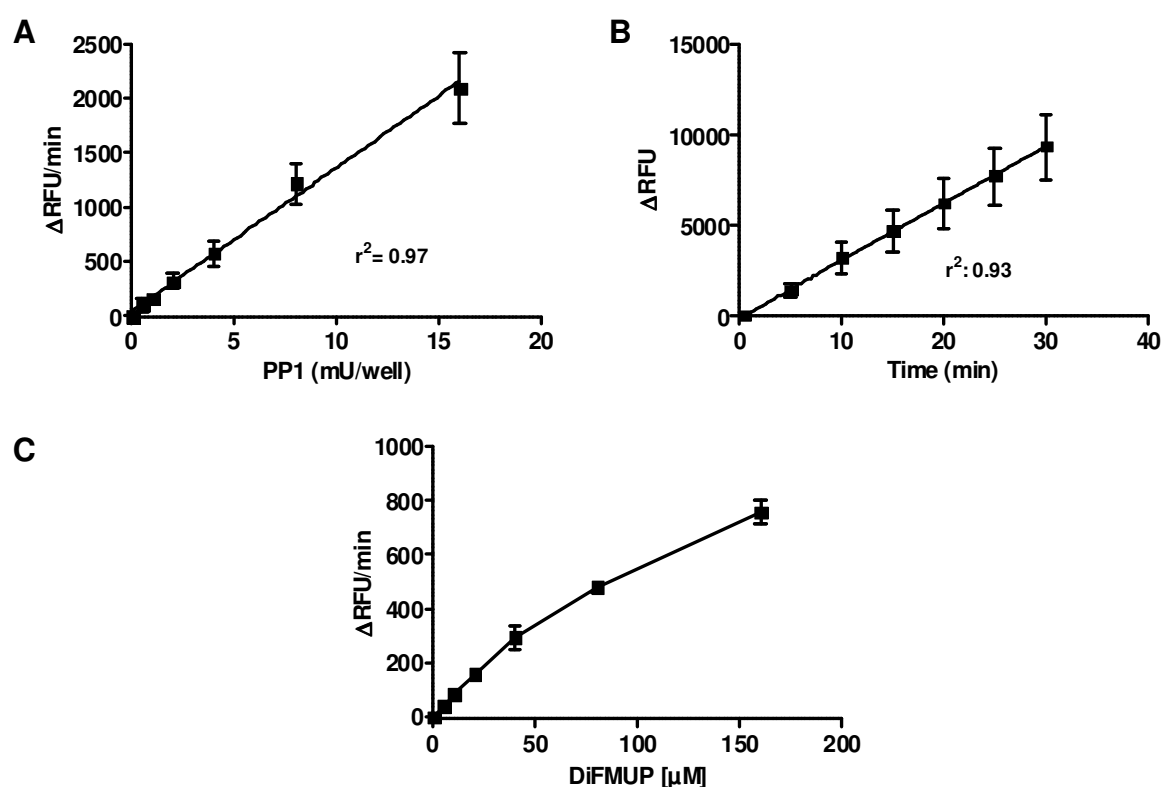


Figure 4.4 DiFMUP as a substrate for PP1. **A)** Hydrolysis rate of 50 μM DiFMUP was recorded using various concentrations of recombinant PP1. **B)** Time course of the reaction with 0.002 U PP1 and 50 μM DiFMUP for 30 min. **C)** The saturation curve of substrate was plotted in the presence of 0.002 U PP1 and different concentrations of DiFMUP. The presented data are mean \pm SD of $n=6$.

The high sensitivity of PP1 against DiFMUP allowed using a lower amount of PP1 catalytic subunit than colorimetric assay (500-fold). The inhibitory activities of I-2, cantharidin, OA and calyculin A were investigated in the presence of 0.002 U PP1

(Fig 4.5 A). Under these conditions, of I-2 and calyculin A were more than in the colorimetric assay with the high concentration of PP1 (~20-fold and 8-fold, respectively), while cantharidin and OA exhibited almost the same IC_{50} values. Unlike in the colorimetric assay, I-1^P was active against recombinant PP1 in the fluorescence assay. I-1^P inhibited PP1 activity concentration-dependently with an IC_{50} value of 14 nM. This value was relative close to the value obtained with native PP1 using phosphorylase a as substrate (1-2 nM; Nimmo & Cohen 1978).

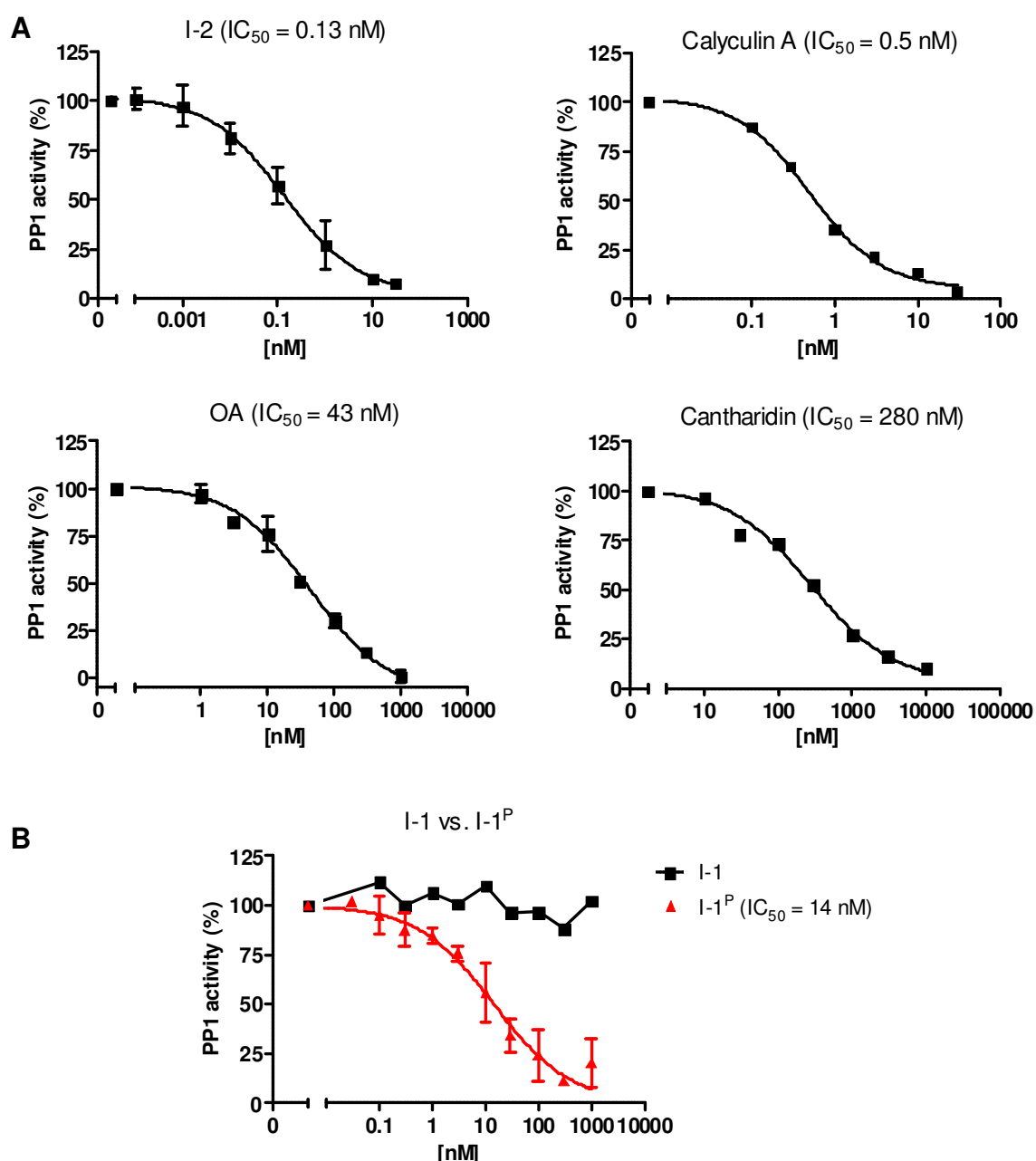


Figure 4.5 PP1 inhibitors in the fluorescence assay. Concentration-inhibition curves of **A)** I-2, calyculin A, OA, cantharidin and **B)** I-1 versus I-1^P after preincubation with 0.002 U PP1.

The presented activities are percentage of control without inhibitor. The data expressed mean of $n=2$ or mean \pm SD of $n=3-4$.

Recombinant PP1 differs from native PP1 in term of substrate sensitivity (Alessi et al. 1993; Zhao et al. 1994; Armstrong et al. 1998). Using the same amounts (0.004 U), native PP1 exhibited lower DiFMUP phosphatase activity than recombinant PP1 (Fig 4.6 A). However, I-1^P inhibited both recombinant and native PP1 with similar IC₅₀ values (12 and 16 nM, respectively; Fig 4.6 B). Western blot analysis revealed that a low amount (0.004 U) of both recombinant and native PP1 did not affect I-1^P, whereas a high amount (1 U) resulted in 100% and ~35% attenuation of I-1 phosphorylation state by recombinant and native PP1, respectively (Fig 4.6 C).

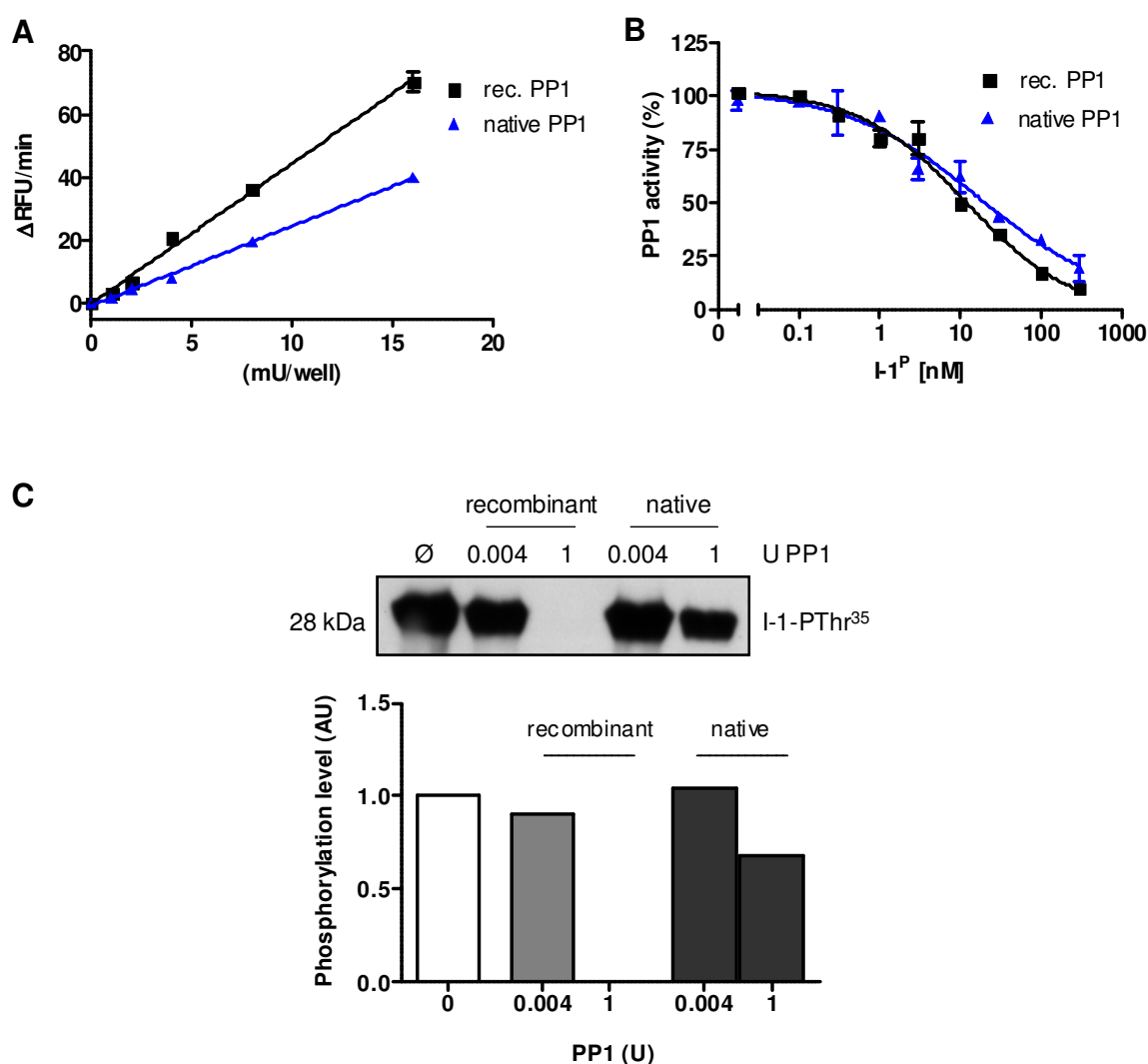


Figure 4.6 Comparison of recombinant versus native PP1. **A)** The hydrolysis rates of 50 μM DiFMUP were monitored in the presence of various concentrations of recombinant (rec.) or native catalytic subunit of PP1. The r^2 were 0.99 for both enzymes. **B)** Inhibition-

concentration curves of I-1^P in the presence of 0.004 U either rec. PP1 or native PP1. Mean±SEM of n=3. **C)** PP1-mediated dephosphorylation of I-1^P. Western blot and statistical analysis demonstrated the effects of different amounts (0.004 U and 1 U) of rec. PP1 versus native PP1 on the phosphorylation state of I-1, using phospho-specific antibodies.

4.2 Investigation of PP1-I-1 interactions using mutant I-1 proteins

Earlier studies implicated the essential role of I-1 N-terminus for its inhibitory activity toward PP1 (Endo et al. 1996; Huang et al. 1997). In current work, we investigated the critical role of the N-terminal domain of I-1 on the physical interaction with PP1 by mutant I-1 proteins. Site directed mutagenesis was performed to generate I-1 Δ KIQF by deletion of the ⁹KIQF¹² motif, I-1_{KIQ/RLN} by replacement of ⁹KIQ¹¹ by RLN, and I-1_{R/A} via substitution of positive charged arginines (³⁰RRRR³³) by uncharged alanines (Fig 4.7 A). The WT I-1 plasmid (pGEX-2T-I-1) was used as template and mutations were induced using primers described in Tab 2 9.1. DNA Sequencing confirmed the achievement of mutagenesis. Finally, GST-tagged mutant proteins were expressed in bacteria and purified as described for WT I-1 (Fig 4.7 B). PKA phosphorylation was carried out as described before (4.1) and phosphorylation levels of the proteins were evaluated by Western blot analysis using phospho-specific antibody. Interestingly, there was no phosphorylation signal with I-1_{R/A}, whereas all other mutant proteins were phosphorylated similar as the WT protein (Fig 4.7 C).

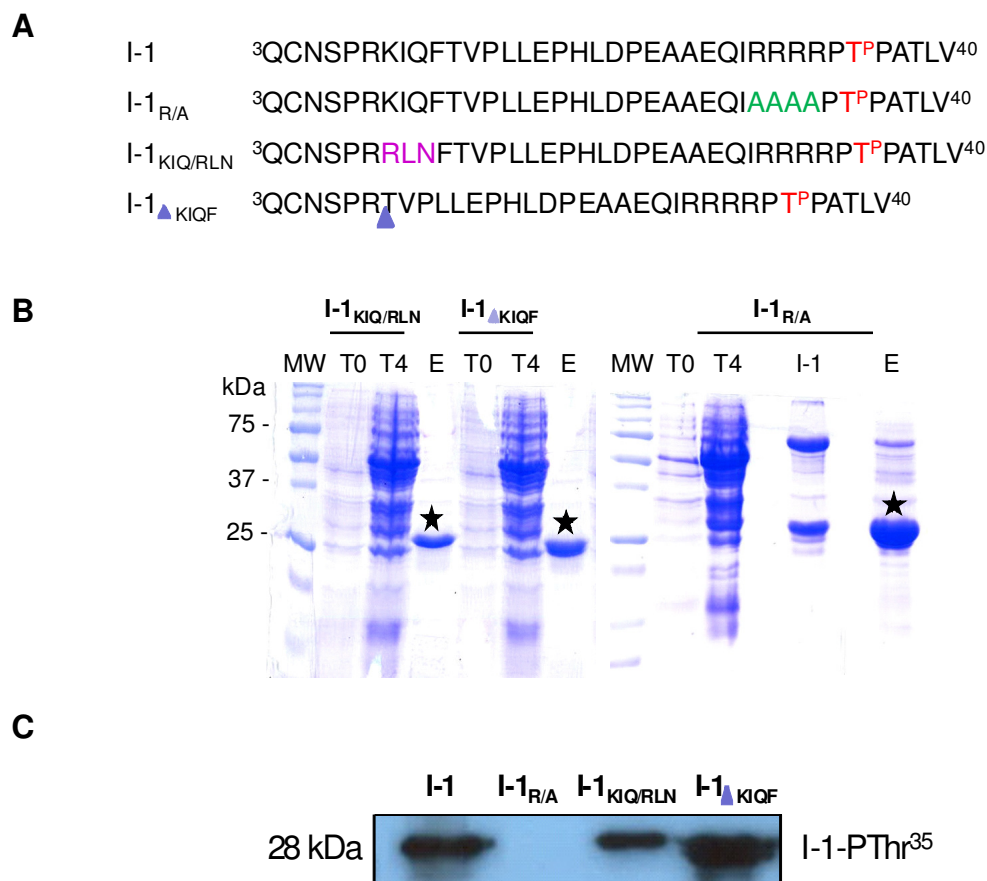


Figure 4.7 Generation and phosphorylation of I-1 mutant proteins. **A)** Sequences of WT and mutant I-1 proteins. **B)** Coomassie stains of the mutant proteins after bacterial expression. T0 and T4 are the times before and after protein generation induction by bacteria. The eluted proteins (28 kDa) are signed with stars. **C)** PKA phosphorylation of WT and mutant I-1 proteins were investigated by Western blot analysis using I-1 phospho-specific antibodies.

The binding affinities of WT and mutant I-1 proteins with PP1 were analyzed using surface plasmon resonance (SPR) measurements by the Biacore™ system. Biotinylation of I-1 proteins on Cys¹¹⁴ and Cys¹⁴⁷ were introduced to allow protein binding to the sensor chip via biotin-streptavidin interaction. The biotin-conjugated proteins were phosphorylated by PKA and immobilized on a streptavidin-coated sensor chip.

Recombinant PP1 was added to the immobilized proteins, resulting in an increased resonance. After reaching its equilibrium state, PP1 was washed out and its dissociation from the I-1 complexes was monitored.

From the dissociation curves of I-1^P versus I-1, at different PP1 concentrations, the K_a and K_d rate constants were obtained and from the ratio of K_d/K_a , equilibrium

constants (K_D) was calculated (Fig 4.8). The obtained K_D value for PP1 interaction with I-1^P (~0.2 nM) was ~2400-fold lower than that for I-1 (470 nM) indicating a considerable higher binding affinity to PP1 than non-phosphorylated I-1, which is depicted in the sensorgram (Fig 4.8).

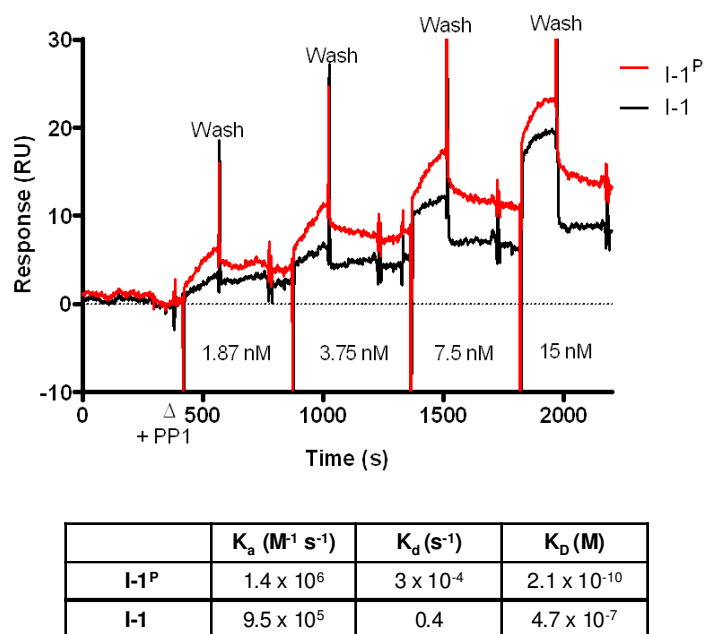


Figure 4.8 Surface plasmon resonance analysis of I-1 vs. I-1^P binding to PP1. The curves represent the applied concentrations of recombinant PP1 (1.87, 3.75, 7.5, 15, 30 nM) to immobilized I-1 and I-1^P. The values of association kinetic rate (K_a) and dissociation kinetic rate (K_d) were obtained from fitting to the corresponding curves.

Comparison of binding affinities of the mutant I-1 proteins was performed in the presence of a single concentration of PP1. I-1^P_{KIQ/RLN} demonstrated 1.4-fold lower binding signal compared to I-1^P. However, the binding signals of both I-1_{R/A} and I-1^P_{ΔKIQF} were abolished, similar to the non-phosphorylated I-1 (Fig 4.9 A-B).

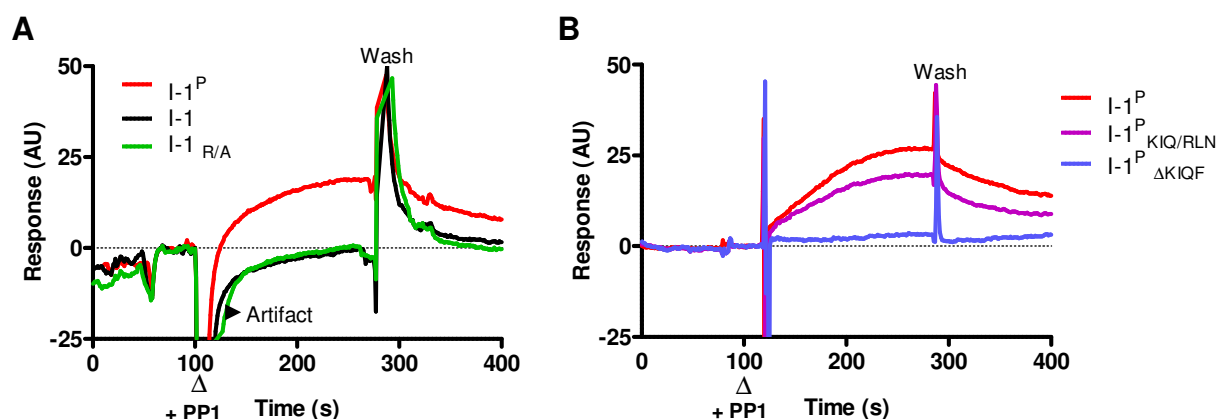


Figure 4.9 PP1 binding abilities of WT versus mutant I-1 proteins. **A)** The kinetic properties of 3 nM PP1 injected to I-1 (black), I-1^P (red), I-1_{R/A} (green), and **B)** 1,78 nM PP1 to I-1^P, I-1^P_{KIQ/RLN} (violet) and I-1^P_{ΔKIQF} (blue) were depicted on sensorgram. The time point of PP1 injection is noted on the graph. AU = arbitrary unit.

The inhibitory effects of the mutant I-1 proteins on PP1 activity were analyzed in the fluorescence assay. The concentration-inhibition curves for WT and mutant demonstrated a 7.2-fold lower inhibitory effect of I-1^P_{KIQ/RLN} than I-1^P (IC₅₀ values were 280 nM and 39 nM, respectively), whereas the highest inhibitory effect of I-1_{R/A} and I-1^P_{ΔKIQF} were 46% and 30%, respectively (Fig 4.10).

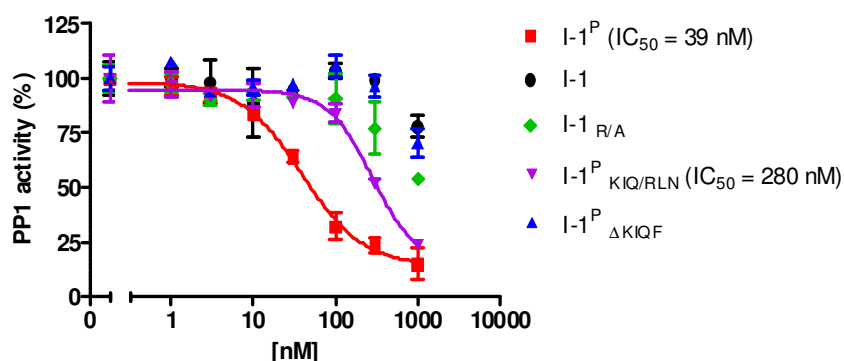


Figure 4.10 Inhibitory effects of WT versus mutant I-1 on PP1 activity. PP1 activities were measured after preincubation with various concentrations of I-1, I-1^P, I-1_{R/A}, I-1^P_{KIQ/RLN} and I-1^P_{ΔKIQF}. The activity of PP1 without inhibitors was considered as 100%. The data represent mean±SD of n=3.

These data collectively indicated that both N-terminal KIQF motif and phosphothreonine-35 are essential for I-1 binding to PP1 and subsequently inhibiting the PP1 activity. The role of RRRR motif in PP1/I-1 interaction showed to be correlated with PKA phosphorylation of Thr³⁵.

4.3 Investigation of I-1 peptides for PP1-I-1 interaction inhibition

Another strategy to elucidate PP1-I-1 binding sites was to employ small peptides derived from the I-1 protein. Therefore, based on the previous findings, we studied peptides containing critical motifs for PP1-I-1 interactions (Goldberg et al. 1995; Endo et al. 1996; Terrak et al. 2004; Fig 4.11).

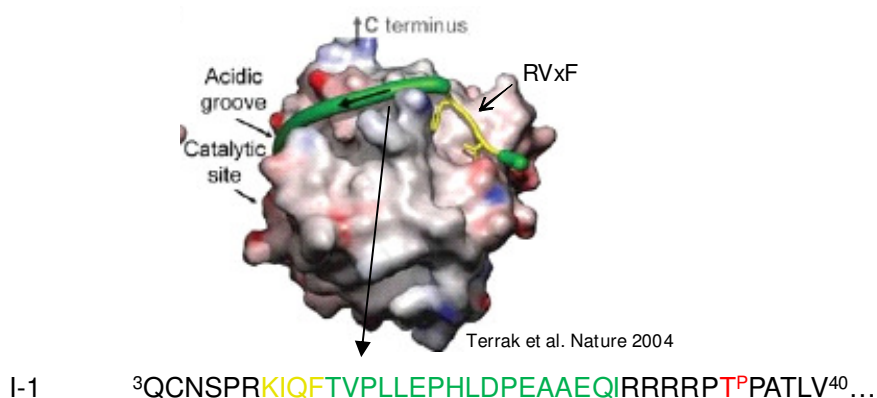


Figure 4.11 Model illustrating I-1 potential interactions with PP1 through the KIQF motif and in the acidic groove.

4.3.1 Characterization of I-1 peptides

Peptides with the sequences ⁶SPRKIQFTV¹⁴, ¹⁹PHLDPEAAEQI²⁹ and ²⁵AAEQIRRRR³³ were examined in both the colorimetric and fluorescence assays. The phosphatase activities were measured after preincubation of these peptides with the PP1-I-1 holoenzyme. The peptide containing the KIQF motif (I-1^{SPRKIQFTV}) antagonized the activities of both I-1^{SP} and I-1^P with IC₅₀ values of 27 μM and 3 μM, respectively (Fig 4.12 A-B). In contrast, the peptides containing the four Arg before the phosphothreonine at 35, ²⁵AAEQIRRRR³³ and the ¹⁹PHLDPEAAEQI²⁹ peptide did not affect I-1 inhibitory activity.

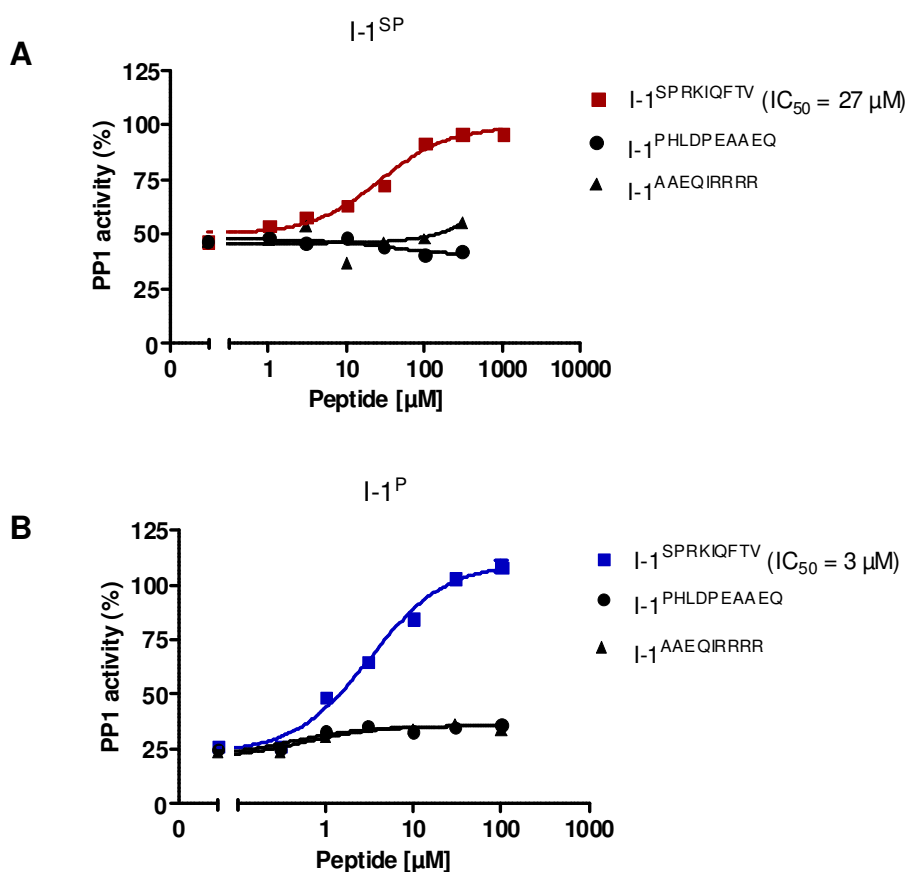


Figure 4.12 The effects of I-1 peptides on I-1 inhibitory activities in the colorimetric and fluorescence assays. Concentration-response curves of $I-1^{\text{SPRKIQFTV}}$, $I-1^{\text{PHLDPEAAEQ}}$ and $I-1^{\text{AAEQIRRRR}}$ in **A)** the pNPP-based assay containing PP1- $I-1^{\text{SP}}$ complex and **B)** the DiFMUP-based assay containing PP1- $I-1^{\text{P}}$ complex. The data are presented as mean of $n=2$ or $\text{mean} \pm \text{SEM}$ of $n=3$.

In order to test the specificity of $I-1^{\text{SPRKIQFTV}}$ for PP1-I-1 interaction, the effect of this peptide was examined in the presence of other PP1 inhibitors including I-2 and calyculin A. The peptide was able to antagonize I-2 activity concentration-dependently with an IC_{50} value of 190 μM , whereas the effects of calyculin A, up to 1000 μM , remained unchanged (Fig 4.13).

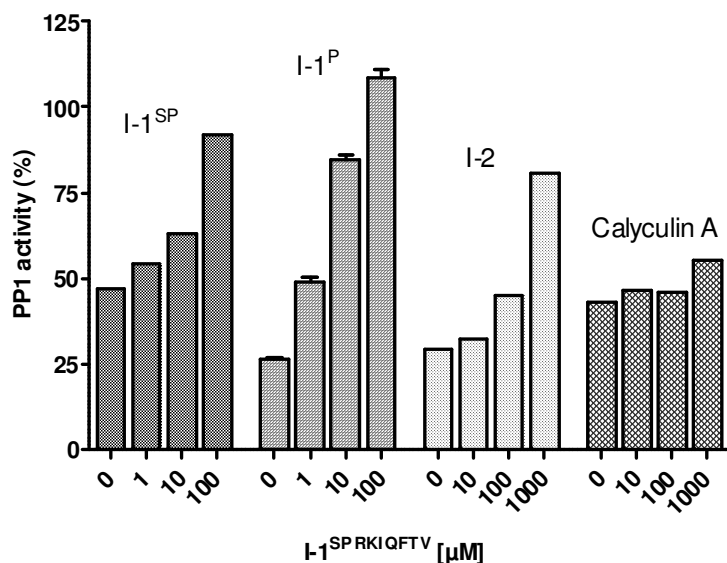


Figure 4.13 Antagonizing effects of I-1^{SPRKIQFTV}. PP1 activities were measured after preincubation of different concentrations of I-1^{SPRKIQFTV} with 700 nM I-1^{SP}, 50 nM I-1^P, 10 nM I-2 and 10 nM calyculin A. Mean of n=2, mean±SEM of n=3.

A peptide with a scrambled sequence (I-1^{KSIPRQTFV}) was applied to test for sequence specificity. The effects of I-1^{SPRKIQFTV} and I-1^{KSIPRQTFV} on PP1 activity and on the PP1/I-1^P holoenzyme were examined in the fluorescence assay. I-1^{SPRKIQFTV} inhibited the PP1-I-1^P interaction, without affecting directly PP1 activity. The scrambled peptide did not change I-1^P inhibitory activity, but had a minor effect on PP1 activity itself (Fig 4.14). It should be noted that the effect of I-1^P and I-1^{SP} on PP1, as the basal condition for testing effects of peptides, varied between assays (compare Fig 4.13 [~75% inhibition] and Fig 4.14 [40% inhibition]).

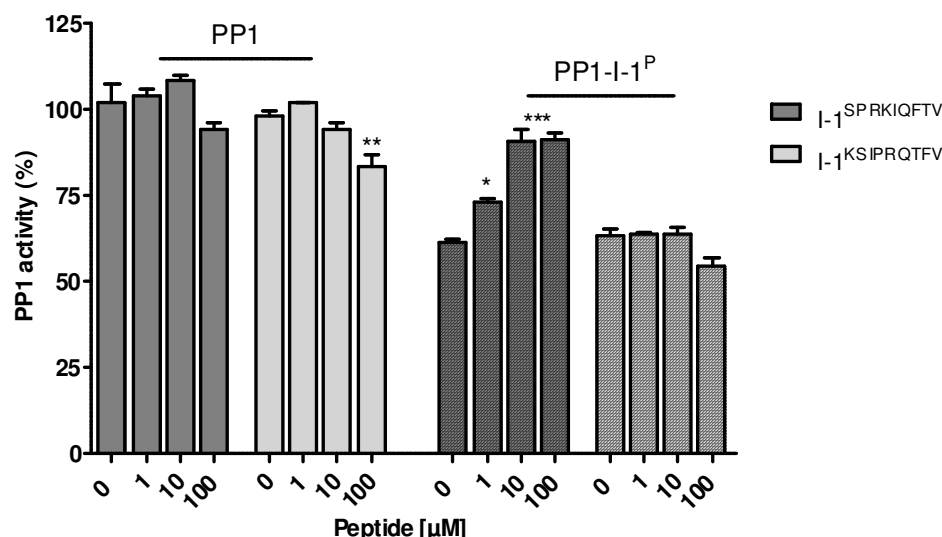


Figure 4.14 I-1^{SPRKIQFTV} versus a scrambled control peptide (I-1^{KSIPRQTFV}). The activities of PP1 were measured after preincubation of different concentrations of I-1^{SPRKIQFTV} or I-1^{KSIPRQTFV} with either 0.002 U PP1c or PP1 complex with 50 nM I-1^P. Mean±SEM of n=3-4. *P<0.05, **P<0.01, ***P<0.001 without vs. with peptide, from one-way ANOVA.

Here, we showed that only the peptide containing KIQF was able to compete with I-1 inhibitory effect either phosphorylated or thiophosphorylated. I-1^{KSIPRQTFV} could also affect the inhibitory effect of I-2 in higher concentrations than I-1, without affecting the inhibitory effect of chemical toxins such OA (data not shown) and calyculin A.

4.3.2 Effects of I-1^{SPRKIQFTV} in cardiac cells

A poly-Arg chain consisting 11 arginines was fused to the C-terminus of I-1^{SPRKIQFTV} and I-1^{KSIPRQTFV} to make them cellular permeable for biological investigations. A FITC-labeled form of the modified I-1^{SPRKIQFTV} was used to monitor the intracellular localization (Fig 4.15).

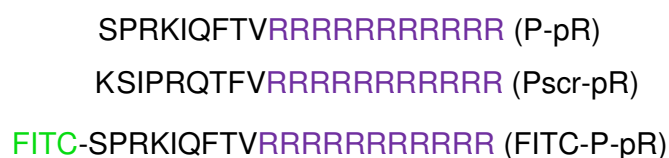


Figure 4.15 The sequences of poly Arg modified peptides.

Engineered heart tissues (EHTs) represent an appropriate 3D model for functional and biological investigations (Hansen et al. 2010). Therefore, we aimed at studying the effects of our modified peptides in EHTs from neonatal rat cardiomyocytes.

Fluorescence microscopy of living EHTs after incubation with 10 μ M FITC-P-pR demonstrated green EHTs (Fig 4.16 A). However, as immunohistological staining was performed to detect cellular localization, the confocal microscopy revealed complete lack of peptide internalization in the cardiomyocytes (Fig 4.16 B). Further optimizations of the conditions e.g. medium \pm serum/BDM or incubation temperature/time, did not lead to intracellular localization of the peptide within the cardiomyocytes.

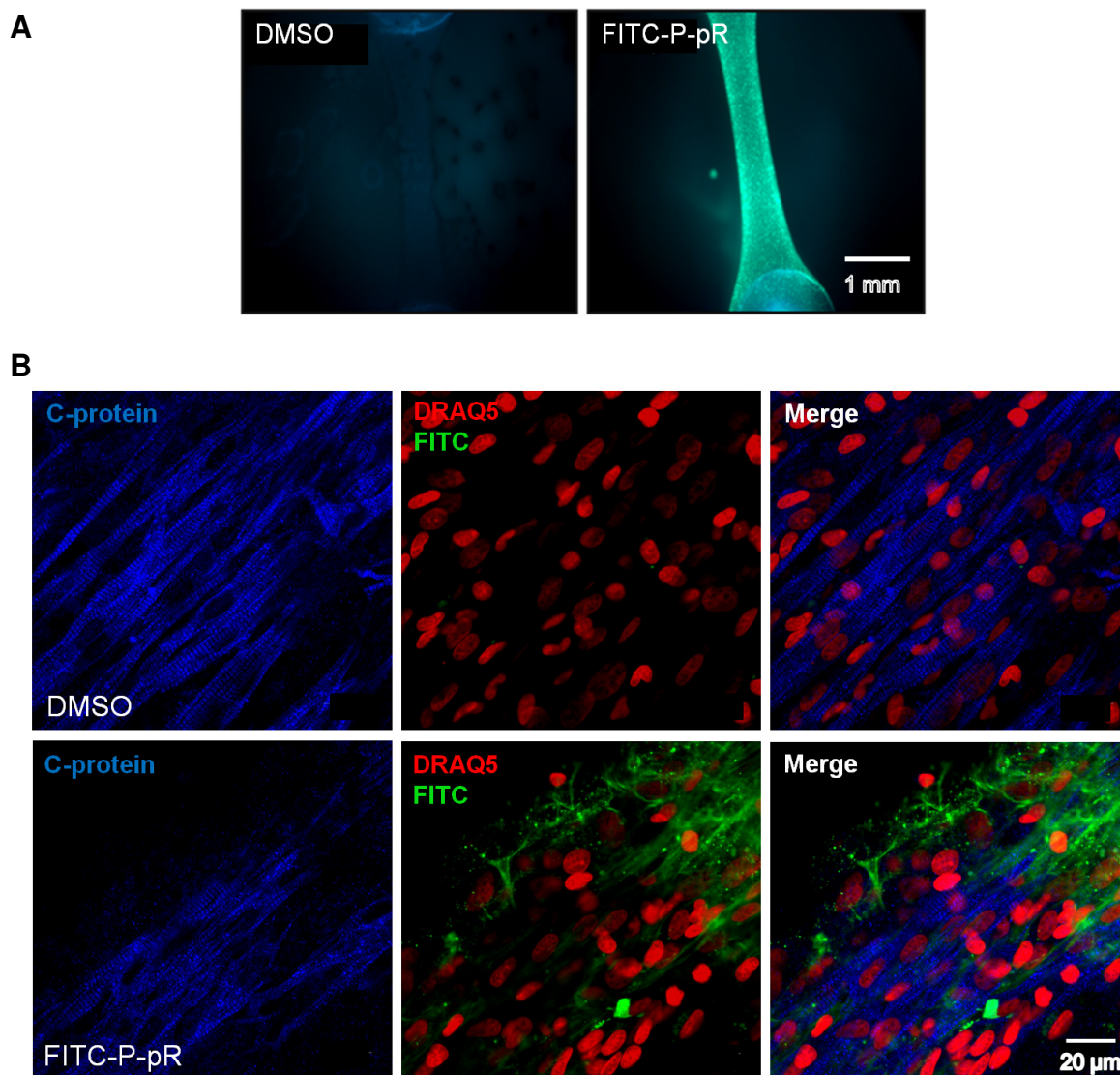


Figure 4.16 lack of uptake of FITC-P-pR into cardiomyocytes in EHTs. **A)** Fluorescence microscopic imaging of EHTs incubated with either DMSO or FITC-P-pR for 60 min, at 37 °C. Magnification x2.5. **B)** Confocal laser microscopy of immunostained EHTs after treatment with DMSO (upper panel) or FITC-labeled P-pR (lower panel). Antibodies against C-protein (MyBP-C) were used to detect sarcomeric structure of cardiomyocytes (blue) and DRAQ5 for the nuclei (red). Magnification x63.

Due to inefficient uptake of the peptide into the EHTs, we employed adult mouse cardiomyocytes (AMCMs) for investigation of functional effects. The cells were incubated with either 0.1% DMSO or 3 and 10 μ M P-pR for video-optical measurements using the IonOptix system. In parallel, some cells were incubated with 3 μ M FITC-P-pR to monitor uptake. Fluorescence confocal microscopy of living AMCMs demonstrated a quite low uptake rate of the intact cells (<20%), but a lot of green dead cells (Fig 4.17 A). Contractile parameters were investigated under basal

condition and after β -adrenergic stimulation with isoprenaline. The analyses showed that isoprenaline (10 nM) increased sarcomere shortening amplitude in DMSO treated cells, whereas this effect was abolished in the cells preincubated with 3 μ M peptide P-pR (Fig 4.17 B). Interestingly, cells treated with 10 μ M P-pR showed severe arrhythmia after isoprenaline addition that contractility measurements were not possible.

Nevertheless, due to suboptimal uptake of the FITC-labeled peptide, evaluation of the effect of the peptide in AMCMs remained unclear.

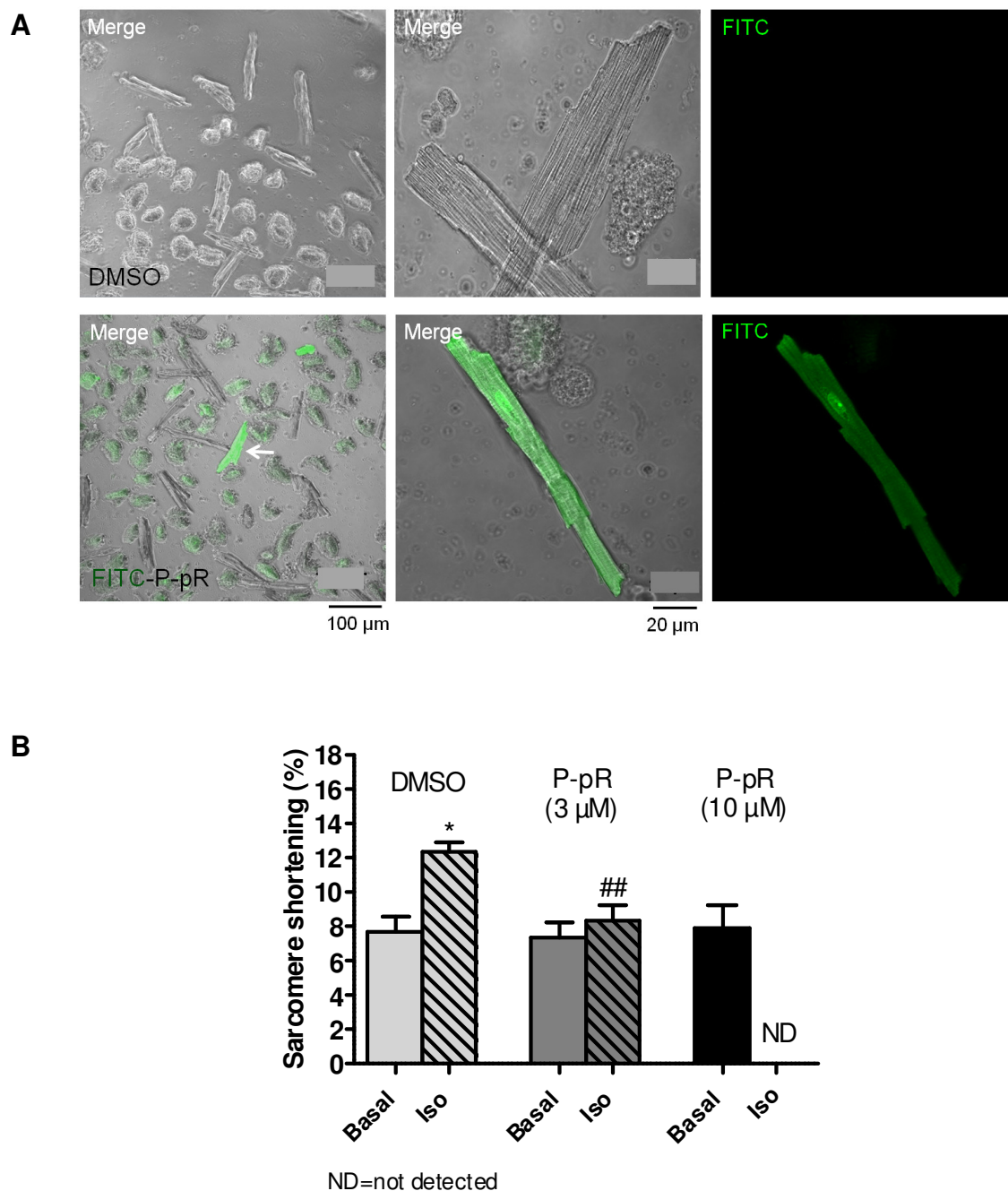


Figure 4.17 Investigation of poly Arg modified peptides in AMCMs. A) Fluorescence microscopic views of living AMCMs after treatment with DMSO (upper panel) or FITC-labeled (green) P-pR (lower panel). The white arrow shows two intact cells with intracellular peptide. **B)** The effect of P-pR on the contractility of AMCMs. Sarcomere shortenings under basal condition and after isoprenaline addition were analyzed in the treated cells with DMSO, 3 and 10 μ M P-pR for 2 h at 37 °C. The presented data are mean \pm SEM of n=7. *P<0.05 vs. + Iso, one-way ANOVA. ##P<0.01 vs. DMSO + Iso, two-way ANOVA.

Next, we analyzed the effect of P-pR in neonatal rat cardiomyocytes (NRCMs). Immunohistological staining was performed after treatment of the cells with DMSO or

3 μ M FITC-P-pR. Confocal microscopic images confirmed efficient internalization of the peptide into the cardiomyocytes (Fig 4.18 A).

The effects of P-pR on isoprenaline-induced phosphorylation levels of PLB on Ser¹⁶ and Thr¹⁷ were investigated by Western immunoblotting using antibodies against PLB-PSer¹⁶ and PLB-PThr¹⁷, respectively. The cells were treated with DMSO (0.1%) as vehicle control and Pscr-pR (10 μ M) as peptide control and 10 μ M P-pR. After isoprenaline (10 nM) treatment for 5 min, phosphorylation levels of PLB on Ser¹⁶ were significantly increased in cells treated with DMSO and Pscr-pR, while P-pR effectively (with respect to the both controls) attenuated the isoprenaline induced effect (Fig 4.18 B).

Our findings demonstrated that poly-Arg chain (11 Arg) did not yield efficient uptake of the peptide in EHT and AMCMs. However, the effective uptake of the peptide in NRCMs resulted in decreased phosphorylation of PLB at Ser¹⁶ after β -adrenergic stimulation.

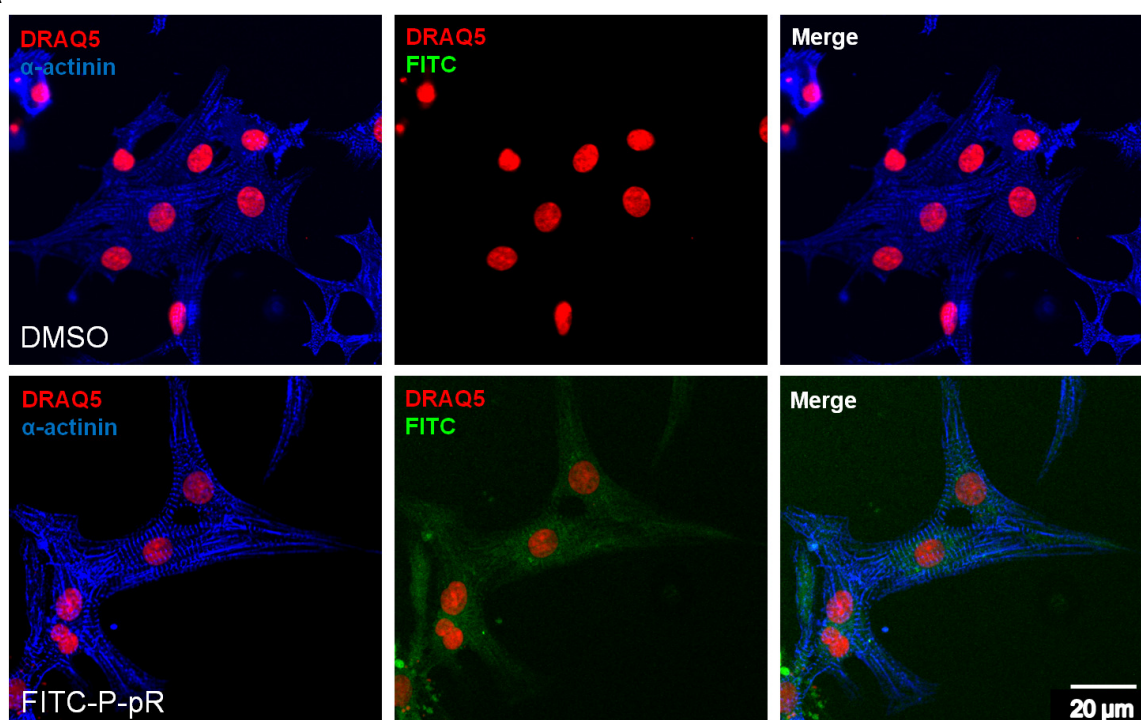
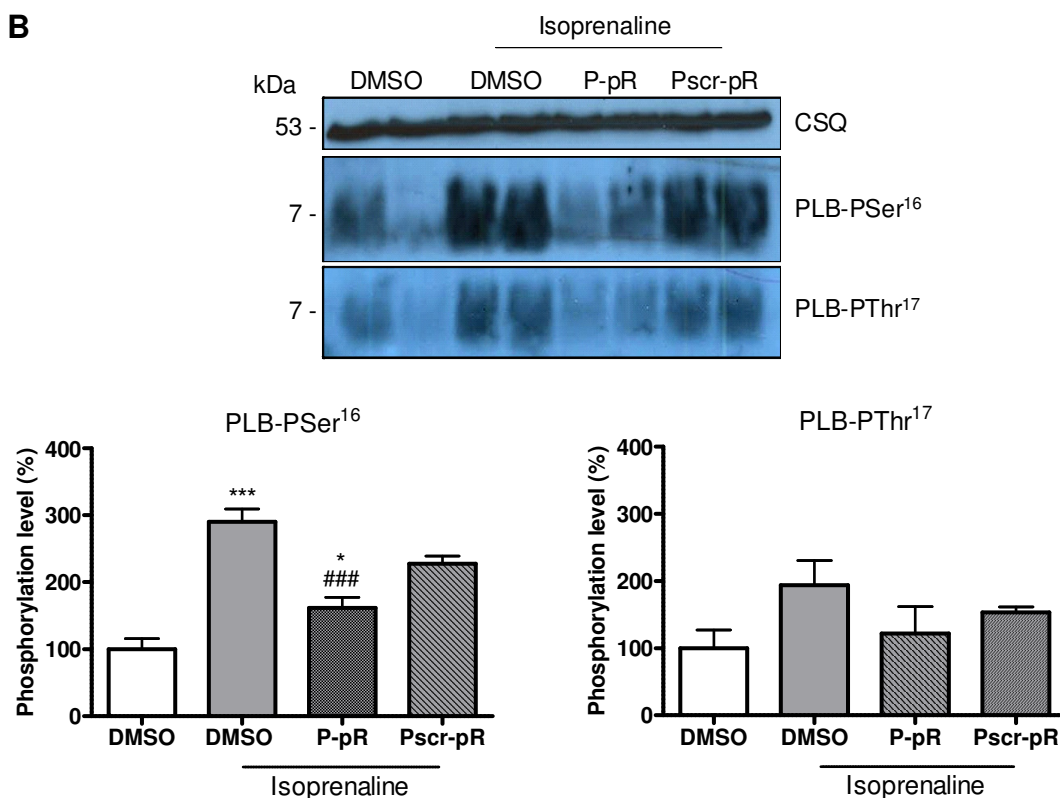
A**B**

Figure 4.18 Investigation of poly Arg modified peptides in NRCMs. A) Immunohistological staining of NRCMs with DMSO (upper panel) or FITC labeled (green) P-pR (lower panel). α-actinin and DRAQ5 staining show the sarcomeric structure of cardiac cells (blue) and nuclei (red), respectively. Magnification x63. **B)** Western blot and statistical

analysis demonstrate the isoprenaline-dependent phosphorylation rates of PLB on Ser¹⁶ (left panel) and Thr¹⁷ (right panel) after treatment with DMSO, 10 μ M P-pR and 10 μ M Pscr-pR. Calsequestrin (CSQ) was used as a marker for the cardiomyocytes. Densitometry analyses were performed after normalization of signals from PLB-PSer¹⁶ and PLB-PThr¹⁷ to CSQ. The presented data are mean \pm SEM of n=3-6. ***P<0.001 vs. DMSO, ###P<0.001 vs. DMSO + Iso, *P<0.05 vs. Pscr-pR, one-way ANOVA.

4.4 Screening of small molecules

Compound screening was performed by fluorescence-based assay due to its advantages over the colorimetric-based assay. The reactions were performed first in a 96-well format with 220 μ l end-volume, and were then minimized to 100 μ l in 384-well plate. A primary screen was performed after preincubation of PP1-I-1 mixture with a single concentration (10-22 μ M) of a compound library. Thus, the hydrolysis rates of DiFMUP were monitored in the presence of PP1 and I-1 preincubated with either DMSO or the indicated compounds (Fig 4.19). Compounds that increased PP1 activity more than 50% of control were considered as hits. Kinetic measurements facilitated the distinction between auto-fluorescent compounds and I-1 inhibitors (~10% of all). Among the first 600 compounds, none of them showed I-1 inhibitory effect, which was not unexpected due to the low number of screened compounds.

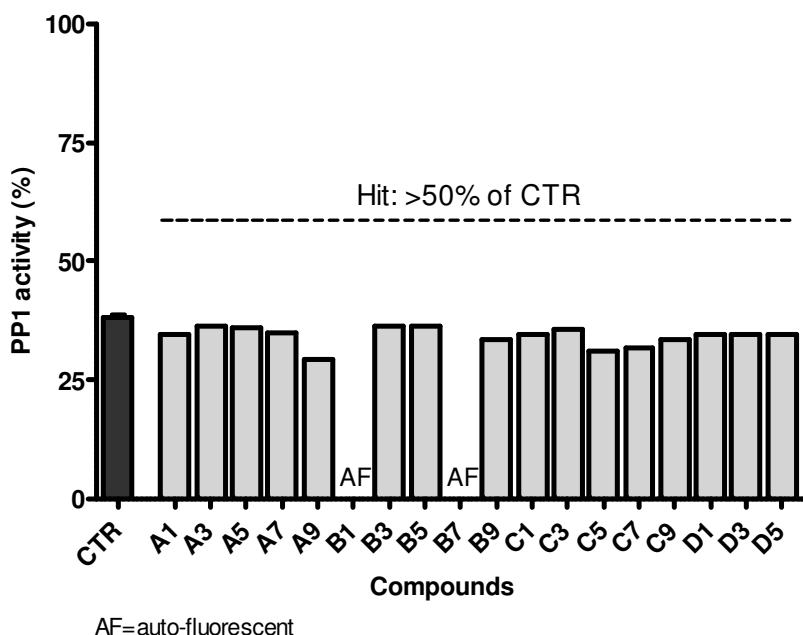


Figure 4.19 Representative compound screen using the fluorescence-based assay. PP1 activities were measured after preincubation of a single concentration of different compounds with PP1-I-1^P complex. The CTR contained 0.004 U PP1 and 50 nM I-1^P. The activity of PP1 alone was considered as 100%. The potential hits were recognized by 50% higher phosphatase activity than CTR. AF referred to the auto-fluorescent compounds with non-detectable activities. Mean (CTR)±SEM of n=5, mean (compounds) of n=2.

4.4.1 Screening of *in silico* selected compounds

Virtual screening was performed to find structures with high affinity to PP1 molecular surface, using available crystal structures of the PP1 catalytic subunit. We first focused on the acidic groove of PP1, which is proposed to be crucial for PP1/I-1 interaction (Fig 4.20 A; Goldberg et al. 1995, Terrak et al. 2004). The “AutoDock” program was used for the screening process providing a flexible ligand-protein docking. Subsequently, 100,000 compounds from the ZINC database were docked with different conformations of five amino acids lying within the acidic groove (Fig 4.20 B). Evaluation of various conformations was performed using the AutoDock scoring function. The central criteria for scoring were localization and interaction of an effective ligand within the acidic groove through at least one H-bond. Thus, compounds with scorings higher than 9.9 were re-docked with the acidic groove for more accuracy and then selected for screening in the phosphatase assay.

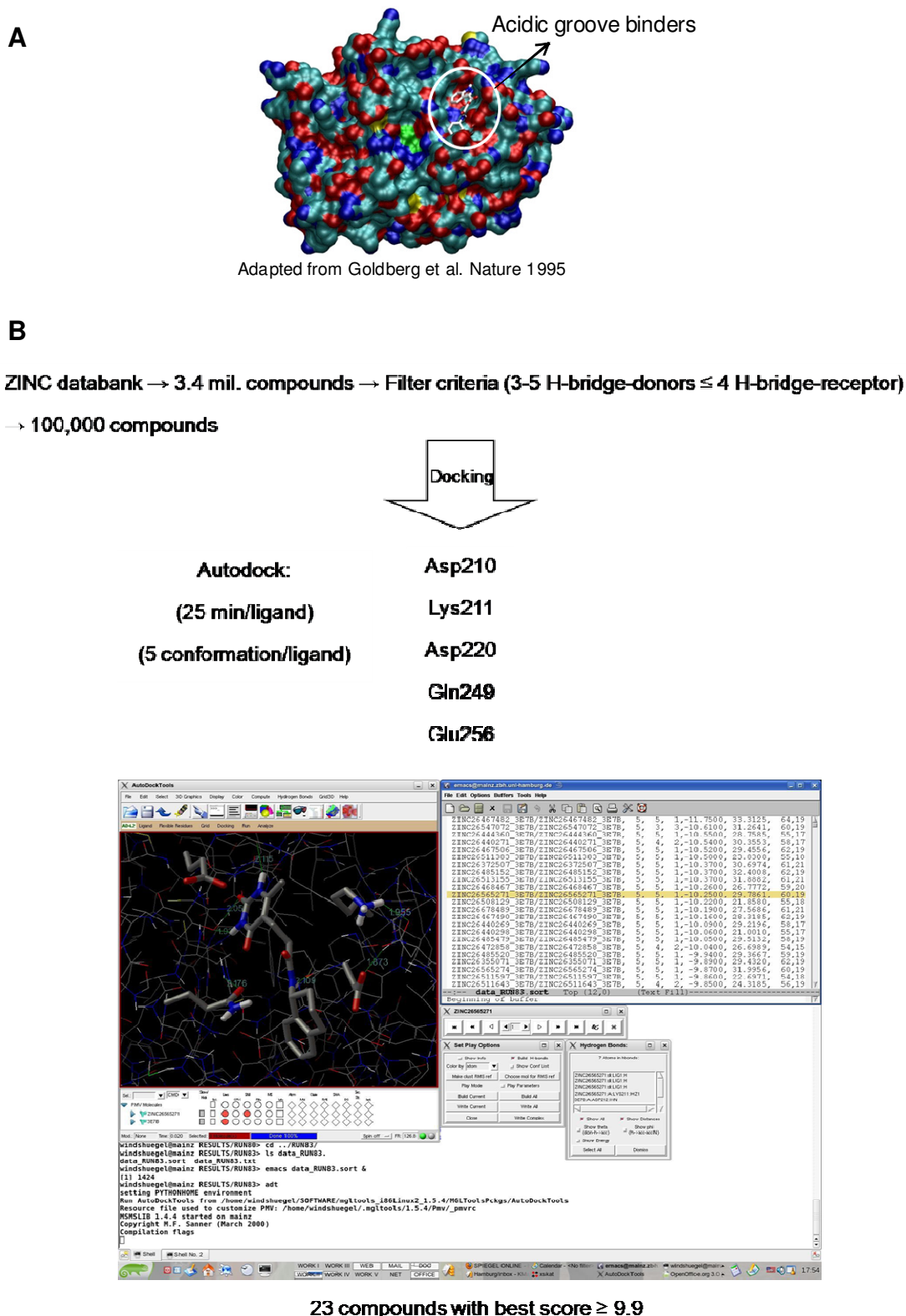


Figure 4.20 Scheme for virtual screening of compounds with potential binding to PP1 within the acidic groove. A) A compound positioned in the acidic groove of PP1 molecular surface is marked with a white circle. **B)** From the ZINC database, 3.4 million lead-like compounds were filtered through their hydrogen bond donors and receptors (≥ 4). The structures of nearly 100,000 restricted compounds were docked with 5 flexible amino acids

lying in the acid groove of PP1 using AutoDock program. Every ligand docking took 25 min generating 5 flexible conformations. All conformations were analyzed by AutoDock scoring program and ligands with scores ≥ 9.9 were again docked with acidic groove of PP1. This time for a precise docking, 20 conformations were analyzed, which took 12 h for each compound. Finally 23 ligands with best scores were nominated for further experiments.

Due to the limitations of compounds supply, from 23 selected ligands, 13 compounds have been experimentally investigated so far. The effects of these compounds on PP1 directly or on the PP1-I-1^P complex were examined in the fluorescence assay (Fig 4.21). Two compounds, D7 and G3, showed ~60% increase of PP1 activity compared to PP1-I-1^P control, but they also increased PP1 activity directly by ~10% and ~30%, respectively. Concentration-response curves could not confirm the inhibitory activity of D7 and G3 against I-1^P (data not shown).

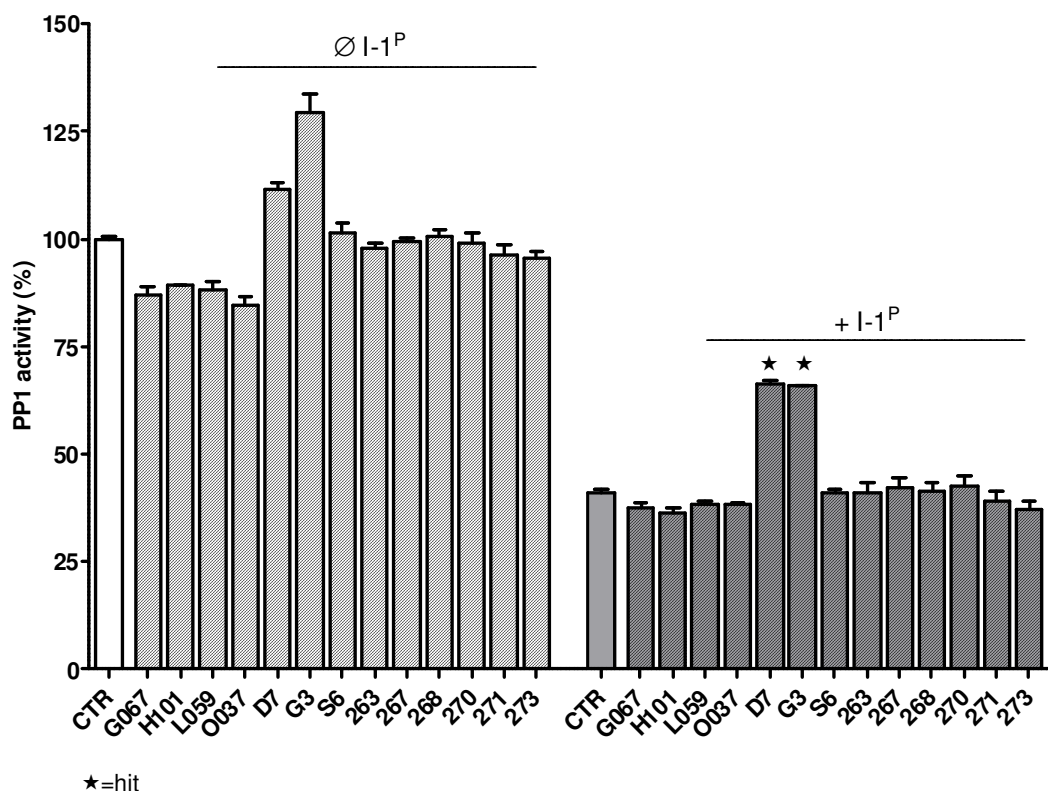


Figure 4.21 Screening of *In silico* selected compounds in the fluorescence assay. The hydrolysis rates of DiFMUP were monitored after preincubation of either PP1c (0.004 U) or PP1-I-1^P (50 nM I-1^P) with 10 μ M of selected compounds with acidic groove binding possibility. The obtained hits are signed with star symbols. The presented data are percentage of PP1 activity alone. Mean \pm SD of n=3.

4.4.2 High-throughput screening (HTS)

The high-throughput format enabled us to quickly conduct thousands of measurements in a short time. Collaboration with European ScreeningPort (ESP) allowed the employment of an automated robotic system and a large selection of compound library. For the HTS approach, the assay was miniaturized to a 10 μ l final volume.

4.4.2.1 Determination of Z'-factor for the fluorescence assay

The Z'-factor is a statistic parameter that reflects both the dynamic signal range and standard deviation, thus providing a useful tool for estimation of the quality of assays, particularly for HTS. As shows in Tab 4.1, the Z' value should be between 0.5 and 1. We monitored the fluorescence signals of 64 wells containing buffer without enzyme (blank), PP1 or PP1-I-1^P for 60 min (Fig 4.21 A). The Z' values were calculated between blank and PP1, and between PP1 and PP1-I-1^P complex. The obtained values were higher than 0.5 10 min after initiation of the reaction, for both PP1 (0.74) and PP1-I-1^P (0.67; Fig 4.21 B). This data confirmed the suitability of our fluorescence assay system for HTS and suggested an incubation time between 20-30 min for screening processes to achieve an optimal Z'-value.

Table 4.1 Characterization of the screening assay quality by the value of Z' factor.

Z'-factor value	Structure of assay	Related to screening
1	SD = 0 (no variation), or the dynamic range	An ideal assay
$1 > Z' \geq 0.5$	Separation band is large	An excellent assay
$0.5 > Z' > 0$	Separation band is small	A double assay
0	No separation band, the sample signal variation and control signal variation bands touch	A "yes/no" type assay
< 0	No separation band, the sample signal variation and control signal variation bands overlap	Screening impossible

Zhang et al. 1999

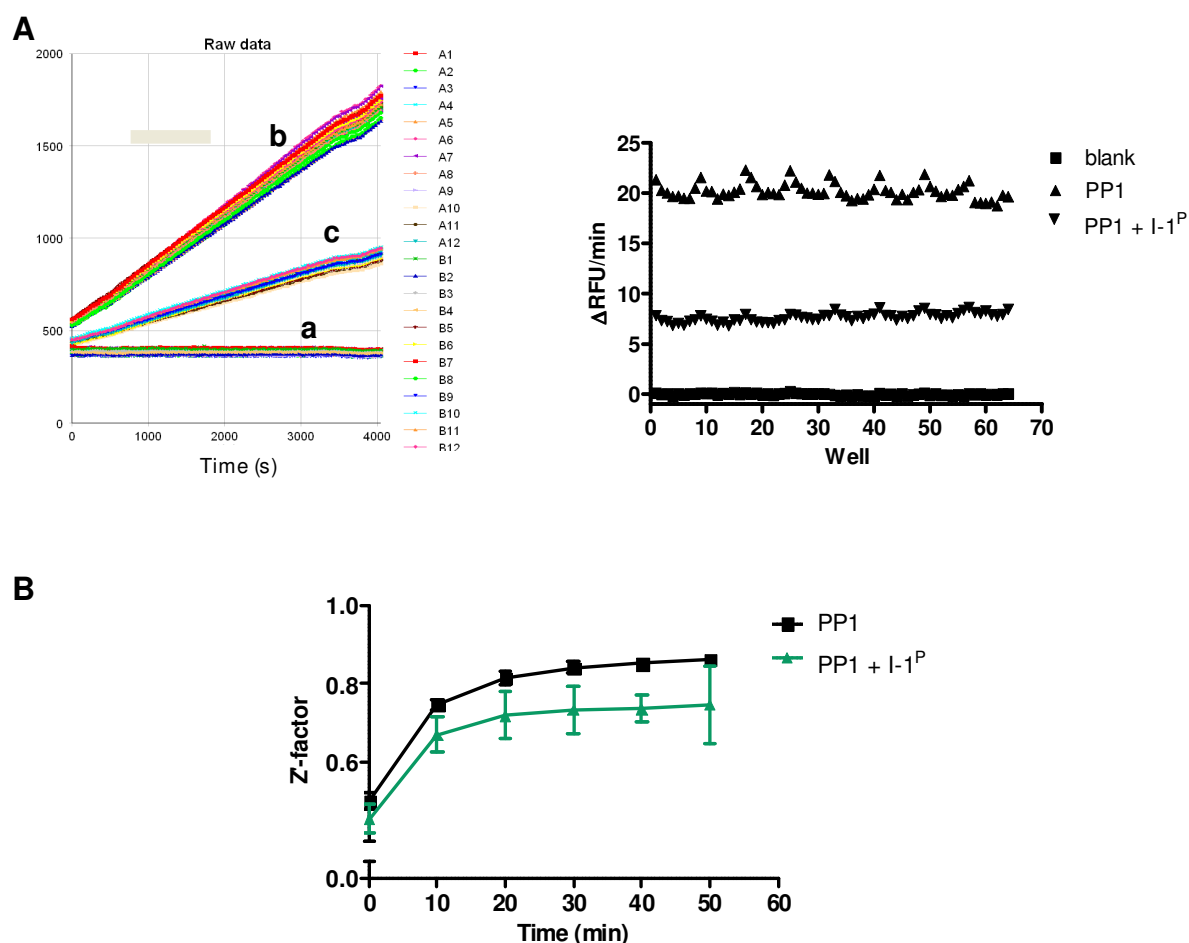


Figure 4.21 Estimation of the Z'-factor. A) Investigation of signal to noise ratio. The raw data of DiFMUP hydrolysis (RFU) in blank 'a, PP1 'b and PP1 + I-1^P 'c, at 30 °C, for ~60 min (left panel). The hydrolysis rates of DiFMUP (Δ RFU/min) were measured for blanks (no enzyme; n=64), PP1 samples (0.004 U; n=64) and PP1-I-1^P samples (0.004 U PP1 + 50 nM I-1^P; n=64). **B)** The estimated Z' values between blank and PP1, and PP1 and PP1-I-1^P were plotted against measurement times. Mean \pm SD, n=128 from two separate experiments.

4.4.2.2 Single-point measurements of HTS

In the first run of HTS, 3560 compounds consisting of FDA approved drugs, natural and drug-like compounds were screened in the DiFMUP-based assay. The compounds (10-20 μ M) were tested in three assays, counter screen (PP1 + DiFMUP + compounds, without incubation), PP1-I-1^P screen (PP1-I-1^P + compounds, 30 min incubation + DiFMUP) and PP1 screen (PP1 + compounds, 30 min incubation + DiFMUP).

A counter screen was performed to identify the interfering compounds with auto-fluorescence or quenching effect. In order to distinguish real signal from artifact, the

compounds were added into the wells containing PP1 after initiation of the reaction and then the fluorescence intensities were measured, immediately (Fig 4.22). Compounds that apparently increased fluorescence intensities 20% over the control were considered as auto-fluorescent compounds. This was true for 14.2% of all the compounds. The quenchers were defined by >20% reduction of fluorescence signals to compare with the signals from PP1 control. About 0.7% of the indicated compounds showed quenching effect. Finally, compounds that demonstrated fluorescence signal similar to PP1 controls were considered as clean compounds (85%).

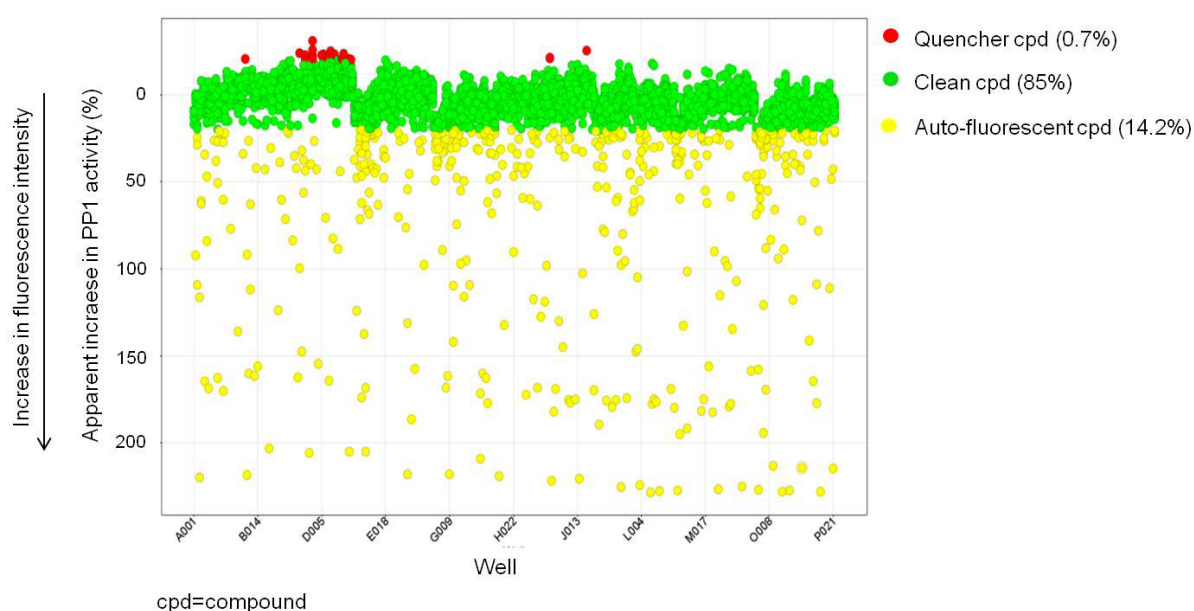


Figure 4.22 The counter screen. The fluorescence intensities were measured in different wells. The compounds (20 μ M) were added after reaction initiation by addition of 5 μ M DiFMUP. The control wells contained only 21.6 pM PP1c (0.002 U).

In the PP1-I-1^P assay, the compounds were examined for their effects of I-1 inhibitory activity. The fluorescence intensities were recorded 30 min after initiation of the reaction. 122 compounds (3.4%) affected PP1 inhibition \geq 50% more than the PP1-I-1^P control (Fig 4.23 A). Among these compounds, 47 compounds that antagonized I-1^P activity between 50-100% (red circle) were considered as I-1 hits. Compounds that showed more than 100% reduction in the PP1 inhibition rate were defined as PP1 activators (Fig 4.23 A). The effects of the indicated compounds on PP1 activity, directly, were investigated in PP1 screen (Fig 4.23 B). 22 compounds (0.6%) were able to inhibit PP1 activity >20%, while they were clean in the counter screen.

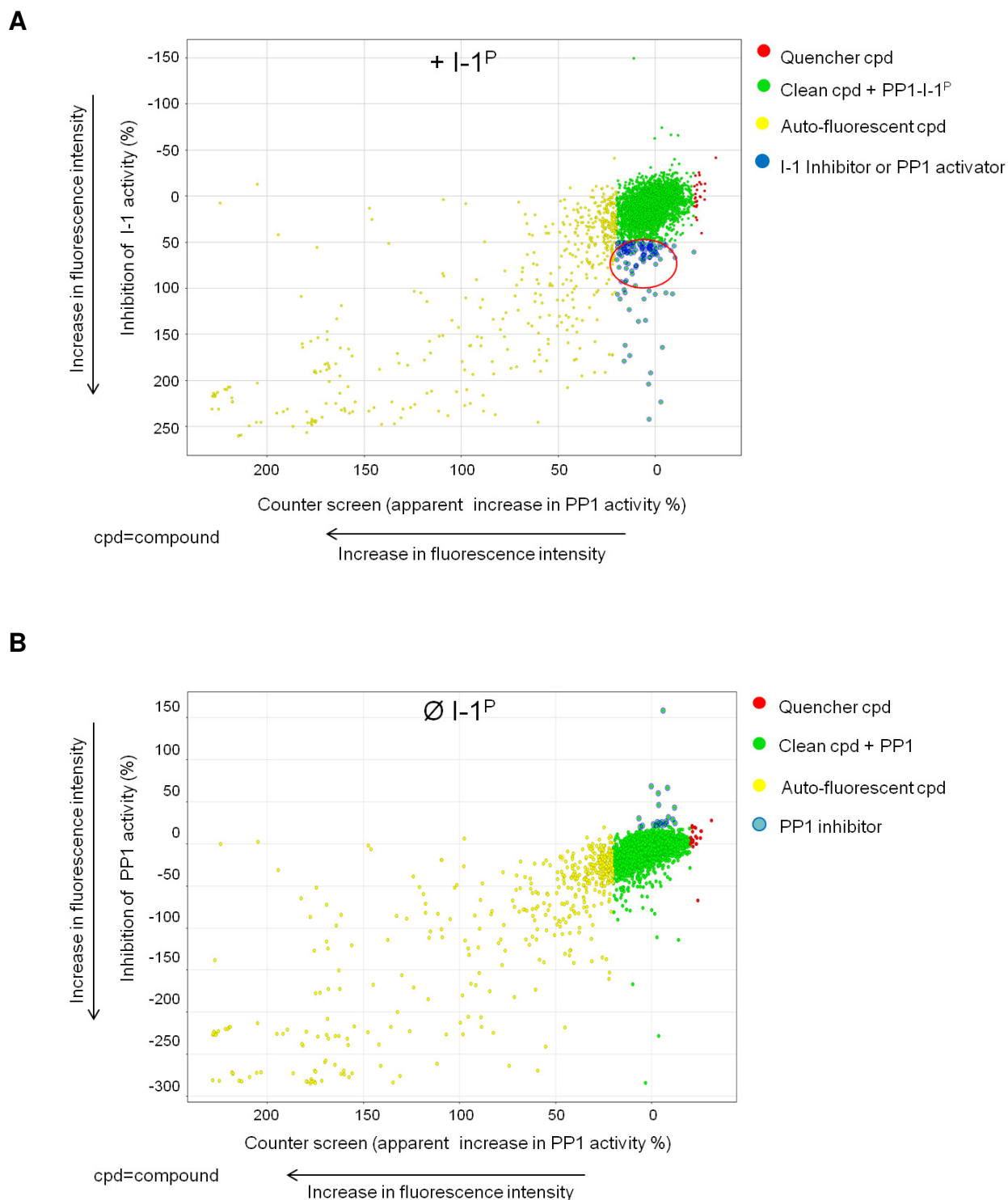


Figure 4.23 Screenings of compounds with single-point measurements. A) I-1^P screen. The compounds were preincubated with PP1-I-1^P complex (21.6 pM + PP1c 30 nM I-1^P) for 10 min prior reaction initiation. The compounds that were clean in counter screen and reduced PP1 inhibition $\geq 50\%$ were considered as either I-1 inhibitors or PP1 activators. The red circle marked the hits with I-1 inhibitory effect. **B)** PP1 screen. The fluorescence signals were measured after preincubation of compounds (20 μ M) with 21.6 pM (0.002 U) PP1c 10 min prior to reaction initiation. The clean compounds in counter screen with $>20\%$ PP1 inhibitory effect were signed as blue dots.

Validation of the hits was performed using the original assay format with increasing concentrations of the selected compounds. Tab 4.2 shows the analyzed data of representative hits. The effects of these compounds were investigated in the presence of PP1-I-1^P or PP1 alone (Fig 4.24 A-B). As positive control, I-1^{SPKIQGTV} was applied in the assays. However, except of ibandronate, none of the selected hits showed significant effects on I-1 or PP1 activities. Ibandronate was able to inhibit PP1 activity, concentration-dependently with an IC₅₀ value of ~3 μ M (Fig 4.24 C). Lack of any confirmed hit for I-1 inhibitory effect indicated of existing of artifacts that could not be recognized by counter screen.

Table 4.2 Representative hits with the obtained values from counter, PP1 and PP1-I-1^P screens.

Name	Counter Screen%	I-1 ^P Inhibition%	PP1 Inhibition%
Ampicillin	-16.2	60.7	-20.6
Florexacin	-16.4	53.4	-10.7
Apramycin	-11.1	61.4	-11.9
Ibandronate	2.5	68.5	6.6
Oxatomide	-6.5	68.9	6.1

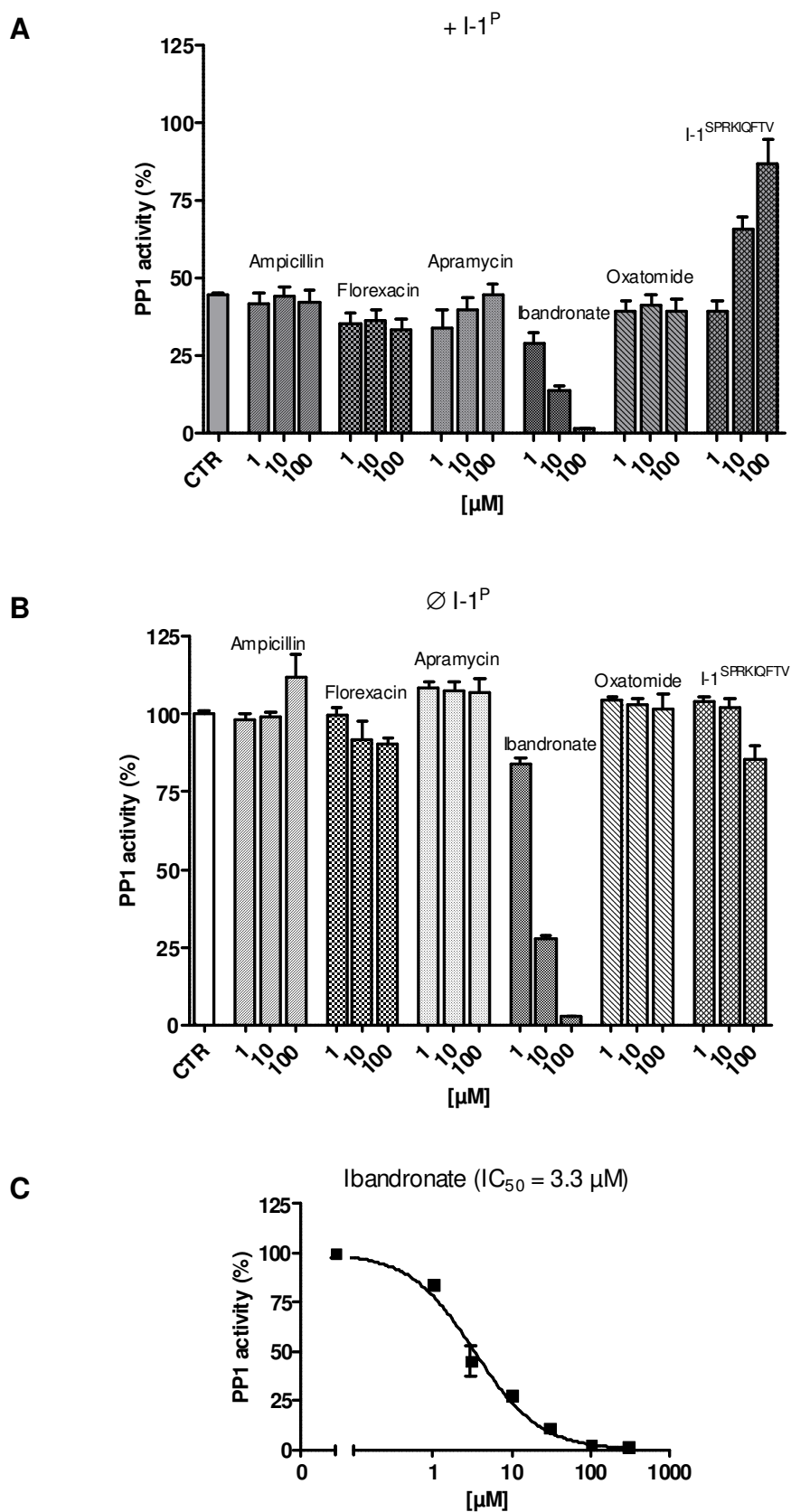
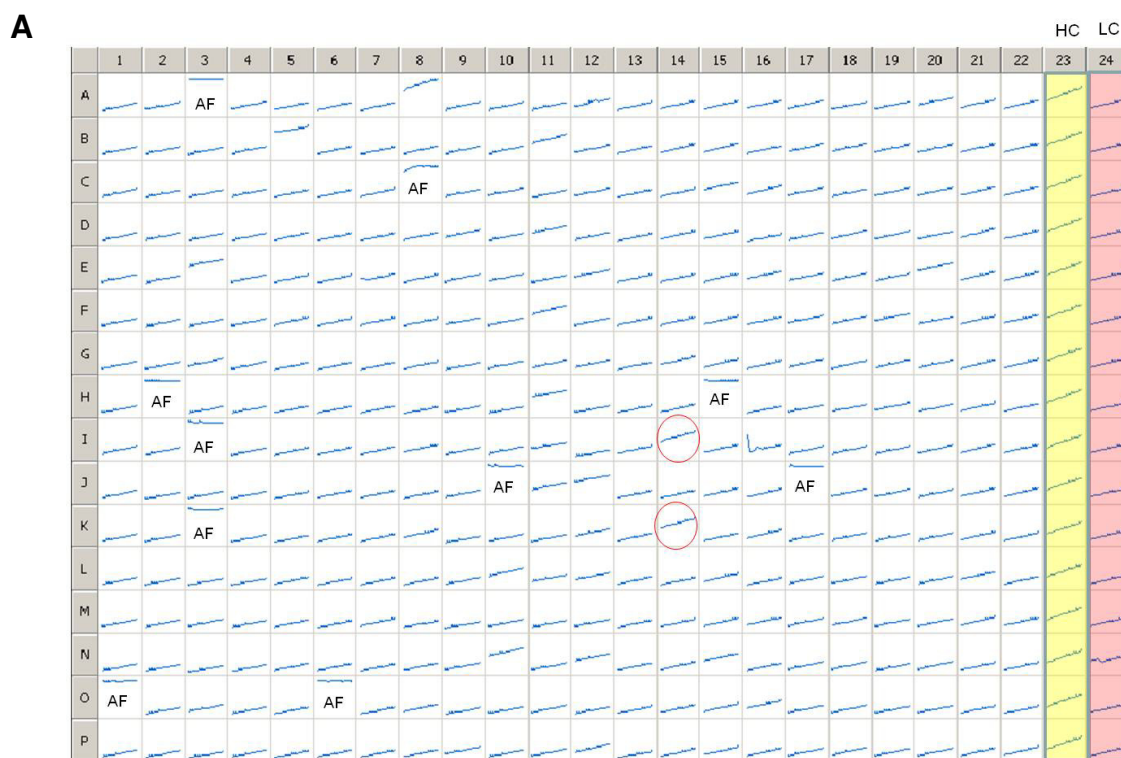


Figure 4.24 Concentration-response effects of potential hits from the single-point measurements. Phosphatase activities were measured after preincubation of various concentrations of selected hits with **A)** The PP1- $I-1^P$ complex containing 21.6 pM PP1 and 30

nM I-1^P or **B**) 21.6 pM PP1c. The data are expressed as percentages of PP1 activity (alone) and are mean±SEM of n>3. **C**) Concentration-inhibition curve of ibandronate was plotted against PP1 activity after preincubation of different concentrations with 21.6 pM PP1c. Mean±SEM of n=3.

4.4.2.3 Kinetic measurements of HTS

In the second run of HTS, 5280 compounds were screened for their effects on I-1 activity, using kinetic measurements. A single concentration of the compounds was preincubation with the PP1-I-1^P complex. Fluorescence intensities were measured after incubation of the reactions with substrate for 30 min. Fig 4.25 A shows the signals in a 384-well plate during the measurement time. Gradients of the signals were calculated and plotted against signal intensities, yielding a linear regression between high controls (PP1c) and low controls (PP1-I-1^P; Fig 4.25 B). Compounds that fell within this linear area and demonstrated ≥50% activity higher than low controls were considered as potential hits (Fig 4.24 B). The kinetic measurements enabled the discrimination of interfering auto-fluorescent compounds (high signal intensity and low gradient) and quenchers (low signal intensity and low gradient), without requirement of a counter screen. It was also possible to recognize compounds with both auto-fluorescence and I-1 antagonizing effect (high signal intensity and high gradient) or quenching and I-1 antagonizing effect (low signal intensity and high gradient). To increase the accuracy of hit identification, the screen was repeated at other time point with the same compounds. Finally, compounds that were effective in both screenings were considered as hits.



HC=high control, LC=low control, AF=auto-fluorescent cpd

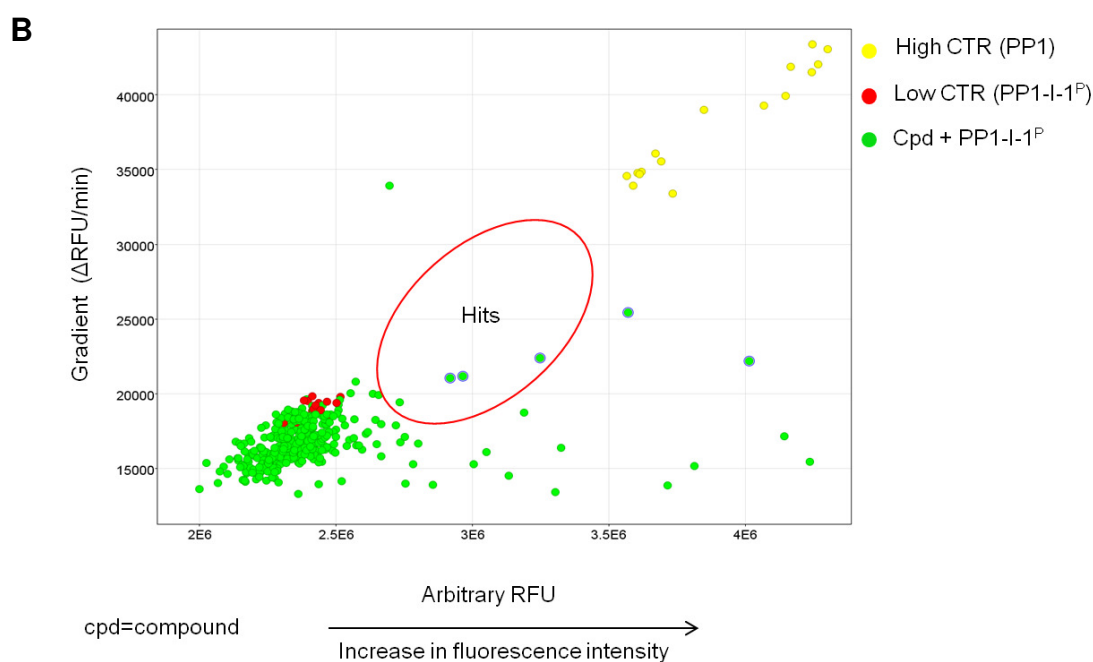


Figure 4.25 Representative kinetic measurements of the HTS. A) Raw data from a 384-well plate. The wells containing 21.6 pM PP1c as high controls (HC) or PP1-I-1^P (21.6 pM PP1 + 30 nM I-1^P) as low controls (LC) are highlighted in yellow and red, respectively. The signal intensities were recorded after preincubation of compounds (20 μM) with PP1-I-1^P, for 15 min prior to reaction initiation. Compounds with low gradient and high background were considered as auto-fluorescent compounds (AF). The wells containing potential hits of I-1 are marked with red circles. **B)** Gradients (ΔRFU/min) were plotted against fluorescence signals (RFU) in a representative plate. High CTRs and low CTRs are depicted as yellow dots and

Bar chart showing PP1 activity (%) for various peptides and concentrations. The y-axis ranges from 0 to 100%. The x-axis shows concentrations of 1, 10, and 30 μ M for each peptide. Peptides include CTR, A02, A16, C16, E02, F05, I03, J03, J09, K03, K21, M03, N02, P03, and ND. The peptide I-1 SP RKIQFTV shows the highest activity, reaching approximately 80% at 30 μ M.

Peptide	1 μ M	10 μ M	30 μ M
CTR	~40	~40	~40
A02	~40	~38	~30
A16	~42	~40	~38
C16	~45	~43	~42
E02	~38	~40	~38
F05	~38	~38	~35
I03	~38	~38	~35
J03	~35	~32	~35
J09	~38	~35	~32
K03	~40	~32	~28
K21	~42	~40	~38
M03	~40	~32	~25
N02	~42	~42	~42
P03	~32	~25	ND
I-1 SP RKIQFTV	~58	~72	~80

ND=non-detected

105

4.5 Determination of endogenous PP1 activity in the fluorescence assay

We investigated the suitability of our fluorescence assay as a simple tool for the detection and quantification of endogenous phosphatase activities. Based on the reported IC₅₀ values of chemical inhibitors of Ser/Thr phosphatases (Tab 4.3; Herzig & Neuman et al. 2000; Swingle et al. 2007), we applied OA and tautomycin (TTM), as global Ser/Thr phosphatase inhibitors and I-2 as a specific PP1 inhibitor for discrimination purposes.

Table 4.3 The inhibitory potencies of natural toxins against different Ser/Thr phosphatases (Swingle et al. 2007).

Inhibition of Ser/thr Protein Phosphatase activity (IC ₅₀ ^{**})						
Compound	PP1	PP2A	PP2B (calcineurin)	PP4	PP5	PP7
Okadaic acid	15–50	0.1–0.3	~4,000	0.1	3.5	>1,000
Microcystin-LR	0.3–1	<0.1–1	~1,000	0.15	1.0	>1,000
Nodularin	2.4	0.3	>1,000	ND	~4	>1,000
Calyculin A	0.4	0.25	>1,000	0.4	3	>1,000
Tautomycin	0.23–22	0.94–32	>1,000	0.2	10	ND
Cantharidin	1,100	194	>10,000	50	600	ND
Fostriecin	45,000–58,000	1.5–5.5	>100,000	3.0	50,000–70,000	ND

ND, not determined

Phosphatase activities of homogenates of HEK 293 cells, mouse heart and skeletal muscle were measured in the classic radioactive and our fluorescence assays (Fig 4.27 A-B). For the radioactive assay, [³²P]-labeled phosphorylase a was used as a substrate. This substrate is selectively cleaved by PP1 and PP2A (Cohen et al. 1989). The total PP1 and PP2A phosphatase activity in HEK 293 cells was higher than in heart and skeletal muscle (25% and 17%, respectively; Fig 4.27 A). The inhibitory activity of 3 nM OA, expected to inhibit mainly PP2A and PP4, was 54%, 43% and 38% in HEK 293 cells, heart and skeletal muscle, respectively (Fig 4.27 A). The fractions of PP1, based on I-2 inhibitory effect, were 58% in HEK 293 cells and skeletal muscle, and 50% of total PP1 + PP2A activity in the heart (Fig 4.27 A). Using DiFMUP as a universal phosphatase substrate, the total hydrolysis rate in HEK 293 cells was ~2-fold higher than in heart and skeletal muscle (Fig 4.27 B). The inhibitory activities of 50 nM TTM indicating the proportion of PP1, PP2A, PP4 & PP5 (Tab

4.2), were 61% in the HEK 293, 76% in the heart and 65% of total phosphatase activity in the skeletal muscle. I-2, which selectively inhibits PP1, reduced total phosphatase activity by 8% and 19% in HEK 293 cells and heart, respectively (Fig 4.27 B). Interestingly, the total phosphatase activity in skeletal muscle was slightly (3%) increased after incubation with I-2. These data indicated that our fluorescence assay was able to distinguish Ser/Thr phosphatases from other types of phosphatases by using tautomycin as a global inhibitor of Ser/Thr PP. However, recognition of PP1 activity using specific inhibitors such as I-1 (data not shown) and I-2 was not efficient, likely because its fraction of total PP activities is too low.

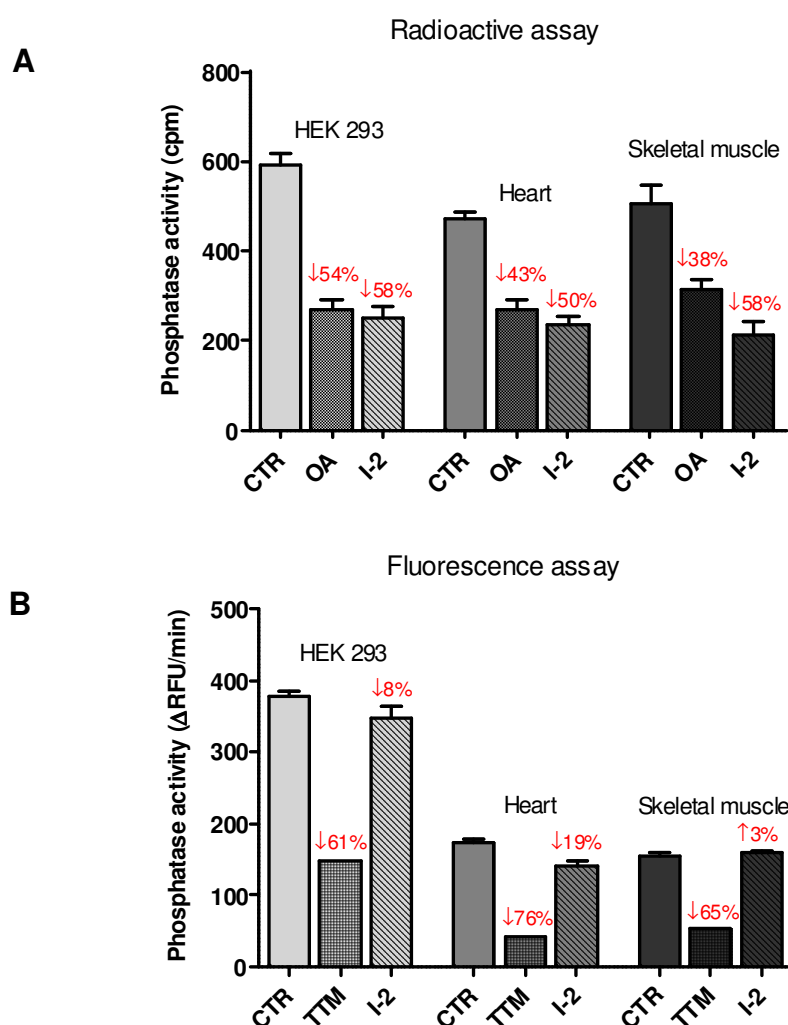


Figure 4.27 Comparison of endogenous phosphatase activities in radioactive and fluorescence assays. A) Phosphorylase a phosphatase activities were monitored in the diluted homogenates of HEK 293 cells (1:16), mouse heart (1:10) and skeletal muscle (1:20) in the presence of OA (3 nM) and I-1 (1 μ M). The data are expressed as total counts of free γ -[32 P]-phosphate per min. Mean \pm SEM of $n=3$. **B)** The hydrolysis rates of 50 μ M DiFMUP were measured after preincubation of 5 μ g proteins of HEK 293 cells, mouse heart and

skeletal muscle homogenates with 50 nM TTM or 260 nM I-2. Mean \pm SEM of n=3 (mean of n=2 for TTM).

In the next step, we compared the phosphatase activities in left ventricle homogenates of human hearts from non-failing (NF), ischemic cardiomyopathy (ICM) and dilated cardiomyopathy (DCM) patients in the fluorescence assay. Total phosphatase activity in the NF group did not differ from the ICM group, but was 24% higher than in the DCM group (non-significant, Fig 4.28). The inhibitory effect of 10 nM OA was ~60% in all samples, indicating similar proportions of PP2A, PP4 and PP5. The inhibition rates by I-2 representing the fractions of PP1 were 8%, 11% and 13% in the NF, ICM and DCM groups, respectively. (Fig 4.28). The significant increase of I-2 inhibitory activity in the DCM group showed that despite generally inefficient quantification of PP1 activity, subgroup corresponding variations could be detected in the fluorescence assay.

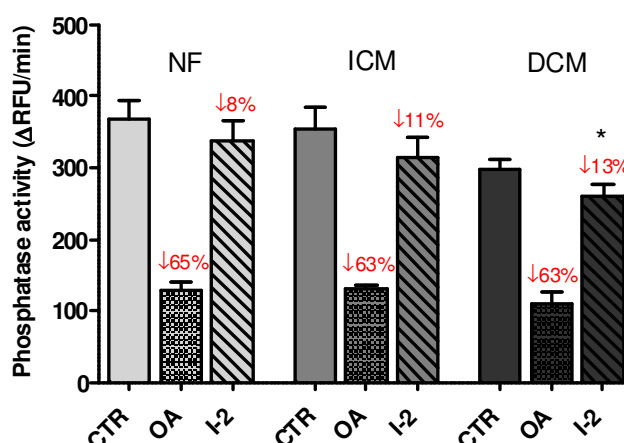


Figure 4.28 Comparison of phosphatase activities in human NF, ICM and DCM hearts. Measurement of total phosphatase activities of human heart homogenates (5 μ g proteins); non-failing (NF), ICM (ischemic cardiomyopathy) and DCM (dilated cardiomyopathy) patients were measured after preincubation with 10 nM OA or 1 μ M I-2. Mean \pm SEM of n=4. *P<0.05 vs. I-2 of NF, two-way ANOVA.

We compared the phosphatase activities of recombinant PP1 and HEK 293 homogenate, before and after incubation together to gain more insights into the deficiency of our fluorescence assay for the determination of endogenous PP1. Hydrolysis rates of DiFMUP in the presence of 1 U recombinant PP1 was 40% higher than in HEK 293 homogenate alone (Fig 4.29 A). By addition of recombinant PP1 to the cell lysate, we expected an increased phosphatase activity up to ~140% compared to HEK 293 lysate alone. However, total phosphatase activity in the

mixture was only ~20% more than HEK 293 extract alone (Fig 4.29 A). This indicated that a huge part of PP1 activity towards DiFMUP was deactivated in HEK 293 cell extract. The activity of recombinant PP1 catalytic subunit was inhibited by OA (300 nM) up to ~70% and by I-2 (30 nM) almost completely (97%; Fig 4.29 A). In a similar manner, OA and I-2 inhibited the active part of PP1 (~20%) in the mixture. Western blot analysis demonstrated considerable presence of PP1 protein in HEK 293 homogenate using an antibody against PP1 catalytic subunit (Fig 4.29 B). These data collectively demonstrated that various cellular parameters were contributed to the reduced sensitivity of PP1 towards DiFMUP and subsequently the inhibitors.

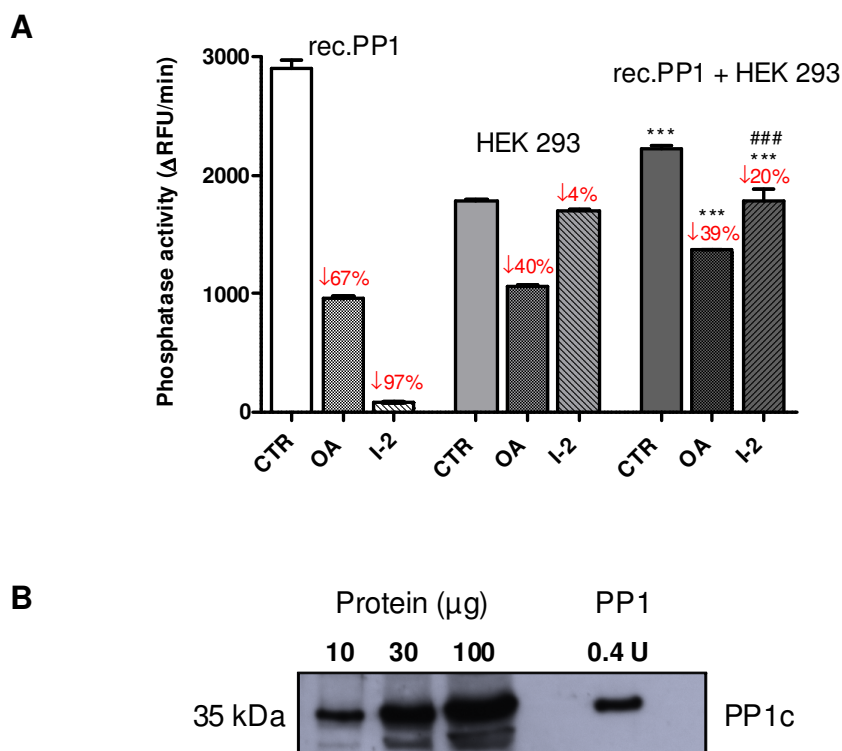


Figure 4.29 Comparison of phosphatase activities of HEK 293 and PP1c. A) The hydrolysis rates of DiFMUP were measured in the presence of 1 U recombinant PP1, HEK 293 homogenate (30 μg proteins) and 1 U recombinant PP1 plus HEK 293 homogenate after preincubation with 300 nM OA or 30 nM I-2. Mean±SD of n=3. ***P<0.001 vs. recombinant PP1, two-way ANOVA. ###P<0.001 vs. CTR, one-way ANOVA. **B)** Representative Western blot of 10, 30 and 100 μg protein of HEK 293 lysate and 0.4 U PP1 derived from rabbit skeletal muscle, using an antibody directed against PP1 catalytic subunit.

5 Discussion

Based on the previous findings (El-Armouche et al. 2003a; El-Armouche et al. 2004), the essential roles of PP1/I-1 holoenzymes in cardiac biological regulatory signaling cascades introduce I-1 as a potential candidate for the treatment of heart failure. Nowadays, modulation of PP1 regulatory subunits has become a substantial aim in many pathological pathways (for review see by Peti et al. 2012). Targeting complexes of PP1/DARPP-32 in the cytoplasm or the nucleus offers therapeutic interventions in neurological disorders such as Parkinson's disease and drug addiction (Yger & Girault 2011). Small molecules that could block the interaction of PP1/G_L (liver glycogen-targeting subunit) to its allosteric inhibitor, phosphorylase a, are promising drugs for diabetes through increased hepatic glycogen synthase activity (Armstrong et al. 1998). Inhibition of PP1 complex with its regulatory subunit M₁₁₀ seems to be beneficial for hypertension due to a smooth muscle relaxant effect (Uehata et al. 1997). Recently, the screen of small molecules yielded salubrinal (Boyce et al. 2005) and guanabenz (Tsaytler et al. 2011) as selective inhibitors of the PP1/GADD34 (growth arrest and DNA damage-inducible protein) complex. These molecules could target pathological pathways involved in endoplasmic reticulum (ER) stress and viral infections via disruption of the stress-induced dephosphorylation of the α subunit of translation initiation factor 2 (eIF2 α). In this regard, we hypothesized that intracellular modulation of cardiac cells via small molecules targeting PP1/I-1 complex might be beneficial for cardiac disorders as already demonstrated in our previous studies (El-Armouche et al. 2008; Wittköpper et al. 2010). Thus, in the current work, we aimed at investigating the drugability of I-1 and screening for small molecules with PP1/I-1 inhibitory effect using a suitable screening system.

5.1 Development of a non-radioactive phosphatase assay facilitates the monitoring of PP1/I-1 activity

Following identification and validation of I-1 as a potential therapeutic target, the development of an appropriate assay was a basic requirement to search for I-1 antagonists. The commonly used assays for PP1 activity are radioactive using [³²P]-labeled substrates. Although such substrates are quite specific, they are expensive, hazardous and the preparation is time-consuming. Therefore we employed p-

nitrophenyl phosphate (pNPP) as a chromogenic substrate and 6, 8-difluoro-4-methylumbelliferone (DiFMUP) as a fluorogenic substrate to develop a non-radioactive PP1/I-1 assay systems. Both pNPP and DiFMUP are non-selective phosphatase substrates that have been mostly used to identify toxins with phosphatase inhibitory effects (Vieytes et al. 1997; Bouaïcha et al. 2002). Indeed, their economic, safe and easy-to-use properties made them appropriate candidates for screening procedures. Thus, we established a colorimetric and a fluorescence PP1 assay in a multi-well plate format using a recombinant catalytic subunit of PP1 (PP1c). Due to the superior sensitivity of DiFMUP to pNPP, the fluorescence assay required 500-fold lower amount of the enzyme than the colorimetric assay, emphasizing the cost-effectiveness of the DiFMUP-based assay. After achievement of robust conditions, both assays were characterized via protein and chemical inhibitors including I-2 as a PP1 selective protein inhibitor and okadaic acid (OA), calyculin A and cantharidin as non-selective Ser/Thr phosphatase inhibitors. Published data reporting the potency of phosphatase inhibitors vary widely. Therefore, we compared the obtained IC_{50} values from both colorimetric and fluorescence assays together and with the reported values to define the sensitivity and accuracy of our assays. While OA and cantharidin showed similar IC_{50} values using either pNPP or DiFMUP, the potencies of I-2 and calyculin A were ~20-folds and 8-fold higher, respectively, in the fluorescence assay. This feature might arise from a different mode of inhibitory activities, independent or dependent on the amount of enzyme. Ultimately, all obtained IC_{50} values of the indicated inhibitors were compatible with the reported values by others (Herzig & Neumann 2000; Swingle et al. 2007), indicating the principal feasibility of both assay systems.

Once having an optimal condition for determining PP1 activity, we attempted to expand these assays as PP1/I-1 assay systems. Thus, we started the titration of I-1 in the presence of constant amounts of PP1c. Recombinant I-1 was bacterially expressed and subsequently phosphorylated by PKA for activation. Nevertheless, in the pNPP-based assay, PP1 activity was not inhibited by phosphorylated I-1 ($I-1^P$) up to 1000 nM. Western blot analysis using phospho-specific antibodies revealed a complete loss of the phosphorylation state of I-1 in the presence of PP1. This feature was previously described by Endo et al. (1997) as an unexpected property of recombinant PP1. In contrast to freshly purified catalytic subunit of PP1 from

mammalian tissues, bacterially expressed PP1 is Mn^{2+} -dependent resulting in changes of some regulation modes (Endo et al. 1997). For instance, while phosphatase activities of Mn^{2+} -dependent PP1 increased toward pNPP and histone H1, its inhibition by I-1 was reduced up to 500-fold (Alessi et al. 1993). The alteration of one or more interactions of PP1/I-1 is supposed to impair PP1 regulation by I-1, in which PP1 becomes able to dephosphorylate and deactivate I-1 (Endo et al. 1997). Interestingly, native PP1 is also converted into a Mn^{2+} -dependent enzyme after long-term storage (Endo et al. 1997), which is accelerated by phosphatase inhibitors such NaF, ATP and sodium pyrophosphate (Brautigan et al. 1982; Burchell & Cohen 1978). This could be explained by the loss of metals from the active site of enzyme (Egloff et al. 1995), leading to structural and functional alterations. However, the activities of I-2 and PP1 chemical inhibitors toward recombinant PP1 tend to be conserved (Endo et al. 1997). It is also worth to mention that in contrast to PP1, recombinant I-1 possesses the same properties as isolated I-1 from rabbit skeletal muscle (Endo et al. 1996). In order to overcome this undesired property of recombinant PP1, we used thiophosphorylated I-1 ($I-1^{SP}$) for our colorimetric assay, as a non-hydrolysisable form, to prevent PP1 dephosphorylation. $I-1^{SP}$ was partially protected against recombinant PP1-mediated dephosphorylation and inhibited PP1 activity with an IC_{50} value of ~300 nM, which was expected according to published data (Alessi et al. 1993). Interestingly, Western blot analysis showed that in contrast to the applied amount of recombinant PP1 in the colorimetric assay, 100-folds lower amounts as indicated by the fluorescence assay were not able to dephosphorylate $I-1^P$. In line with to the Western blot data, $I-1^P$ was able to inhibit PP1 activity in the DiFMUP-based assay with an IC_{50} value that was very close to the physiological value (Nimmo & Cohen 1978; Ingebritsen et al. 1983; Connor et al. 1998). In addition, we compared DiFMUP phosphatase activities using equal amounts of native and recombinant PP1. Although, the activity of native PP1 was ~2-fold lower than recombinant PP1, the inhibition rates of both of them by $I-1^P$ were identical. This highlights the reliability of our fluorescence assay as a surrogate system for monitoring PP1 activity.

5.2 The I-1 N-terminal KIQF motif and Thr-P³⁵ are essential for PP1 binding and inhibition

The free catalytic subunit of PP1 has poor substrate specificity. More than 200 regulators determine its substrate specificity in a distinct manner. However, a detailed understanding about how these proteins direct PP1 at a molecular level is lacking. Up to now, only the structures of 15 PP1 holoenzymes have been determined to atomic resolution (Tab 5.1). Notably, all of these complexes have been generated bacterially, because no native PP1 holoenzyme has been yet achieved through isolation process. In addition to crystallography, mutations in critical binding sites and screening of a peptide library with PP1c have been mainly used to map PP1 holoenzymes (Zhang et al. 1994; Zhao & Lee 1997). Elucidation of PP1/I-1 interaction would help to identify essential areas that could be targeted by potential drugs. Due to the lack of a crystal structure of the PP1/I-1 complex, a precise interaction model is missing. However, several lines of evidences implicated that the N-terminal domains of I-1 and that of its neuronal homologue DARPP-32, together with the phosphothreonine (at residue 35 for I-1 and 34 for DARPP-32), are crucial parts for binding and inhibition of PP1 (Endo et al. 1996; Huang et al. 1999). For deeper molecular insights, we generated three mutants of the I-1 protein by site-directed mutagenesis or by deletion of the ⁹KIQF¹² motif as well as mutations within ³⁰RRRR³³ motif. The properties of the PKA phosphorylated forms of these mutants toward PP1 activity were investigated using surface plasmon resonance (SPR) for binding abilities and the fluorescence phosphatase assay for the corresponding activities. We showed that deletion of the ⁹KIQF¹² motif eliminated both the I-1 binding to and inhibition of PP1. Similar results were shown by Endo et al. (1996) as an N-terminal fragment of I-1 (I-1¹³⁻⁵⁴) with deleted KIQF failed to inhibit PP1 activity. Substitution of RLN (arginine-leucine-asparagine) residues with KIQ (lysine-isoleucine-glutamine) led to attenuated binding (~1.5-fold) and activity (~7-fold). This is consistent with previous findings showing that mutations in valine or phenylalanine destroyed the interaction between PP1c and NIPP1 (Beullens et al. 1999), spinophilin (Hsieh-Wilson et al. 1999) and AKAP 220 (Schillace & Scott 1999). Obviously, the nonpolar valine (V) and phenylalanine (F) residues bind to hydrophobic amino acids on the PP1 surface, while basic residues such arginine (R) build hydrogen bounds to PP1 (Egloff et al. 1997). Although arginine, leucine (L) and

asparagine (N) provide the same charge and polarity as lysine (K), isoleucine (I) and glutamine (Q), the alleviated binding and activity of mutant I-1 may implicate the distinct roles of these residues for PP1 interaction. Interestingly, swapping of KIQF to the RVxF motif of NIPP1 (¹⁹⁷RVTF²⁰⁶) has been reported to increase I-1 inhibitory effects on PP1c due to increased affinity (Wakula et al. 2003). The abolished activities of the mutants, I-1_{ΔKIQF} and I-1_{KIQ/RLN}, after PKA-dependent phosphorylation, emphasize the necessity of a primary binding site as supporter for further interactions. In addition, we showed that mutations of basic residues, ³⁰RRRR³³, to neutral amino acids, ³⁰AAAA³³, abrogate both I-1 binding and activity towards PP1. Western blot analysis demonstrated absolute deficit of Thr³⁵ phosphorylation of the I-1_{R/A} mutant. This could be explained by an essential role of ³⁰RRRR³³, as a PKA consensus motif for Thr³⁵ phosphorylation. Therefore, replacing the uncharged alanines seems to eliminate the PP1/I-1 interaction due to a lack of phosphorylation on Thr³⁵ rather than an impaired binding to acidic groove of PP1. Similarly, we observed that non-phosphorylated I-1 has >2000-fold less affinity to PP1 than I-1^P. This reduced affinity may explain the abolished inhibitory activity of non-phosphorylated I-1 in the phosphatase assay. These findings contradict earlier reports by Endo et al. (1996), showing that binding of I-1 to PP1 is independent of the I-1 phosphorylation state and thus does not account for its inhibitory activity. However, in a later study, Connor et al. (1998) demonstrated a loss of PP1/I-1 interaction with the I-1 mutants, T35A and T35D, emphasizing the requirement of phosphorylation of Thr³⁵ for binding to PP1. Our data collectively support the concomitant importance of KIQF and phospho-Thr³⁵ for both binding and activity of I-1 towards PP1.

Table 5.1 Overview of all currently determined PP1 structures (Peti et al. 2012).

PP1 Complex ¹	PP1 isoform	Res (Å)	Metals	PDB	Year	Ref
Ligand bound						
tungstate:PP1 ²	gamma	2.50	Mn/Fe	n/a	1995	[32]
Toxin bound						
microcystin:PP1 ³	alpha	2.10	Mn/Mn	1FJM	1995	[30]
okadaic acid:PP1	gamma	1.90	Mn/Mn	1JK7	2001	[34]
caluculin A:PP1	gamma	2.00	Mn/Mn	1IT6	2002	[33]
motuporin:PP1	gamma	2.10	Mn/Mn	2BCD	2006	[64]
dihydromicrocystin-LA:PP1	gamma	2.30	Mn/Mn	2BDX	2006	[64]
*nodularin-R:PP1	alpha	1.63	Mn/Mn	3E7A	2009	[6]
*tautomycin:PP1	alpha	1.70	Mn/Mn	3E7B	2009	[6]
RVxF peptide bound						
G _m (63-75):PP1	gamma	3.00	Mn/Mn	n/a*	1997	[38]
Rb(870-882):PP1	alpha	3.20	Mn/Mn	3N5U	2010	[65]
Regulatory protein bound						
MYPT1:PP1	delta	2.70	Mn/Mn	1S70	2004	[28]
Inhibitor-2:PP1	gamma	2.50	Mn	2O8G	2006	[29]
*Inhibitor-2:PP1 ⁴	alpha	NMR/SAXS	Mn/Mn		2010	[11]
*Spinophilin:PP1 ⁴	alpha	1.85	Mn/Mn	3EGG	2010	[26]
*Spinophilin:PP1 ⁴	alpha	SAXS	Mn/Mn		2011	[66]
*Neurabin:PP1	alpha	2.20	Mn/Mn	3HVQ	2010	[26]
Triple Complex						
*PP1:Spinophilin:Nodularin-R	alpha	2.00	Mn/Mn	3EGH	2010	[26]
*PP1:Spinophilin:Inhibitor-2 ⁴	Alpha	NMR/SAXS	Mn/Mn		2011	[5]

¹PP1 protein for all PP1 crystal structures determined to date produced in *E. coli*. In all cases, expression medium was supplemented with 1 mM MnCl₂. In most cases, purification and final protein buffers were also supplemented with MnCl₂ (0.2 – 1.0 mM).

²Proton induced X-ray emission (PIXE) used to identify 1 Mn and 0.5 Fe in the active site.

³Metals listed as Mn²⁺ in 1FJM; reported that the presence of a strong anomalous signal rules out Mg, Ni, Cu or Zn, but could not discriminate between Mn, Fe or Co.

⁴ICP-AES spectroscopy experiments have confirmed that PP1 holoenzymes prepared using the protocol described in this review, such as PP1:Spinophilin, contain 2 Mn ions at the active site (MnCl₂ is used only during expression, not during purification).

*Structures of PP1 complexes determined by the authors.

5.3 The binding site of the KIQF motif is a promising druggable target for PP1/I-1 interaction inhibitors

Based on the data discussed above, we investigated the effects of small synthetic peptides derived from I-1 on PP1/I-1 interactions. Identification of peptides that affect the PP1/I-1 holoenzyme could be useful for several reasons: I) a better understanding of protein-protein interactions and dynamics, II) development of a peptide-based drug as an I-1 antagonist, III) elucidation of potential targeting sites or hot spots for small molecules. For decades now, the importance of small peptides

(less than 50 amino acids) in the molecular biology has been substantially increased, due to their multifunctional roles. The application of small peptides has been expanded from structural and functional studies of proteins to therapeutic and diagnostic approaches (Fuchs et al. 2003; Tsang et al. 2009). Since 2000, the number of peptides entering clinical studies as NBEs has been enormously increased (Lax 2010). According to the recent report of Peptide Therapeutic Foundation (2010), 54 therapeutic peptides are currently on the market worldwide, in which the most treatment areas include oncology (17%), obstetrics/gynecology (9%), allergy and immunology (9%). In this regard, we designed three peptides containing the critical N-terminal sequences of the I-1 protein: I) a nonapeptide encompassing PP1 the well-known binding consensus, ${}^6\text{SPRKIQFTV}^{14}$, II) a 11-residue peptide comprising the sequences between RVxF motif and Thr-P³⁵, ${}^{19}\text{PHLDPEAAEQI}^{29}$, and III) a nonapeptide, ${}^{25}\text{AAEQIRRRR}^{33}$ that include the four arginines preceding Thr-P³⁵. We showed that among these peptides only I-1^{SPRKIQFTV} was able to affect the PP1/I-1 complex and antagonized I-1 inhibitory activity. The obtained IC₅₀ values varied from the colorimetric assay to the fluorescence assay, depending on the indicated amount of PP1/I-1 complex. Since I-1^{SPRKIQFTV} comprises the “general” PP1 binding motif, we examined the selectivity of this peptide using other PP1 interactors. Interestingly, I-1^{SPRKIQFTV} antagonized the effect of I-2 with a 7-fold lower efficacy (IC₅₀ = 190 μM) than I-1^{SP}, whereas the PP1 holoenzymes with the toxins such as OA (data not shown) and calyculin A remained completely unchanged. The inhibitory effect of I-1^{SPRKIQFTV} on I-2 protein could be described as a competition with interaction between the KLHY sequence in I-2, which is proposed to be the corresponding RVxF motif (Yang et al. 2000). Such inhibitory activities of I-1^{SPRKIQFTV} are also expected for other PP1 interactors e.g. DARPP-32 and spinophilin that contain similar RVxF motifs. Therefore, for therapeutic approaches more investigations are required to define the selectivity of I-1^{SPRKIQFTV} for I-1, which also is dependent on its potencies. Furthermore, we verified the sequence specificity of I-1^{SPRKIQFTV} comparing it to a scrambled peptide (I-1^{KSIPRQTFV}), which was not able to affect the PP1/I-1 complex. The efficacy of the KIQF containing peptide together with the obtained I-1 mutagenesis data underline the fundamental role of the KIQF motif as a potential hot spot for specific PP1 interaction, and subsequently its target-ability or drugability. The definition of a hot spot is used for certain areas that mediate the interaction of

proteins. Identification of hot spots is mainly carried out by mutagenesis studies, which revealed residues contributed in binding free energy to the interaction (Clackson & Wells 1995). Indeed, peptides derived from one binding partner disrupt the protein-protein interaction via competing with the native protein for binding to the corresponding hot spot. Hence, small molecules that could affect these hot spots by mimicking the inhibitory peptides could be promising for therapeutic approaches. The lack of effect of I-1^{PHLDPEAAEQI} and I-1^{AAEQIRRRR} may indicate the non-involvement of these sequences in the PP1/I-1 binding, and underlines the fact that the PP1 peptide binding site is confined to the KIQF motif. Our results are compatible with findings from Connor et al. (1998) showing that mutations of six negative charged amino acids to neutral residues placed within the PP1 acidic groove did not change the sensitivity of PP1 to I-1. Therefore, we screened additional six small peptides containing 4x-Arg motif; ³⁰RRRR³³, ²⁸QIRRRR³³, ²⁸QIRRRRP³⁴, ²⁸QIRRRRP³⁵, ³⁰RRRRP³⁵ and ³⁰RRRRPTPA³⁷. These peptides neither affected PP1/I-1 holoenzyme nor PP1c (data not shown). These data, collectively, challenge the proposed interaction model of four arginines preceding phosphothreonine with the PP1 acidic groove illustrated by Goldberg and Terrak.

Following the biochemical validations, we attempted to characterize the biological and functional consequences of I-1^{SPRKIQFTV} in cardiac cells. Because I-1 is an intracellular protein, we modified the peptide by conjugating it to a C-terminal poly-arginine (poly-Arg) chain consisting of 11 arginines to allow cell-permeability. Arginine-rich peptides are a subgroup of the cell-penetrating peptides (CPPs) that are capable of entering most mammalian cells and therefore are widely used for carrying bioactive molecules like drugs, proteins, oligonucleotides and liposomes into the cells (Tünnemann et al. 2008). Their entering mechanisms are still under discussion, but two main mechanisms seem to be involved: I) active uptake through endocytosis and subsequent release of the enclosed compounds from endosomes or lysosomes (Ferrari et al. 2003; Richard et al. 2003) and II) energy-independent uptake across cell membrane via transient pores (Duchardt et al. 2007; Herce et al. 2009). Nevertheless, all of these studies uniquely implicated the ability of poly-Arg peptides, with optimal numbers of arginines (9-11), to translocate across the cells efficiently, without inducing toxicity (Tünnemann et al. 2008). Labeling the poly-Arg peptide with FITC, facilitated the monitoring of intracellular localization.

First, we used neonatal rat engineered heart tissues (EHTs) for investigation of functional effects of poly-Arg modified I-1^{SPRKIQFTV} (P-pR). The EHT model represents a 3-D heart-tissue-like system of cardiomyocytes that allow determination of contractile parameters under isometric condition. Confocal microscopy of immunohistological stained EHTs revealed inefficient uptake of the peptide by cardiac cells, despite successful translocation into the EHTs. One reason could be the barrier effect of matrix components via unspecific bindings. In line with the microscopic observations, video-optical analyses of treated EHTs with P-pR showed no change in the contractile parameters (data not shown). In the next step, we examined the functional consequences of P-pR on the contractility of isolated adult mouse cardiomyocytes (AMCMs). Confocal microscopy of living cells indicated a suboptimal translocation (<20%) of the peptide into the cardiac cells. On the other hand, our observation of many dead cells containing the peptide might argue for hypersensitivity and consequently rapid death of the cells after an effective uptake of the peptide. However, video-optical analyses demonstrated a significant attenuation of the isoprenaline-induced positive inotropic effect in the treated cells with P-pR with unchanged basal contractility. The current results are consistent with our previous study (El-Armouche et al. 2008) showing that the lack of I-1 in KO mice was associated with desensitization to the isoprenaline induced positive inotropic effect without changing the basal contractility. Interestingly, treatment of the cells with a higher concentration of P-pR induced severe spontaneous contractions indicating arrhythmias and cell death after β -adrenergic stimulation. This feature might be described either as a concentration-dependent proarrhythmic effect of P-pR or as a toxic side-effect of poly-Arg chain by interrupting the physiological processes of cell membrane (Herce et al. 2009). Further functional investigations with optimized conditions (e.g. improved cellular uptake and/or using selective cells containing peptide) are required to manifest these findings. Finally, we investigated the biological effects of I-1^{SPRKIQFTV} in neonatal rat cardiomyocytes (NRCMs). Confocal microscopy indicated efficient translocation of the peptide into the cells. This was associated with significantly attenuated phosphorylation levels of PLB in response to isoprenaline, whereas the phosphorylation levels of PLB-Thr¹⁷ and TnI-Ser^{23/24} remained unchanged (data not shown). The sequence-related specificity of this effect was verified using the scrambled peptide (Pscr-pR) as control. The reduced

phosphorylation of PLB on Ser¹⁶ by P-pR confirms the obtained results from functional investigations in AMCMs and is in agreement with the findings from I-1 KO mice. As reported by our group (El-Armouche et al. 2008), the protective mechanism of I-1 ablation in the mice heart against catecholamines detrimental effects were associated with hypophosphorylation of RyR2 and PLB. Increased steady-state phosphorylation levels of RyR2 and PLB upon β -adrenergic stimulation contribute to an increased contraction-relaxation cycle in the heart. Reduced PKA phosphorylation of PLB leads to reduced diastolic Ca²⁺ uptake in the SR and therefore low SR Ca²⁺ load. This is considered as an adverse effect, but concomitant hypophosphorylation of RyR2 reduces Ca²⁺ release to gain a new balance of Ca²⁺ transient at a lower level. This situation may explain the protective effect of I-1 ablation. Interestingly, other PKA targets including myofilament proteins, TnI and MyBP-C were found to be unaffected in I-1 KO hearts. This data implicate that I) a small peptide of I-1 containing KIQF is able to compete with endogenous I-1, II) competitive inhibition of I-1 mimics the effect of genetically I-1 ablation in terms of PLB phosphorylation, III) therefore, peptide inhibition of I-1 similar to I-1 KO might protect role against β -adrenergic stress. The effect of P-pR on phosphorylation states of RyR2 and MyBP-C needs to be examined in future studies.

5.4 High throughput screening using the fluorescence assay would be an appropriate system to detect small molecule inhibitors for PP1/I-1 interaction

Identification of an interfering peptide for PP1/I-1 interaction was a satisfying achievement. However, identifying small molecules that inhibit PP1/I-1 protein-protein interaction was much more challenging. Indeed, for protein-protein interactions, peptides are more effective than small molecules due to the characteristics of protein interaction surfaces (Wells & McClendon 2007). Moreover, the structural relationship between drug peptides and proteins is associated with ~20% less side-effect compared to small molecules (Lax 2010). Yet, despite these advantages, application of peptides is still limited because of: I) expensive and difficult synthesis, II) limited stability III) non-oral administration due to proteolytic degradation in the gastrointestinal system, IV) suboptimal entering into the cells despite poly-Arg or stearate modifications, therefore difficulties to control their intracellular

concentrations, and V) immunogenic reactions (Lax 2010; Christian et al. 2011). Small molecules are kinetically advantageous over peptides due to intercalation between protein-protein interactions leading to an increased dissociation rate of the interacting proteins (Tang et al. 2006). Furthermore, small molecules can allosterically disrupt protein-protein interaction by induction of conformational changes from a distant binding site (Buchwald 2010). Although both the colorimetric and fluorescence assays were reliable and robust systems for screening purposes, we employed mainly our DiFMUP-based PP1-I-1^P assay, due to its advantages over the colorimetric assay (discussed in 5.1). In our laboratory, we tested ~600 compounds including *in silico* selected compounds. Because of the low number of the screened compounds together with the complexity of protein-protein interactions, we did not identify any validated hit with a distinct I-1 antagonizing effect. However, we managed to further fine-tune our assay conditions for getting more optimized signal to noise ratio, in particular for big scale screenings such as high-throughput screening (HTS). We used bioinformatic tools for virtual (*in silico*) screening of a large database (ZINC) to refine our compound library. Considerable advances in computer-based methods and determination of 3D structures by x-ray crystallography and NMR have made virtual screening techniques as a crucial tool for drug discovery (Bajorath 2002). Since a crystal structure of PP1/I-1 holoenzyme is missing, we counted on the suggested interaction models and targeted the acidic groove of PP1 as I-1 feasible specific binding site. Using our selection criteria, based on chemical properties (number of hydrogen-bond acceptors and donors), and a ligand-protein docking program (AutoDock), compounds with the highest affinity to the PP1 acidic groove were identified. Such compounds may disrupt I-1 interactions via competitive or allosteric inhibitory mechanisms. However, among the experimentally investigated compounds, none of them yielded any confirmed hit. On the other hand, the obtained results from the peptides and the mutant I-1 proteins may argue for non-relevant role of PP1 acidic groove for I-1 interaction or otherwise lack of any binding site for small molecules, as discussed above. In this regard, computational searching for the molecules that potentially affect KIQF binding to PP1 RVxF motif may be more promising as direct I-1 antagonists. Finally, we attempted to employ our fluorescence PP1/I-1 assay for HTS approaches. Since 1980, high-throughput technologies have become a cornerstone of drug discovery with constantly increasing miniaturization

and automation (Smith 2002; Baker 2010). Nowadays, the conventional 96-well plates have been widely replaced by 384-well plates. The robotic equipments made the screenings fully automated in each part including liquid handling, sample preparation and data analysis (Bajorath 2002; Eckstein 2008). The ultimate goal of such modernizations was screening of more compounds in less time. Thus, today, screening of up to 100,000 compounds in a single day is a usual speed for pharmaceutical companies. Nevertheless, only highly qualified assays are able to increase the final output of HTS. Therefore, the assays should be evaluated for sufficient stability, robustness and statistics prior entering HTS.

We verified the suitability of our fluorescence assay by estimation of the Z' -factor, as the most commonly used parameter for assay quality assessments. In the first run, nearly 3,600 compounds were applied for HTS using single-point measurements. A counter screen was performed to identify the compounds with artifact signals. Some molecules show intrinsic light emission, especially at the wavelength below 500 nm. This was reflected by ~10% of all indicated compounds as an auto-fluorescence effect, while a much lower numbers of compounds interfered by signals quenching effect. Screening for I-1 antagonists resulted in 3.4% compounds with either I-1 inhibitory effect or PP1 activation. In addition, the indicated compounds were examined for their direct effect on PP1c. Among the selected compounds as potential hits none of them were validated by subsequent concentration-response studies. One possible reason could be low accuracy of hit the finding process from only one measured point. Interestingly, one of putative hits, ibandronate, showed a non-competitive PP1 inhibitory activity concentration-dependently. Ibandronate is a biphosphonate used for treatment of post-menopausal osteoporosis by inhibiting osteoclasts. Biphosphonates are structural homologues of pyrophosphate (PPi), and their inhibitory effect on farnesyl pyrophosphate synthase (FPPS), the key enzyme in the mevalonate pathway, have been described as their main anticatabolic mechanism (Russell & Rogers 1999). Although the phosphatase inhibitory effect of biphosphonates, particularly on PTP has been earlier reported (Bauss & Schimmer 2006), up to now, there is no report about inhibition of PP1. This finding may represent an unknown additional mechanism of ibandronate. In the next step, we ran a PP1/I-1 HTS of ~5,000 new compounds by kinetic measurements, similar to the original assay format. The advantages of kinetic measurement over single-point

measurement are: i) discrimination of effective and interfering compounds in the very same assay, and subsequently no requirement for an additional counter screen, and ii) recognition of effective compounds with simultaneous auto-fluorescence activity. Double screening of the indicated compound was done to provide enhanced accuracy and reliability. Finally, 13 compounds with reproducible I-1 antagonizing activity were considered as putative hits. However, none of them could be validated in the concentration-response assays. Actually, the reliability of the assay itself has been continuously substantiated by I-1^{SPRKIQFTV}, which was used in the validation experiments as a positive control. On the other hand, it is not very likely to find a real hit from only ~9,000 compounds for a protein-protein interaction, while the gold standard in the pharma industry is 1,000,000 compounds per desired target (Smith 2002; Bajorath 2002). Another important limitation is referred to the complexity in the nature of protein-protein interaction. Although there are several examples of small molecules as protein-protein interaction inhibitors such as tirofiban, a $\alpha_{IIb}\beta_3$ /fibrinogen inhibitor (Fry 2006) and maraviroc a CCR5/gp-120 inhibitor (Dorr et al. 2005), finding small molecules that target protein-protein interfaces is traditionally a big challenge. The contact surface of a protein-protein interaction is ~1500-3000 Å², while a protein-small molecule contact surface involves ~300-1,000 Å² (Jones & Thornton 1996; Cheng et al. 2007). Furthermore, the surfaces of the proteins that interacted with the other are not well targetable by small molecules due to the lack of any binding pocket (Wells & McClendon 2007). Even some evidences demonstrated that HTS has regularly failed to identify small molecules that disrupt protein-protein interfaces (Spencer 1998; Cochran 2000). Despite all these hitches, the mentioned successful examples provide hopes to find effective small molecules via competition with hot spots. Subsequently, the interest of targeting of the interfaces of interacting proteins is increasing (Wells & McClendon 2007). In our case, the KIQF binding site could be a substantial hot spot for PP1/I-1 interaction, as discussed before. Thus, for the future, it seems to be useful to identify compounds that are similar to I-1^{SPRKIQFTV} using virtual screening.

5.5 Determination of endogenous PP1 activity in the fluorescence assay is challenging

Having established well-functioning non-radioactive phosphatase assays motivated us to extend these assay systems for quantification of endogenous phosphatase activity, particularly PP1, in cell/tissue extracts. Due to the ubiquitous expression and multifunctional role of PP1 in living cells, development of simple and rapid activity assays may provide many advances for biological and clinical investigations. Although the routine radioactive assays, especially using phosphorylase a as specific substrate for PP1 and PP2A, are used widely as reliable tools for activity measurements, there is still a need for non-radioactive assays. However, lack of selective chromogenic and/or fluorogenic substrates has delayed this effort. In this regard, we employed our fluorescence assay system for investigation of phosphatase activities in cell and tissue lysates. Due to the unselective property of DiFMUP, we used I-2 as a PP1 specific inhibitor and toxins such as OA and tautomycin (TTM), Ser/Thr phosphatase inhibitors, as discriminative tools. Several lines of evidences have shown that most toxic inhibitors are very potent (nanomolar range) inhibitors of PP1, PP2A, PP4 and PP5, whereas their activities are limited against PP2B, PP7, PPM-family Ser/Thr phosphatases and phosphotyrosine phosphatases (Honkanen & Golden 2002; Swingle et al. 2007). Based on the data from Swingle et al. (2007), the most selective inhibitors are OA ($\sim 10^2$ -fold selectivity for PP2A/PP4 vs PP1/PP5), fostreicin (PP2A/PP4 vs PP1/PP5 selectivity $\geq 10^4$ -fold) and TTM (~ 5 -fold selectivity for PP1 vs PP2A/PP4). Since the unstable property of fostreicin limits its application, we investigated the abilities of OA and TTM for phosphatase studies. Comparison of the phosphatase activities in HEK 293 cells, mouse heart and skeletal muscle in both radioactive and fluorescence assays demonstrated higher phosphatase activity in HEK 293 cells. However, the ratio of this difference was ~ 5 -fold larger in the fluorescence assay due to the unselective substrate. The radioactive assay using phosphorylase a, demonstrated the activities of only PP1 and PP2A (and PP2A-like phosphatases). The inhibition rate of phosphatase activity by OA indicated the fragment of PP2A, while I-1 inhibitory activity reflected the proportion of PP1 demonstrating 40-50% of the total activities. In the fluorescence assay, DiFMUP was hydrolysed by all types of phosphatases. The inhibitory activity of TTM were 60-70% in HEK 293 cells, heart and skeletal muscle, which discriminated the fraction of

Ser/Thr phosphatases including PP1, PP2A, PP4, PP5 and PP6 from PP2B, PP2C and non-Ser/Thr phosphatases. However, inhibition of PP1 corresponding activity by I-2 was relative low (up to 20%), even in some cases I-2 showed a slight increase in DiFMUP phosphatase activities (skeletal muscle in Fig 4.27 and other data that not shown). This feature could be due to a low amount of PP1 compared to the other phosphatases or was associated with altered sensitivity and selectivity of PP1 holoenzyme. The latter is favoured by the fact that PP1 does not exist freely in the cells (Cohen 2002; Virshup & Shenoliker 2009). We also compared the phosphatase activities of human non-failing (NF), ischemic cardiomyopathy (ICM) and dilated cardiomyopathy (DCM) donor hearts using DiFMUP as substrate. The total hydrolysis rates of DiFMUP were overall similar with a tendency to lower levels in the DCM group. The similar inhibitory activities of OA (PP2A sensitive concentration) in the all groups demonstrated the invariant ratios of PP2A and PP2A-like phosphatases. However, the slight increase of inhibition rates by I-2 in the ICM and DCM groups might be associated with an increased PP1 activity. This is in line with the previous data (El-Armouche 2004; Neumann et al. 1997) that showed PP1 activity to be elevated in the failing heart, albeit the inhibition ratio by I-2 did not exceed 20%. Therefore, we examined the effects of OA at a PP1 sensitive concentration and I-2 on recombinant PP1c, before and after preincubation with HEK 293 cell extract. The idea was to investigate the behavior of PP1 either “alone” or in association with its physiological environment e.g. in the presence of other cellular components. The activity of recombinant PP1 catalytic subunit was considerably suppressed after incubation with HEK 293 extract. Subsequently, the inhibitory effects of OA and I-2 were dropped in the mixture compared to PP1c alone. This experiment highlighted the altered sensitivity of PP1 towards substrate accompanied with other proteins that regulate its activity. This could be confirmed by Western blot analysis using antibody against PP1c that showed an abundant presence of PP1 in the cell extract. Presumably, I-2 was able to target only the proportion of PP1 that was available for DiFMUP. Similarly, Ragusa et al. (2010) showed that spinophilin was able to inhibit PP1c activity on phosphorylase a, whereas it had no effect on the activity of PP1 for other substrates like GluR1 and pNPP. Another example is the so-called PP1/I-2 inactive complex. I-2 acts not only as an inhibitor of PP1 but also a regulator. One of the PP1 complexes with I-2 that is termed ATP-Mg²⁺-dependent phosphatase is

inactive against phosphorylase a (Yang et al. 1981), which could be reactivated after treatment with trypsin or GSK-3 in the presence of Mn^{2+} . Trypsin degrades the regulatory subunits leading to released full active PP1 catalytic subunit, which is supposed to be trypsin-resistant (Endo et al. 1996). However, using trypsin treatment did not improve PP1 quantification using DiFMUP or pNPP (data not shown). Furthermore, based on the unselective property of DiFMUP, the competition with other phosphatases (alkaline, acid and tyrosine phosphatase) for one substrate may result in a lower fraction of PP1 activity compared to the total phosphatase activity. All together, our DiFMUP-based fluorescence assay is principally able to distinguish different groups of phosphatases, particularly PP2A, PP4 and PP5, using appropriate inhibitors. However, due to the complexity of PP1 holoenzymes achievement of optimal conditions using non-radioactive substrates for measurement of endogenous PP1 in the cell/tissue extracts is still challenging.

6 Summary

Reversible protein phosphorylation accomplished by kinases and phosphatases is a major regulatory mechanism. Out of several families of protein phosphatases, serine/threonine phosphatases quantitatively prevail. The functional diversity of the serine/threonine phosphatase type-1 (PP1) *in vivo* results from the association of its catalytic subunit (PP1c) with different regulatory or inhibitory subunits. One of them is inhibitor-1 (I-1) that inhibits PP1c only in its PKA-phosphorylated form (I-1-Thr³⁵^P). Disruption of the I-1 gene in mice resulted in protection from catecholamine-induced lethal arrhythmias and cardiac hypertrophy. This suggested that pharmacological I-1 blockade may represent a therapeutic strategy in heart failure. Therefore, the aim of this study was to screen a library of chemical compounds that inhibit I-1 and to characterize promising candidates *in vitro* for efficiency and toxicity. However, current assay systems for PP1 and/or I-1 activity based on PP1-mediated dephosphorylation of radioactively labeled phosphorylase a are expensive and not suitable for high-throughput screening (HTS). Therefore, first it was crucial to develop a non-radioactive, reliable and cost-efficient assay system for PP1/I-1 activity. Indeed, we succeeded to establish one colorimetric and one fluorescence assay system using pNPP and DiFMUP as substrates, respectively. The principal feasibility of both assays was confirmed with well-characterized chemical and protein inhibitors of PP1. However, the fluorescence assay exhibited a significantly higher sensitivity (with 500-fold lower requirement for recombinant PP1) and, in contrast to the colorimetric assay, showed similar sensitivity of either the recombinant (14 nM) or native PP1 (16 nM) for the activated I-1 within the assay. We also investigated the effects of mutant I-1 proteins, which implicated the importance of the KIQF motif and Thr-P³⁵ within the conserved N-terminal region of I-1 for binding to and activity against PP1. Screening of selected small peptides derived from I-1 yielded peptides with inhibitory activity against PP1/I-1 interaction. For instance, a nonapeptide containing the KIQF motif antagonized I-1 inhibitory activity with an IC₅₀ value of 3 μM. Notably, a cell-permeable poly-Arg modified peptide attenuated beta-adrenoceptor induced phosphorylation of PLB on Ser¹⁶ in neonatal rat cardiomyocytes, indicating biological functionality. Finally, we started to screen a selected, but undirected compound library and a number of *in silico* designed compounds, which should specifically interfere with the interaction of PP1 with Thr³⁵-phosphorylated I-1. The Z'-factor

amounted to 0.86 and 0.73 for PP1 alone and PP1 + I-1^P, respectively, which confirmed the suitability of the fluorescence assay for HTS. Nearly 9,000 small molecules were tested in a HTS format using either single-point or kinetic measurements. However, none of them could be validated in secondary assays, suggesting that screening of more compounds is required to identify validated hits. Furthermore, we investigated the aptitude of our fluorescence assay to quantify endogenous phosphatase activities in the cell/tissue extracts. Using okadaic acid (OA) and tautomycin (TTM), this assay enabled us to distinguish the fraction of toxin-sensitive PPP family phosphatases (PP2A, PP4, PP5 and PP6), from insensitive phosphatases (PP2B, PP7, PPM family, PTPases, ACP and AP). Conditions for the specific quantification of PP1 holoenzymes activity still need to be defined. In conclusion, a reliable assay system for the specific detection of I-1 inhibitory compounds has been developed and forms the basis to identify promising small molecule candidates, which could pave the way for the development of clinically applicable drugs to treat patients with chronic heart failure.

7 Zusammenfassung

Bei der reversiblen Phosphorylierung von Proteinen handelt es sich um einen essentiellen Regulationsmechanismus der Proteinfunktion. Durch Kinasen und Phosphatasen wird hierbei die Phosphorylierung bzw. die Dephosphorylierung der Proteine realisiert, beispielsweise auch jener, welche im Herzen die Kontraktilität regulieren. Generell bilden in der Gruppe der Proteinphosphatasen die Serin/Threonin-Phosphatasen den Hauptanteil. Die funktionelle Vielfalt der Serin/Threonin-Phosphatase Typ 1 (PP1) im lebenden Organismus wird durch die Assoziation einer katalytischen Untereinheit (PP1c) mit verschiedenen modulierenden Untereinheiten erreicht. Eine Untereinheit stellt hierbei das PP1 hemmende Protein Inhibitor-1 (I-1) dar, dessen inhibierende Wirkung nur im seinerseits phosphorylierten Zustand (I-1-Thr35^P) erreicht wird. Im Mausmodell wurde gezeigt, dass eine Ausschaltung des Gens, welches für I-1 kodiert, Herzmuskelzellen vor Katecholamin-induzierten tödlichen Arrhythmien oder vor Hypertrophie schützt. Dies führt zu der Hypothese, dass eine pharmakologische Blockade von I-1 einen therapeutischen Effekt bei Herzinsuffizienz darstellen könnte. Basierend auf dieser Hypothese war das Ziel dieser Studie, eine große Bandbreite chemischer Substanzen im Großmaßstab automatisiert zu analysieren, um somit vielversprechende Kandidaten zu identifizieren, welche das Protein I-1 hemmen und zur Therapie geeignet sein könnten. Weiterhin sollten die gefundenen Substanzen hauptsächlich *in vitro* hinsichtlich Effizienz und Toxizität untersucht werden. Die Analyseverfahren für PP1- und/oder I-1-Aktivitätsuntersuchungen, welche bis dato etabliert wurden, basieren auf PP1-vermittelter Dephosphorylierung von radioaktiv markierter Phosphorylase. Diese Verfahren sind zum einen teuer, zum anderen nicht für eine Analyse im Großmaßstab (sogenanntes '*High-throughput screening*') geeignet. Aus diesem Grund wurde zunächst ein nicht-radioaktives Analyseverfahren etabliert, welches durch seine hohe Verlässlichkeit eine kostengünstige Alternative zu bisheriger PP1/I-1 Aktivitätsmessungsmethodik darstellte. In diesem Rahmen entwickelten wir ein kalorimetrisches und ein Fluoreszenz-basiertes Messsystem mit geeigneten pNPP- und DiFMUP-Substraten. Die verlässliche Durchführbarkeit beider Messsysteme wurde mithilfe von bekannten PP1-Inhibitoren getestet. Hierbei stellte sich heraus, dass die Fluoreszenzmessungen eine deutlich höhere Sensitivität als

die kalorimetrischen Messungen aufwiesen, was mit einem 500-fach geringeren Verbrauch von eingesetzt rekombinanten PP1 einherging. Weiterhin zeichneten sich die Fluoreszenzmessungen durch eine ähnliche Empfindlichkeit von entweder rekombinanten (14 nM) oder nativem PP1 (16 nM) für das aktivierte I-1 innerhalb der Messmethode aus. Außerdem untersuchten wir die Effekte von mutierten I-1-Proteinen in unserem Messsystem, wodurch wir feststellen konnten, dass das KIQF-Motiv und das phosphorylierte Thr35^P innerhalb der erhaltenen N-terminalen Region des I-1 eine essentielle Voraussetzung für seine Bindung an PP1 war. Wir untersuchten in der Folge eine selektive Auswahl an kleinen Peptiden mit inhibitorischer Wirkung auf die PP1/I-1-Interaktion in unserem Messsystem. Hierbei konnten wir exemplarisch feststellen, dass ein Nonapeptid, welches das KIQF-Motiv enthielt, eine antagonisierende Wirkung auf I-1 zeigte ($IC_{50} = 3 \mu M$). Ein Peptid dieser Art, welches durch eine Poly-Argininkette modifiziert wurde, verringerte die beta-Adrenozeptor-vermittelte Phosphorylierung von Phospholamban an Ser16 in neonatalen Rattenkardiomyozyten. Mit dem etablierten Messsystem untersuchten wir eine Reihe weiterer ausgewählter sowie einige *in silico*-entwickelte Substanzen, welche spezifisch nur mit dem an Thr35-phosphorylierten I-1 gebundenen PP1 interagieren sollten. Der Z'-Faktor, welcher die Übertragbarkeit des etablierten Fluoreszenzmesssystems auf Messungen im Großmaßstab determiniert (Soll: $Z' > 0,5$), lag hierbei für PP1 bei 0,86 und für PP1 + I-1^P bei 0,73. Etwa 9.000 kleinere Moleküle wurden mittels Einpunkt- oder kinetischen Messungen im Großmaßstab getestet. Leider konnte keine der vermeintlich identifizierten Substanzen in weiteren Messungen validiert werden. Dies zeigte uns, dass die Notwendigkeit besteht, eine größere Anzahl weiterer Substanzen im Großmaßstab zu testen um etwaige 'Treffer' in weiteren Analysen zu bestätigen. Weiterhin charakterisierten wir die Amplitude unserer Fluoreszenzmessung um den Gehalt endogener Phosphataseaktivität in Zellen oder Gewebeproben zu bestimmen. Der Einsatz von Okadasäure (OA) und Tautomycin (TTM) ermöglichte es uns, die Fluoreszenzmessungen zur Unterscheidung von Toxin-empfindlichen PPP Phosphatasen (PP2A, PP4, PP5 und PP6) und unselektiven Phosphatasen (PP2B, PP7, PPM-Familie, PTPasen, ACP und AP) heranzuziehen. Es bedarf weiterer Optimierung der Messbedingungen für die gerichtete Quantifizierung der PP1-Holoenzymenaktivität.

Zusammenfassend kann gesagt werden, dass eine reproduzierbare Messmethodik entwickelt wurde, um mit hoher Spezifität I-1-antagonisierende Substanzen zu testen, was zukünftig die Identifikation von Kleinmolekül-I-1-Inhibitoren ermöglicht. Dieses Messsystem könnte also den Weg für die Entdeckung klinisch applizierbarer Substanzen ebnen, welche zur Behandlung der chronischen Herzinsuffizienz eingesetzt werden könnten.

8 References

- Ahmad, Z., Green, F.J., Subuhi, H.S. & Watanabe, A.M., 1989. Autonomic regulation of type 1 protein phosphatase in cardiac muscle. *The Journal of biological chemistry*, 264(7), pp.3859-63.
- Ajuh, P.M., Browne, G.J., Hawkes, N.A., Cohen, P.T., Roberts, S.G. & Lamond, A.I., 2000. Association of a protein phosphatase 1 activity with the human factor C1 (HCF) complex. *Nucleic acids research*, 28(3), pp.678-86.
- Alessi, D.R., MacDougall, L.K., Sola, M.M., Ikebe, M. & Cohen, Philip, 1992. The control of protein phosphatase-1 by targetting subunits. The major myosin phosphatase in avian smooth muscle is a novel form of protein phosphatase-1. *European journal of biochemistry / FEBS*, 210(3), pp.1023-35.
- Alessi, D.R., Street, a J., Cohen, Philip & Cohen, P.T., 1993. Inhibitor-2 functions like a chaperone to fold three expressed isoforms of mammalian protein phosphatase-1 into a conformation with the specificity and regulatory properties of the native enzyme. *European journal of biochemistry / FEBS*, 213(3), pp.1055-66.
- Anker, S.D. & Coats, A.J.S., 2002. How to RECOVER from RENAISSANCE? The significance of the results of RECOVER, RENAISSANCE, RENEWAL and ATTACH. *International journal of cardiology*, 86(2-3), pp.123-30.
- Aoyama, H., Ikeda, Y., Miyazaki, Y., Yoshimura, K., Nishino, S., Yamamoto, T., Yano, M., Inui, M., Aoki, H. & Matsuzaki, M., 2011. Isoform-specific roles of protein phosphatase 1 catalytic subunits in sarcoplasmic reticulum-mediated Ca(2+) cycling. *Cardiovascular research*, 89(1), pp.79-88.
- Armstrong, C.G., Doherty, M.J. & Cohen, P.T.W., 1998. Glycogen and protein phosphatase 1. *Insulin*, 704, pp.699-704.
- Bajorath, J., 2002. INTEGRATION OF VIRTUAL AND HIGH-THROUGHPUT SCREENING. *Nature Publishing Group*, 1(November), pp.882-894.
- Baker, M., 2010. Academic screening goes high-throughput. *Nature Publishing Group*, 7(10), pp.787-792.
- Barford, D., Das, A.K. & Egloff, M.P., 1998. The structure and mechanism of protein phosphatases: insights into catalysis and regulation. *Annual review of biophysics and biomolecular structure*, 27, pp.133-64.
- Bartel, S., Stein, B., Eschenhagen, T., Mende, U., Neumann, J., Schmitz, W, Krause, E.G., Karczewski, P. & Scholz, H, 1996. Protein phosphorylation in isolated trabeculae from nonfailing and failing human hearts. *Molecular and cellular biochemistry*, 157(1-2), pp.171-9.

- Bauss, F. & Schimmer, R.C., 2006. Ibandronate: the first once-monthly oral bisphosphonate for treatment of postmenopausal osteoporosis. *Therapeutics and clinical risk management*, 2(1), pp.3-18.
- Bers, D.M., 2002a. Cardiac excitation-contraction coupling. *Nature*, 415(6868), pp.198-205.
- Bers, D.M., 2002b. Sarcoplasmic reticulum Ca release in intact ventricular myocytes. *Frontiers in bioscience*: a journal and virtual library, 7, pp.d1697-711.
- Bers, D.M. & Harris, S.P., 2011. Translational medicine: to the rescue of the failing heart. *Nature*, 473(7345), pp.36-9.
- Beullens, M, Eynde, A. Van, Vulsteke, V., Connor, J.H., Shenolikar, S, Stalmans, W & Bollen, M, 1999. Molecular determinants of nuclear protein phosphatase-1 regulation by NIPP-1. *The Journal of biological chemistry*, 274(20), pp.14053-61.
- Bollen, Mathieu, Peti, W., Ragusa, M.J. & Beullens, Monique, 2010. The extended PP1 toolkit: designed to create specificity. *Trends in biochemical sciences*, 35(8), pp.450-8.
- Bouaícha, N., Maatouk, I., Vincent, G. & Levi, Y., 2002. A colorimetric and fluorometric microplate assay for the detection of microcystin-LR in drinking water without preconcentration. *Food and chemical toxicology*: an international journal published for the British Industrial Biological Research Association, 40(11), pp.1677-83.
- Boyce, M., Bryant, K.F., Jousse, C., Long, K., Harding, H.P., Scheuner, D., Kaufman, R.J., Ma, D., Coen, D.M., Ron, D. & Yuan, J., 2005. A selective inhibitor of eIF2 α dephosphorylation protects cells from ER stress. *Science (New York, N.Y.)*, 307(5711), pp.935-9.
- Bradford, M.M., 1976. A rapid and sensitive method for the quantitation of microgram quantities of protein utilizing the principle of protein-dye binding. *Analytical biochemistry*, 72, pp.248-54.
- Braz, J.C., Gregory, K., Pathak, A., Zhao, W., Sahin, B., Klevitsky, R., Kimball, T.F., Lorenz, J.N., Nairn, Angus C, Liggett, S.B., Bodi, I., Wang, S., Schwartz, A., Lakatta, E.G., et al., 2004. PKC- α regulates cardiac contractility and propensity toward heart failure. *Nature medicine*, 10(3), pp.248-54.
- Bristow, M.R., Ginsburg, R., Minobe, W., Cubicciotti, R.S., Sageman, W.S., Lurie, K., Billingham, M.E., Harrison, D.C. & Stinson, E.B., 1982. Decreased catecholamine sensitivity and beta-adrenergic-receptor density in failing human hearts. *The New England journal of medicine*, 307(4), pp.205-11.
- Brodde, O.-E., Bruck, H. & Leineweber, K., 2006. Cardiac Adrenoceptors: Physiological and Pathophysiological Relevance. *Journal of Pharmacological Sciences*, 100(5), pp.323-337.

- Brodde, O.E., 1991. Beta 1- and beta 2-adrenoceptors in the human heart: properties, function, and alterations in chronic heart failure. *Pharmacological reviews*, 43(2), pp.203-42.
- Brodde, O.E. & Michel, M.C., 1999. Adrenergic and muscarinic receptors in the human heart. *Pharmacological reviews*, 51(4), pp.651-90.
- Buchwald, P., 2010. Small-molecule protein-protein interaction inhibitors: therapeutic potential in light of molecular size, chemical space, and ligand binding efficiency considerations. *IUBMB life*, 62(10), pp.724-31.
- Bylund, D.B., Eikenberg, D.C., Hieble, J.P., Langer, S.Z., Lefkowitz, R.J., Minneman, K.P., Molinoff, P.B., Ruffolo, R.R. & Trendelenburg, U., 1994. International Union of Pharmacology nomenclature of adrenoceptors. *Pharmacological reviews*, 46(2), pp.121-36.
- Carr, A.N., Schmidt, A.G., Suzuki, Y., Monte, F. del, Sato, Y., Lanner, C., Breeden, K., Jing, S.-L., Allen, Patrick B, Greengard, Paul, Yatani, A., Hoit, Brian D, Grupp, Ingrid L, Hajjar, R.J., 2002. Type 1 phosphatase, a negative regulator of cardiac function. *Molecular and cellular biology*, 22(12), pp.4124-35.
- Cazorla, O., Szilagyi, S., Vignier, N., Salazar, G., Krämer, E., Vassort, G., Carrier, L. & Lacampagne, A., 2006. Length and protein kinase A modulations of myocytes in cardiac myosin binding protein C-deficient mice. *Cardiovascular research*, 69(2), pp.370-80.
- Ceulemans, H., Stalmans, Willy & Bollen, M, 2002. Regulator-driven functional diversification of protein phosphatase-1 in eukaryotic evolution. *BioEssays*: news and reviews in molecular, cellular and developmental biology, 24(4), pp.371-81.
- Ceulemans, H. & Bollen, M, 2004. Functional diversity of protein phosphatase-1, a cellular economizer and reset button. *Physiological reviews*, 84(1), pp.1-39.
- Ceulemans, H. & Bollen, M, 2006. A tighter RVxF motif makes a finer Sift. *Chemistry & biology*, 13(1), pp.6-8.
- Chang, M.W., Ayeni, C., Breuer, S. & Torbett, B.E., 2010. Virtual screening for HIV protease inhibitors: a comparison of AutoDock 4 and Vina. *PloS one*, 5(8), p.e11955.
- Cheng, A.C., Coleman, R.G., Smyth, K.T., Cao, Q., Soulard, P., Caffrey, D.R., Salzberg, A.C. & Huang, E.S., 2007. Structure-based maximal affinity model predicts small-molecule druggability. *Nature biotechnology*, 25(1), pp.71-5.
- Chiariello, M. & Perrone-Filardi, P., 1999. Pathophysiology of Heart Failure. *Current*, pp.6-10.

- Chisholm, A.A. & Cohen, P., 1988. The myosin-bound form of protein phosphatase 1 (PP-1M) is the enzyme that dephosphorylates native myosin in skeletal and cardiac muscles. *Biochimica et biophysica acta*, 971(2), pp.163-9.
- Christian, F., Szaszák, M., Friedl, S., Drewianka, S., Lorenz, D., Goncalves, A., Furkert, J., Vargas, C., Schmieder, P., Götz, F., Zühlke, K., Moutty, M., Göttert, H., Joshi, M., 2011. Small molecule AKAP-protein kinase A (PKA) interaction disruptors that activate PKA interfere with compartmentalized cAMP signaling in cardiac myocytes. *The Journal of biological chemistry*, 286(11), pp.9079-96.
- Christopoulos, A., 2002. Allosteric binding sites on cell-surface receptors: novel targets for drug discovery. *Nature reviews. Drug discovery*, 1(3), pp.198-210.
- Clackson, T. & Wells, J A, 1995. A hot spot of binding energy in a hormone-receptor interface. *Science (New York, N.Y.)*, 267(5196), pp.383-6.
- Cochran, A.G., 2000. Antagonists of protein-protein interactions. *Chemistry & biology*, 7(4), pp.R85-94.
- Cohen, P., 1989. The structure and regulation of protein phosphatases. *Annual review of biochemistry*, 58, pp.453-508.
- Cohen, P.T., 1988. Two isoforms of protein phosphatase 1 may be produced from the same gene. *FEBS letters*, 232(1), pp.17-23.
- Cohen, P.T., 2002. Protein phosphatase 1--targeted in many directions. *Journal of cell science*, 115(Pt 2), pp.241-56.
- Cohn, J.N., Pfeffer, M.A., Rouleau, J., Sharpe, N., Swedberg, K., Straub, M., Wiltse, C. & Wright, T.J., 2003. Adverse mortality effect of central sympathetic inhibition with sustained-release moxonidine in patients with heart failure (MOXCON). *European journal of heart failure*, 5(5), pp.659-67.
- Communal, C., Singh, K., Sawyer, D.B. & Colucci, W.S., 1999. Opposing effects of beta(1)- and beta(2)-adrenergic receptors on cardiac myocyte apoptosis: role of a pertussis toxin-sensitive G protein. *Circulation*, 100(22), pp.2210-2.
- Connor, J.H., Quan, H.N., Ramaswamy, N.T., Zhang, L., Barik, S., Zheng, J., Cannon, J.F., Lee, E.Y. & Shenolikar, S, 1998. Inhibitor-1 interaction domain that mediates the inhibition of protein phosphatase-1. *The Journal of biological chemistry*, 273(42), pp.27716-24.
- Connor, J.H., Weiser, D C, Li, S, Hallenbeck, J.M. & Shenolikar, S, 2001. Growth arrest and DNA damage-inducible protein GADD34 assembles a novel signaling complex containing protein phosphatase 1 and inhibitor 1. *Molecular and cellular biology*, 21(20), pp.6841-50.
- Cowie, M.R., Mosterd, A., Wood, D.A., Deckers, J.W., Poole-Wilson, P.A., Sutton, G.C., Grobbee, D.E. 1997. The epidemiology of heart failure. *Eur Heart J*. 18(2):208-25.

- Dancheck, B., Nairn, A.C. & Peti, W., 2008. Detailed structural characterization of unbound protein phosphatase 1 inhibitors. *Biochemistry*, 47(47), pp.12346-56.
- Delgado, R.M. & Willerson, J.T., 1999. Pathophysiology of Heart Failure A Look at the Future. , 26(1).
- Depaoli-Roach, A.A., Park, I.K., Cerovsky, V., Csontos, C., Durbin, S.D., Kuntz, M.J., Sitikov, A., Tang, P.M., Verin, A. & Zolnierowicz, S., 1994. Serine/threonine protein phosphatases in the control of cell function. *Advances in enzyme regulation*, 34, pp.199-224.
- Dobson, C.M., 2004. Chemical space and biology. *Nature*, 432(7019), pp.824-8.
- Dorr, P., Westby, M., Dobbs, S., Griffin, P., Irvine, B., Macartney, M., Mori, J., Rickett, G., Smith-Burchnell, C., Napier, C., Webster, R., Armour, D., Price, D., Stammen, B., 2005. Maraviroc (UK-427,857), a potent, orally bioavailable, and selective small-molecule inhibitor of chemokine receptor CCR5 with broad-spectrum anti-human immunodeficiency virus type 1 activity. *Antimicrobial agents and chemotherapy*, 49(11), pp.4721-32.
- Drews, J., 2000. Drug Discovery: A Historical Perspective. *Science*, 287(5460), pp.1960-1964.
- Duchardt, F., Fotin-Mleczek, M., Schwarz, H., Fischer, R. & Brock, R., 2007. A comprehensive model for the cellular uptake of cationic cell-penetrating peptides. *Traffic (Copenhagen, Denmark)*, 8(7), pp.848-66.
- Eckstein, J., 2008. ISOA / ARF Drug Development Tutorial. *Alzheimer Research Forum*.
- Egloff, M.P., Cohen, P.T., Reinemer, P. & Barford, D., 1995. Crystal structure of the catalytic subunit of human protein phosphatase 1 and its complex with tungstate. *Journal of molecular biology*, 254(5), pp.942-59.
- Egloff, M.P., Johnson, D.F., Moorhead, G., Cohen, P.T., Cohen, P. & Barford, D., 1997. Structural basis for the recognition of regulatory subunits by the catalytic subunit of protein phosphatase 1. *The EMBO journal*, 16(8), pp.1876-87.
- El-Armouche, A., Rau, T., Zolk, O., Ditz, D., Pamminger, T., Zimmermann, W.H., Jäckel, E., Harding, S.E., Boknik, P., Neumann, J. & Eschenhagen, T., 2003a. Evidence for protein phosphatase inhibitor-1 playing an amplifier role in beta-adrenergic signaling in cardiac myocytes. *The FASEB journal*: official publication of the Federation of American Societies for Experimental Biology, 17(3), pp.437-9.
- El-Armouche, A., Zolk, O., Rau, T. & Eschenhagen, T., 2003b. Inhibitory G-proteins and their role in desensitization of the adenylyl cyclase pathway in heart failure. *Cardiovascular research*, 60(3), pp.478-87.

- El-Armouche, A., Pamminger, T., Ditz, D., Zolk, O. & Eschenhagen, T., 2004. Decreased protein and phosphorylation level of the protein phosphatase inhibitor-1 in failing human hearts. *Cardiovascular research*, 61(1), pp.87-93.
- El-Armouche, A., Bednorz, A., Pamminger, T., Ditz, D., Didié, M., Dobrev, D. & Eschenhagen, T., 2006a. Role of calcineurin and protein phosphatase-2A in the regulation of phosphatase inhibitor-1 in cardiac myocytes. *Biochemical and biophysical research communications*, 346(3), pp.700-6.
- El-Armouche, A., Boknik, P., Eschenhagen, T., Carrier, L., Knaut, M., Ravens, U. & Dobrev, D., 2006b. Molecular determinants of altered Ca²⁺ handling in human chronic atrial fibrillation. *Circulation*, 114(7), pp.670-80.
- El-Armouche, A., Pohlmann, L., Schlossarek, S., Starbatty, J., Yeh, Y.-H., Nattel, S., Dobrev, D., Eschenhagen, T. & Carrier, L., 2007a. Decreased phosphorylation levels of cardiac myosin-binding protein-C in human and experimental heart failure. *Journal of molecular and cellular cardiology*, 43(2), pp.223-9.
- El-Armouche, A., Singh, J., Naito, H., Wittköpper, K., Didié, M., Laatsch, A., Zimmermann, W.H. & Eschenhagen, T., 2007b. Adenovirus-delivered short hairpin RNA targeting PKC alpha improves contractile function in reconstituted heart tissue. *Journal of molecular and cellular cardiology*, 43(3), pp.371-6.
- El-Armouche, A., Wittköpper, K., Degenhardt, F., Weinberger, F., Didié, M., Melnychenko, I., Grimm, M., Peeck, M., Zimmermann, W.H., Unsöld, B., Hasenfuss, G., Dobrev, D. & Eschenhagen, T., 2008. Phosphatase inhibitor-1-deficient mice are protected from catecholamine-induced arrhythmias and myocardial hypertrophy. *Cardiovascular research*, 80(3), pp.396-406.
- El-Armouche, A. & Eschenhagen, T., 2009. Beta-adrenergic stimulation and myocardial function in the failing heart. *Heart failure reviews*, 14(4), pp.225-41.
- El-Armouche, A., Wittköpper, K., Fuller, W., Howie, J., Shattock, M.J. & Pavlovic, D., 2011. Phospholemman-dependent regulation of the cardiac Na/K-ATPase activity is modulated by inhibitor-1 sensitive type-1 phosphatase. *The FASEB journal*: official publication of the Federation of American Societies for Experimental Biology, 25(12), pp.4467-75.
- Elbrecht, A., DiRenzo, J., Smith, R.G. & Shenolikar, S., 1990. Molecular cloning of protein phosphatase inhibitor-1 and its expression in rat and rabbit tissues. *The Journal of biological chemistry*, 265(23), pp.13415-8.
- Endo, S., Zhou, X., Connor, J.H., Wang, B. & Shenolikar, S., 1996. Multiple structural elements define the specificity of recombinant human inhibitor-1 as a protein phosphatase-1 inhibitor. *Biochemistry*, 35(16), pp.5220-8.
- Endo, S., Connor, J.H., Forney, B., Zhang, L., Ingebritsen, T.S., Lee, E.Y. & Shenolikar, S., 1997. Conversion of protein phosphatase 1 catalytic subunit to a Mn(2+)-dependent enzyme impairs its regulation by inhibitor 1. *Biochemistry*, 36(23), pp.6986-92.

- Eschenhagen, T., 2008. Beta-adrenergic signaling in heart failure-adapt or die. *Nature medicine*, 14(5), pp.485-7.
- Feldman, D.S., Carnes, C.A., Abraham, W.T. & Bristow, M.R., 2005. Mechanisms of Disease□: β -adrenergic receptors — alterations in signal transduction and pharmacogenomics in heart failure REVIEW CRITERIA. *Nature Clinical Practice Cardiovascular Medicine*, 2(9), pp.475-483.
- Ferrari, A., Pellegrini, V., Arcangeli, C., Fittipaldi, A., Giacca, M. & Beltram, F., 2003. Caveolae-mediated internalization of extracellular HIV-1 tat fusion proteins visualized in real time. *Molecular therapy□: the journal of the American Society of Gene Therapy*, 8(2), pp.284-94.
- Fischmeister, R., Castro, L.R.V., Abi-Gerges, A., Rochais, F., Jurevicius, J., Leroy, J. & Vandecasteele, G., 2006. Compartmentation of cyclic nucleotide signaling in the heart: the role of cyclic nucleotide phosphodiesterases. *Circulation research*, 99(8), pp.816-28.
- Fontal, O.I., Vieytes, M.R., Baptista de Sousa, J.M., Louzao, M.C. & Botana, L.M., 1999. A fluorescent microplate assay for microcystin-LR. *Analytical biochemistry*, 269(2), pp.289-96.
- Foulkes, J.G., Jefferson, L.S. & Cohen, P., 1980. The hormonal control of glycogen metabolism: dephosphorylation of protein phosphatase inhibitor-1 in vivo in response to insulin. *FEBS letters*, 112(1), pp.21-4.
- Fry, D.C., 2006. Protein – Protein Interactions as Targets for Small Molecule Drug Discovery. *Biopolymers*, 84(July), pp.535-552.
- Fuchs, S., Kasher, R., Balass, M., Scherf, T., Harel, M., Fridkin, M., Sussman, J.L. & Katchalski-Katzir, E., 2003. The binding site of acetylcholine receptor: from synthetic peptides to solution and crystal structure. *Annals of the New York Academy of Sciences*, 998, pp.93-100.
- Gee, K.R., Sun, W.C., Bhargat, M.K., Upson, R.H., Klaubert, D.H., Latham, K.A. & Haugland, R.P., 1999. Fluorogenic substrates based on fluorinated umbelliferones for continuous assays of phosphatases and beta-galactosidases. *Analytical biochemistry*, 273(1), pp.41-8.
- Geladopoulos, T.P., Sotiroidis, T.G. & Evangelopoulos, A.E., 1991. A malachite green colorimetric assay for protein phosphatase activity. *Analytical biochemistry*, 192(1), pp.112-6.
- Goldberg, J., Huang, H.B., Kwon, Y.G., Greengard, P, Nairn, A C & Kuriyan, J., 1995. Three-dimensional structure of the catalytic subunit of protein serine/threonine phosphatase-1. *Nature*, 376(6543), pp.745-53.
- Goodman, I.S., 1996. No Title. In *Goodman and GilmanŌs. The Pharmacological Basis of Therapeutics*. McGraw-Hill.

- Gordon, J.A., 1991. Use of vanadate as protein-phosphotyrosine phosphatase inhibitor. *Methods in enzymology*, 201, pp.477-82.
- Gupta, R C, Neumann, J, Watanabe, A.M., Lesch, M. & Sabbah, H N, 1996. Evidence for presence and hormonal regulation of protein phosphatase inhibitor-1 in ventricular cardiomyocyte. *The American journal of physiology*, 270(4 Pt 2), pp.H1159-64.
- Gupta, Ramesh C, Mishra, S., Rastogi, S., Imai, M., Habib, O. & Sabbah, H.N., 2003. Cardiac SR-coupled PP1 activity and expression are increased and inhibitor 1 protein expression is decreased in failing hearts. *American journal of physiology. Heart and circulatory physiology*, 285(6), pp.H2373-81.
- Hansen, A., Eder, A., Bönstrup, M., Flato, M., Mewe, M., Schaaf, S., Aksehirlioglu, B., Schwörer, A., Uebeler, J. & Eschenhagen, T., 2010. Development of a drug screening platform based on engineered heart tissue. *Circulation research*, 107(1), pp.35-44.
- Hemmings, H.C., Nairn, A C & Greengard, P, 1984. DARPP-32, a dopamine- and adenosine 3':5'-monophosphate-regulated neuronal phosphoprotein. II. Comparison of the kinetics of phosphorylation of DARPP-32 and phosphatase inhibitor 1. *The Journal of biological chemistry*, 259(23), pp.14491-7.
- Hemmings, H.C., Girault, J.A., Nairn, A C, Bertuzzi, G. & Greengard, P, 1992. Distribution of protein phosphatase inhibitor-1 in brain and peripheral tissues of various species: comparison with DARPP-32. *Journal of neurochemistry*, 59(3), pp.1053-61.
- Herce, H.D., Garcia, A.E., Litt, J., Kane, R.S., Martin, P., Enrique, N., Rebolledo, A. & Milesi, V., 2009. Arginine-rich peptides destabilize the plasma membrane, consistent with a pore formation translocation mechanism of cell-penetrating peptides. *Biophysical journal*, 97(7), pp.1917-25.
- Herzig, S. & Neumann, J., 2000. Effects of serine/threonine protein phosphatases on ion channels in excitable membranes. *Physiological reviews*, 80(1), pp.173-210.
- Ho, K.K., Pinsky, J.L., Kannel, W.B., Levy, D. 1993. The epidemiology of heart failure: the Framingham Study. *J Am Coll Cardiol* (4 Suppl A):6A-13A
- Hoekema, A., 2007. Sharing risks and rewards—basis for a turnkey pharma-biotech alliance in osteoarthritis. *Drug Disc. World Spring*, 54.
- Honkanen, R. E., Zwiller, J., Moore, R.E., Daily, S.L., Khatra, B.S., Dukelow, M. & Boynton, A.L., 1990. Characterization of microcystin-LR, a potent inhibitor of type 1 and type 2A protein phosphatases. *The Journal of biological chemistry*, 265(32), pp.19401-4.
- Honkanen, R. E., 1993. Cantharidin, another natural toxin that inhibits the activity of serine/threonine protein phosphatases types 1 and 2A. *FEBS letters*, 330(3), pp.283-6.

- Honkanen, R. E. & Golden, T., 2002. Regulators of serine/threonine protein phosphatases at the dawn of a clinical era? *Current medicinal chemistry*, 9(22), pp.2055-75.
- Hsieh-Wilson, L.C., Allen, P B, Watanabe, T., Nairn, A C & Greengard, P, 1999. Characterization of the neuronal targeting protein spinophilin and its interactions with protein phosphatase-1. *Biochemistry*, 38(14), pp.4365-73.
- Huang, H.B., Horiuchi, A., Goldberg, J., Greengard, P & Nairn, A C., 1997. Site-directed mutagenesis of amino acid residues of protein phosphatase 1 involved in catalysis and inhibitor binding. *Proceedings of the National Academy of Sciences of the United States of America*, 94(8), pp.3530-5.
- Huang, H.B., Horiuchi, A., Watanabe, T., Shih, S.R., Tsay, H.J., Li, H.C., Greengard, P & Nairn, A. C., 1999. Characterization of the inhibition of protein phosphatase-1 by DARPP-32 and inhibitor-2. *The Journal of biological chemistry*, 274(12), pp.7870-8.
- Huang, H.B., Chen, Y.C., Tsai, L.H., Wang, H., Lin, F.M., Horiuchi, A., Greengard, P, Nairn, A C, Shiao, M.S. & Lin, T.H., 2000. Backbone ¹H, ¹⁵N, and ¹³C resonance assignments of inhibitor-2 -- a protein inhibitor of protein phosphatase-1. *Journal of biomolecular NMR*, 17(4), pp.359-60.
- Hunter, T., 1995. Protein kinases and phosphatases: the yin and yang of protein phosphorylation and signaling. *Cell*, 80(2), pp.225-36.
- Ingebritsen, T.S. & Cohen, P., 1983. The protein phosphatases involved in cellular regulation. 1. Classification and substrate specificities. *European journal of biochemistry / FEBS*, 132(2), pp.255-61.
- Ingebritsen, T.S., Stewart, A.A. & Cohen, P., 1983. The protein phosphatases involved in cellular regulation. 6. Measurement of type-1 and type-2 protein phosphatases in extracts of mammalian tissues; an assessment of their physiological roles. *European journal of biochemistry / FEBS*, 132(2), pp.297-307.
- Jackson, G., Gibbs, C.R., Davies, M.K. & Lip, G.Y.H., 2000. Pathophysiology Myocardial systolic dysfunction Neurohormonal activation. *Heart Failure*, pp.167-170.
- Jones, S. & Thornton, J.M., 1996. Principles of protein-protein interactions. *Proceedings of the National Academy of Sciences of the United States of America*, 93(1), pp.13-20.
- Kadambi, V.J., Ponniah, S., Harrer, J.M., Hoit, B D, Dorn, G.W., Walsh, R.A. & Kranias, E.G., 1996. Cardiac-specific overexpression of phospholamban alters calcium kinetics and resultant cardiomyocyte mechanics in transgenic mice. *The Journal of clinical investigation*, 97(2), pp.533-9.

- Kaye, D.M., Smirk, B., Finch, S., Williams, C. & Esler, M.D., 2004. Interaction between cardiac sympathetic drive and heart rate in heart failure: modulation by adrenergic receptor genotype. *Journal of the American College of Cardiology*, 44(10), pp.2008-15.
- Kita, A., Matsunaga, S., Takai, Akira, Kataiwa, H., Wakimoto, T., Fusetani, N., Isobe, Minoru & Miki, K., 2002. Crystal structure of the complex between calyculin A and the catalytic subunit of protein phosphatase 1. *Structure (London, England)*: 1993), 10(5), pp.715-24.
- Kitchen, D.B., Decornez, H., Furr, J.R. & Bajorath, J., 2004. Docking and scoring in virtual screening for drug discovery: methods and applications. *Nature reviews. Drug discovery*, 3(11), pp.935-49.
- Klabunde, R.E., 2007. Normal heart rhythm. *Cardiovascular physiology concepts*.
- Kranias, E.G. & Salvo, J., 1986. A phospholamban protein phosphatase activity associated with cardiac sarcoplasmic reticulum. *The Journal of biological chemistry*, 261(22), pp.10029-32.
- Kwon, Y.G., Huang, H.B., Desdouits, F., Girault, J.A., Greengard, P & Nairn, A.C., 1997. Characterization of the interaction between DARPP-32 and protein phosphatase 1 (PP-1): DARPP-32 peptides antagonize the interaction of PP-1 with binding proteins. *Proceedings of the National Academy of Sciences of the United States of America*, 94(8), pp.3536-41.
- Lankoff, A., Bialczyk, J., Dziga, D., Carmichael, W.W., Gradzka, I., Lisowska, H., Kuszewski, T., Gozdz, S., Piorun, I. & Wojcik, A., 2006. The repair of gamma-radiation-induced DNA damage is inhibited by microcystin-LR, the PP1 and PP2A phosphatase inhibitor. *Mutagenesis*, 21(1), pp.83-90.
- Lax, R., 2010. The Future of Peptide Development in the Pharmaceutical Industry. *PharManufacturing:The International Peptide Review*, pp.10-15.
- Lefkowitz, R.J., Rockman, H.A. & Koch, W.J., 2000. Catecholamines, cardiac beta-adrenergic receptors, and heart failure. *Circulation*, 101(14), pp.1634-7.
- Lin, T.-H., Tsai, P.-C., Liu, H.-T., Chen, Y.-C., Wang, L.-H., Hsieh, F.-K. & Huang, H.-B., 2005. Characterization of the protein phosphatase 1-binding motifs of inhibitor-2 and DARPP-32 by surface plasmon resonance. *Journal of biochemistry*, 138(6), pp.697-700.
- Lindemann, J.P., Jones, L.R., Hathaway, D.R., Henry, B.G. & Watanabe, A.M., 1983. beta-Adrenergic stimulation of phospholamban phosphorylation and Ca²⁺-ATPase activity in guinea pig ventricles. *The Journal of biological chemistry*, 258(1), pp.464-71.
- Lindemann, J.P. & Watanabe, A.M., 1985. Phosphorylation of phospholamban in intact myocardium. Role of Ca²⁺-calmodulin-dependent mechanisms. *The Journal of biological chemistry*, 260(7), pp.4516-25.

- Lindsay, M. A., 2003. Target discovery. *Nature reviews. Drug discovery*, 2(10), pp.831-8.
- Lohse, M.J., Engelhardt, S. & Eschenhagen, T., 2003. What is the role of beta-adrenergic signaling in heart failure? *Circulation research*, 93(10), pp.896-906.
- Lowes, B.D., Gilbert, E.M., Abraham, W.T., Minobe, W.A., Larrabee, P., Ferguson, D., Wolfel, E.E., Lindenfeld, J., Tsvetkova, T., Robertson, A.D., Quaife, R.A. & Bristow, M.R., 2002. Myocardial gene expression in dilated cardiomyopathy treated with beta-blocking agents. *The New England journal of medicine*, 346(18), pp.1357-65.
- Luo, W., Grupp, I L, Harrer, J., Ponniah, S., Grupp, G., Duffy, J.J., Doetschman, T. & Kranias, E.G., 1994. Targeted ablation of the phospholamban gene is associated with markedly enhanced myocardial contractility and loss of beta-agonist stimulation. *Circulation research*, 75(3), pp.401-9.
- Lüss, H., Klein-Wiele, O., Bokník, P., Herzig, S., Knapp, J., Linck, B., Müller, F.U., Scheld, H.H., Schmid, C., Schmitz, W & Neumann, J., 2000. Regional expression of protein phosphatase type 1 and 2A catalytic subunit isoforms in the human heart. *Journal of molecular and cellular cardiology*, 32(12), pp.2349-59.
- MacDougall, L.K., Campbell, D.G., Hubbard, M.J. & Cohen, P., 1989. Partial structure and hormonal regulation of rabbit liver inhibitor-1; distribution of inhibitor-1 and inhibitor-2 in rabbit and rat tissues. *Biochimica et biophysica acta*, 1010(2), pp.218-26.
- MacDougall, L.K., Jones, L.R. & Cohen, P., 1991. Identification of the major protein phosphatases in mammalian cardiac muscle which dephosphorylate phospholamban. *European journal of biochemistry / FEBS*, 196(3), pp.725-34.
- MacMillan, L.B., Bass, M.A., Cheng, N., Howard, E.F., Tamura, M., Strack, S., Wadzinski, B.E. & Colbran, R J, 1999. Brain actin-associated protein phosphatase 1 holoenzymes containing spinophilin, neurabin, and selected catalytic subunit isoforms. *The Journal of biological chemistry*, 274(50), pp.35845-54.
- Marx, S.O., Reiken, S., Hisamatsu, Y., Jayaraman, T., Burkhoff, D., Rosemblyt, N. & Marks, A.R., 2000. PKA phosphorylation dissociates FKBP12.6 from the calcium release channel (ryanodine receptor): defective regulation in failing hearts. *Cell*, 101(4), pp.365-76.
- Maynes, J.T., Bateman, K.S., Cherney, M.M., Das, a K., Luu, H. a, Holmes, C.F. & James, M.N., 2001. Crystal structure of the tumor-promoter okadaic acid bound to protein phosphatase-1. *The Journal of biological chemistry*, 276(47), pp.44078-82.
- Messer, A.E., Jacques, A.M. & Marston, S.B., 2007. Troponin phosphorylation and regulatory function in human heart muscle: dephosphorylation of Ser23/24 on

- troponin I could account for the contractile defect in end-stage heart failure. *Journal of molecular and cellular cardiology*, 42(1), pp.247-59.
- Mirzaei M, Yen L, Leeder SR. 2007. Epidemiology of chronic heart failure. The Serious and Continuing Illness Policy and Practice Study (SCIPPS), The Menzies Centre for Health Policy
- Molkentin, J. D., Lu, J.R., Antos, C.L., Markham, B., Richardson, J., Robbins, J, Grant, S.R. & Olson, E.N., 1998. A calcineurin-dependent transcriptional pathway for cardiac hypertrophy. *Cell*, 93(2), pp.215-28.
- Moorhead, G.B.G., Trinkle-Mulcahy, L. & Ulke-Lemée, A., 2007. Emerging roles of nuclear protein phosphatases. *Nature reviews. Molecular cell biology*, 8(3), pp.234-44.
- Morrissey, R.P., Czer, L. & Shah, P.K., 2011. Chronic heart failure: current evidence, challenges to therapy, and future directions. *American journal of cardiovascular drugs*: drugs, devices, and other interventions, 11(3), pp.153-71.
- Mountfort, D.O., Kennedy, G., Garthwaite, I., Quilliam, M., Truman, P. & Hannah, D.J., 1999. Evaluation of the fluorometric protein phosphatase inhibition assay in the determination of okadaic acid in mussels. *Toxicology: official journal of the International Society on Toxinology*, 37(6), pp.909-22.
- Mulkey, R.M., Endo, S., Shenolikar, S. & Malenka, R.C., 1994. Involvement of a calcineurin/inhibitor-1 phosphatase cascade in hippocampal long-term depression. *Nature*, 369(6480), pp.486-8.
- Neumann, J., Gupta, Ramesh C, Schmitz, Wilhelm & Scholz, Hasso, 1991. Evidence for Isoproterenol-Induced Phosphorylation of Phosphatase Inhibitor-1 in the Intact Heart. *Circulation Research*.
- Neumann, J., Bokn  k, P., Herzig, S., Schmitz, W, Scholz, H, Wiechen, K. & Zimmermann, N., 1994. Biochemical and electrophysiological mechanisms of the positive inotropic effect of calyculin A, a protein phosphatase inhibitor. *The Journal of pharmacology and experimental therapeutics*, 271(1), pp.535-41.
- Neumann, J., Eschenhagen, T., Jones, L.R., Linck, B., Schmitz, W, Scholz, H & Zimmermann, N., 1997. Increased expression of cardiac phosphatases in patients with end-stage heart failure. *Journal of molecular and cellular cardiology*, 29(1), pp.265-72.
- Nimmo, G.A. & Cohen, P., 1978. The regulation of glycogen metabolism. Purification and characterisation of protein phosphatase inhibitor-1 from rabbit skeletal muscle. *European journal of biochemistry / FEBS*, 87(2), pp.341-51.
- Noble, J.E., Ganju, P. & Cass, A.E.G., 2003. Fluorescent peptide probes for high-throughput measurement of protein phosphatases. *Analytical chemistry*, 75(9), pp.2042-7.

- Olsen, J.V., Blagoev, B., Gnädig, F., Macek, B., Kumar, C., Mortensen, P. & Mann, M., 2006. Global, in vivo, and site-specific phosphorylation dynamics in signaling networks. *Cell*, 127(3), pp.635-48.
- Opie, L.H., 2008. Mechanisms of cardiac contraction and relaxation. In P. Libby, R. O. Bonow, D. P. Zipes, D. L. Mann, & E. Braunwald, eds. *Braunwald's Heart Disease*. pp. 509-520.
- O'Connell, T.D.O., Ni, Y.G., Lin, K.-mean, Han, H. & Yan, Z., 2003. Isolation and Culture of Adult Mouse Cardiac Myocytes for Signaling Studies. *AFCS Research Reports*, 1(5), pp.1-9.
- Pathak, A., Monte, F., Zhao, W., Schultz, J.-E., Lorenz, J.N., Bodi, I., Weiser, D., Hahn, H., Carr, A.N., Syed, F., Mavila, N., Jha, L., Qian, J., Marreez, Y., Chen, G., McGraw, D.W., Heist, E.K., Guerrero, J Luis, DePaoli-Roach, Anna A, Hajjar, Roger J, Kranias, Evangelia G, 2005. Enhancement of cardiac function and suppression of heart failure progression by inhibition of protein phosphatase 1. *Circulation research*, 96(7), pp.756-66.
- Peti, W., Nairn, A. C. & Page, R., 2012. Structural Basis for Protein Phosphatase 1 Regulation and Specificity. *The FEBS journal*.
- Pohlmann, L., Kröger, I., Vignier, N., Schlossarek, S., Krämer, E., Coirault, C., Sultan, K.R., El-Armouche, A., Winegrad, S., Eschenhagen, T. & Carrier, L., 2007. Cardiac myosin-binding protein C is required for complete relaxation in intact myocytes. *Circulation research*, 101(9), pp.928-38.
- Port, J.D. & Bristow, M.R., 2001. beta-Adrenergic receptors, transgenic mice, and pharmacological model systems. *Molecular pharmacology*, 60(4), pp.629-31.
- Poulter, L., Ang, S.G., Gibson, B.W., Williams, D.H., Holmes, C.F., Caudwell, F.B., Pitcher, J. & Cohen, P., 1988. Analysis of the in vivo phosphorylation state of rabbit skeletal muscle glycogen synthase by fast-atom-bombardment mass spectrometry. *European journal of biochemistry / FEBS*, 175(3), pp.497-510.
- Rapundalo, S.T., 1998. Cardiac protein phosphorylation: functional and pathophysiological correlates. *Cardiovascular research*, 38(3), pp.559-88.
- Richard, J.P., Melikov, K., Vives, E., Ramos, C., Verbeure, B., Gait, M.J., Chernomordik, L.V. & Lebleu, B., 2003. Cell-penetrating peptides. A reevaluation of the mechanism of cellular uptake. *The Journal of biological chemistry*, 278(1), pp.585-90.
- Rodriguez, P., Mitton, B., Waggoner, J.R. & Kranias, E.G., 2006. Identification of a novel phosphorylation site in protein phosphatase inhibitor-1 as a negative regulator of cardiac function. *The Journal of biological chemistry*, 281(50), pp.38599-608.
- Russell, R.G. & Rogers, M.J., 1999. Bisphosphonates: from the laboratory to the clinic and back again. *Bone*, 25(1), pp.97-106.

- Sams-Dodd, F., 2005. Target-based drug discovery: is something wrong? *Drug discovery today*, 10(2), pp.139-47.
- Schillace, R.V. & Scott, J.D., 1999. Association of the type 1 protein phosphatase PP1 with the A-kinase anchoring protein AKAP220. *Current biology*: CB, 9(6), pp.321-4.
- Schillace, R.V., Voltz, J W, Sim, A.T., Shenolikar, S & Scott, J.D., 2001. Multiple interactions within the AKAP220 signaling complex contribute to protein phosphatase 1 regulation. *The Journal of biological chemistry*, 276(15), pp.12128-34.
- Schröder, F., Handrock, R., Beuckelmann, D.J., Hirt, S., Hullin, R., Priebe, L., Schwinger, R.H., Weil, J. & Herzig, S., 1998. Increased availability and open probability of single L-type calcium channels from failing compared with nonfailing human ventricle. *Circulation*, 98(10), pp.969-76.
- Shenolikar, S & Nairn, A. C., 1991. Protein phosphatases: recent progress. *Advances in second messenger and phosphoprotein research*, 23, pp.1-121.
- Shi, Y., 2009. Serine/threonine phosphatases: mechanism through structure. *Cell*, 139(3), pp.468-84.
- Smith, A., 2002. Screening for drug discovery: The leading question. *Nature*, 418, pp.453-459.
- Spencer, R.W., 1998. High-throughput screening of historic collections: observations on file size, biological targets, and file diversity. *Biotechnology and bioengineering*, 61(1), pp.61-7.
- Stelzer, J.E., Patel, J.R., Walker, J.W. & Moss, R.L., 2007. Differential roles of cardiac myosin-binding protein C and cardiac troponin I in the myofibrillar force responses to protein kinase A phosphorylation. *Circulation research*, 101(5), pp.503-11.
- Stevenson, L.W., 2003. Clinical use of inotropic therapy for heart failure: looking backward or forward? Part I: inotropic infusions during hospitalization. *Circulation*, 108(3), pp.367-72.
- Swingle, M.R., Ni, L. & Honkanen, R.E., 2007. Small-molecule inhibitors of ser/thr protein phosphatases: specificity, use and common forms of abuse. *Methods in molecular biology (Clifton, N.J.)*, 365, pp.23-38.
- Swingle, M.R., Amable, L., Lawhorn, B.G., Buck, S.B., Burke, C.P., Ratti, P., Fischer, K.L., Boger, D.L. & Honkanen, R.E., 2009. Structure-Activity Relationship Studies of Fostriecin , Cytostatin , and Key Analogs , with PP1 , PP2A , PP5 , and Further Insight into the Inhibitory Actions of Fostriecin Family Inhibitors. *Pharmacology*, 331(1), pp.45-53.

- Takai, A, Sasaki, K., Nagai, H., Mieskes, G., Isobe, M, Isono, K. & Yasumoto, T., 1995. Inhibition of specific binding of okadaic acid to protein phosphatase 2A by microcystin-LR, calyculin-A and tautomycin: method of analysis of interactions of tight-binding ligands with target protein. *The Biochemical journal*, 306 (Pt 3, pp.657-65.
- Tang, C., Iwahara, J. & Clore, G.M., 2006. Visualization of transient encounter complexes in protein-protein association. *Nature*, 444(7117), pp.383-6.
- Teerlink, J.R., 2002. Recent heart failure trials of neurohormonal modulation (OVERTURE and ENABLE): approaching the asymptote of efficacy? *Journal of cardiac failure*, 8(3), pp.124-7.
- Terrak, M., Kerff, F., Langsetmo, K., Tao, T. & Dominguez, R., 2004. Structural basis of protein phosphatase 1 regulation. *Nature*, 429(6993), pp.780-4.
- Terry-Lorenzo, R.T., Carmody, L.C., Voltz, James W, Connor, J.H., Li, Shi, Smith, F.D., Milgram, S.L., Colbran, Roger J & Shenolikar, S., 2002. The neuronal actin-binding proteins, neurabin I and neurabin II, recruit specific isoforms of protein phosphatase-1 catalytic subunits. *The Journal of biological chemistry*, 277(31), pp.27716-24.
- Trinkle-Mulcahy, L., Ajuh, P., Prescott, A., Claverie-Martin, F., Cohen, S., Lamond, A.I. & Cohen, P., 1999. Nuclear organisation of NIPP1, a regulatory subunit of protein phosphatase 1 that associates with pre-mRNA splicing factors. *Journal of cell science*, 112 (Pt 2, pp.157-68.
- Tsang, F.H., Lee, N.P. & Luk, J.M., 2009. The use of small peptides in the diagnosis and treatment of hepatocellular carcinoma. *Protein and peptide letters*, 16(5), pp.530-8.
- Tsaytler, P., Harding, H.P., Ron, D. & Bertolotti, A., 2011. Selective inhibition of a regulatory subunit of protein phosphatase 1 restores proteostasis. *Science (New York, N.Y.)*, 332(6025), pp.91-4.
- Tóth, A., Kiss, E., Herberg, F W, Gergely, P., Hartshorne, D.J. & Erdödi, F., 2000. Study of the subunit interactions in myosin phosphatase by surface plasmon resonance. *European journal of biochemistry / FEBS*, 267(6), pp.1687-97.
- Tünnemann, G., Ter-Avetisyan, G., Martin, R.M., Stöckl, M., Herrmann, A. & Cardoso, M.C., 2008. Live-cell analysis of cell penetration ability and toxicity of oligo-arginines. *Journal of peptide science* □: an official publication of the *European Peptide Society*, 14(4), pp.469-76.
- Uehata, M., Ishizaki, T., Satoh, H., Ono, T., Kawahara, T., Morishita, T., Tamakawa, H., Yamagami, K., Inui, J., Maekawa, M. & Narumiya, S., 1997. Calcium sensitization of smooth muscle mediated by a Rho-associated protein kinase in hypertension. *Nature*, 389(6654), pp.990-4.

- Vieytes, M.R., Fontal, O.I., Leira, F., Baptista de Sousa, J.M. & Botana, L.M., 1997. A fluorescent microplate assay for diarrheic shellfish toxins. *Analytical biochemistry*, 248(2), pp.258-64.
- Virshup, D.M. & Shenolikar, S., 2009. From promiscuity to precision: protein phosphatases get a makeover. *Molecular cell*, 33(5), pp.537-45.
- Vittone, L., Mundiña, C., Chiappe de Cingolani, G. & Mattiazzi, A., 1990. cAMP and calcium-dependent mechanisms of phospholamban phosphorylation in intact hearts. *The American journal of physiology*, 258(2 Pt 2), pp.H318-25.
- Wakula, P., Beullens, M., Ceulemans, H., Stalmans, W. & Bollen, M., 2003. Degeneracy and function of the ubiquitous RVXF motif that mediates binding to protein phosphatase-1. *The Journal of biological chemistry*, 278(21), pp.18817-23.
- Walker, D.H., DePaoli-Roach, A. A. & Maller, J.L., 1992. Multiple roles for protein phosphatase 1 in regulating the *Xenopus* early embryonic cell cycle. *Molecular biology of the cell*, 3(6), pp.687-98.
- Watanabe, T., Huang, H.B., Horiuchi, a, Cruze Silva, E.F. da, Hsieh-Wilson, L., Allen, P B, Shenolikar, S, Greengard, P & Nairn, A.C., 2001. Protein phosphatase 1 regulation by inhibitors and targeting subunits. *Proceedings of the National Academy of Sciences of the United States of America*, 98(6), pp.3080-5.
- Webster, K.A., Discher, D.J. & Bishopric, N.H., 1993. Induction and nuclear accumulation of fos and jun proto-oncogenes in hypoxic cardiac myocytes. *The Journal of biological chemistry*, 268(22), pp.16852-8.
- Wegener, A.D., Simmerman, H.K., Lindemann, J.P. & Jones, L.R., 1989. Phospholamban phosphorylation in intact ventricles. Phosphorylation of serine 16 and threonine 17 in response to beta-adrenergic stimulation. *The Journal of biological chemistry*, 264(19), pp.11468-74.
- Wehrens, X.H.T., Lehnart, S.E., Reiken, S.R. & Marks, A.R., 2004. Ca²⁺/calmodulin-dependent protein kinase II phosphorylation regulates the cardiac ryanodine receptor. *Circulation research*, 94(6), pp.e61-70.
- Weiser, Douglas C, Sikes, S., Li, S. & Shenolikar, S., 2004. The inhibitor-1 C terminus facilitates hormonal regulation of cellular protein phosphatase-1: functional implications for inhibitor-1 isoforms. *The Journal of biological chemistry*, 279(47), pp.48904-14.
- Wells, J. A & McClendon, C.L., 2007. Reaching for high-hanging fruit in drug discovery at protein-protein interfaces. *Nature*, 450(7172), pp.1001-9.
- Wittköpper, K., Fabritz, L., Neef, S., Ort, K.R., Grefe, C., Unsöld, B., Kirchhof, P., Maier, L.S., Hasenfuss, G., Dobrev, D., Eschenhagen, T. & El-Armouche, A., 2010. Constitutively active phosphatase inhibitor-1 improves cardiac contractility

- in young mice but is deleterious after catecholaminergic stress and with aging. *The Journal of clinical investigation*, 120(2), pp.617-26.
- Xie, X.J., Xue, C.-Z., Huang, W., Yu, D.-Y. & Wei, Q., 2006. The beta12-beta13 loop is a key regulatory element for the activity and properties of the catalytic domain of protein phosphatase 1 and 2B. *Biological chemistry*, 387(10-11), pp.1461-7.
- Yang, J., Hurley, T.D. & DePaoli-Roach, A. A., 2000. Interaction of inhibitor-2 with the catalytic subunit of type 1 protein phosphatase. Identification of a sequence analogous to the consensus type 1 protein phosphatase-binding motif. *The Journal of biological chemistry*, 275(30), pp.22635-44.
- Yger, M. & Girault, J.A., 2011. DARPP-32, Jack of All Trades... Master of Which? *Frontiers in behavioral neuroscience*, 5, p.56.
- Zhang, J.H., Chung, T.D.Y. & Oldenbutg, K.R., 1999. A Simple Statistical Parameter for Use in Evaluation and Validation of High Throughput Screening Assays. *Journal of Biomolecular Screening*, 4(2), pp.67-73.
- Zhang, Z., Zhao, S., Bai, G. & Lee, E.Y., 1994. Characterization of deletion mutants of the catalytic subunit of protein phosphatase-1. *The Journal of biological chemistry*, 269(19), pp.13766-70.
- Zhao, S. & Lee, E.Y., 1997. A protein phosphatase-1-binding motif identified by the panning of a random peptide display library. *The Journal of biological chemistry*, 272(45), pp.28368-72.

9 Appendix

9.1 Abbreviations

AA	amino acids
ACE	aldosterone converting enzyme inhibitor
ACP1	acid phosphatase 1
AMCM	adult mouse cardiomyocytes
APS	ammonium persulfate
AP	alkaline phosphatase
ARB	angiotensin receptor blocker
ATP	adenosine 5'-triphosphate
AV	atrioventricular node
AU	arbitrary unit
β -AR	β -adrenergic receptor
BDM	2,3-butanedione monoxime
bp	base pairs
BSA	bovine serum albumin
BW	body weight
°C	degree Celsius
cAMP	cyclic adenosine monophosphate
CaMKII	Ca ²⁺ /calmodulin-dependent kinase II
cDNA	complementary deoxyribonucleic acid
CEE	chick embryo extract
CICR	Calcium-Induced-Calcium-Release
CIP	calf intestinal phosphatase
CMV	cytomegalovirus
cMyBP-C	cardiac myosin binding protein C
CSQ	calsequestrin
Ctr	control
Da	Dalton
DARPP-32	dopamine- and cAMP-regulated neuronal phosphoproteins
DCM	dilated cardiomyopathy

DiFMUP	6, 8-difluoro-4-methylumbelliferyl phosphate
DMEM	Dulbecco's modified Eagle medium
DMF	dimethylformamide
DMSO	dimethyl sulfoxide
DNA	deoxyribonucleic acid
dNTP	deoxynucleoside triphosphate
DTT	dithiothreitol
ECL	enhanced chemiluminescence
EDB	enzyme dilution buffer
EDTA	ethylenediaminetetraacetic acid
EHT	engineered heart tissue
FBS	fetal bovine serum
FCP	TFIIF associating component of RNA polymerase II CTD phosphatase
FCS	fetal calf serum
FFT	Fast Fourier Transform
Fig.	Figure
FITC	fluorescein isothiocyanate
FS	fractional shortening
g	gram
GAPDH	glyceraldehyde-3-phosphate dehydrogenase
GFP	green fluorescent protein
GST	glutathione-S-transferase
h	hours
HBSS	Hank's balanced salt solution
HEK	human embryonic kidney (cells)
HEPES	4-(2-hydroxyethyl) piperazine-1-ethanesulfonic acid
HF	heart failure
HR	homologous recombination
HST	high-throughput screening
HW	heart weight
Hz	hertz
I-1	protein phosphatase-1 inhibitor-1
I-2	protein phosphatase-1 inhibitor-2

IC ₅₀	half maximal inhibitory concentration
ICM	ischemic cardiomyopathy
IgG	immunoglobulin G
IPTG	isopropyl 1-thio-β-D-galactopyranoside
kb	kilo base
kDa	kilo dalton
kg	kilo gram
KM	MEM containing 10% FCS and 1% P/S
KO	knock-out
LB	Luria-Bertani
LSM	laser scanning microscopy
LTCC	L-type Ca ²⁺ tubular channel
LV	left ventricular
LVH	left ventricular hypertrophy
M	molar
mA	milliampere
MEM	minimum essential medium
mg	milligram
mil.	million
min	minutes
ml	milliliter
mM	millimolar
μg	microgram
μl	microliter
μM	micromolar
MOI	multiplicity of infection
mRNA	messenger ribonucleic acid
MUP	4-methylumbelliferyl phosphate
MW	molecular weight (marker)
MyPT1	myosin phosphatase targeting subunit 1
n	number
NF	non-failing
ng	nanogram

nm	nanometer
nM	nanomolar
NRCM	neonatal rat cardiomyocytes
nt	nucleotides
NT	non-treated
NT	non-transfected
PBS	phosphate buffered saline
PCR	polymerase chain reaction
PDE	phosphodiesterase enzyme
PFA	paraformaldehyde
PKA	protein kinase A (also known as cAMP-dependent protein kinase)
PLB	phospholamban
PMP	protein MetalloPhosphatases
pNPP	para-nitrophenyl phosphate
PP1	protein phosphatase 1
PP2A	protein phosphatase 2A
PP2B	protein phosphatase 2B (calcineurin)
PP2C	protein phosphatase 2C
PPM	metal-dependent phosphoprotein
PPP	phosphoprotein phosphatase
P/S	penicillin/streptomycin
PTPN1	tyrosine phosphatase non-receptor type-1
PVDF	polyvinylidene fluoride
OA	okadaic acid
OD	optical density
R	spearman value
RB	reaction buffer
rec.	recombinant
RFU	relative fluorescence unit
RNA	ribonucleic acid
rpm	rotation per minute
RT	room temperature
RyR	ryanodine receptors

s	seconds
SA	sinoatrial node
SCP	small CTD phosphatase
SDS	sodium dodecyl sulfate
SERCA	sarcoplasmic reticulum Ca^{2+} -ATPase
SEM	standard error of the mean
SL2	biosafety level-2
SOC	super optimal broth medium with glucose
SPR	surface plasmon resonance
SR	sarcoplasmic reticulum
TBE	Tris borate EDTA
TBS-T	Tris buffered saline with Tween® 20
TCA	trichloroacetic acid
TE	Tris-HCl EDTA
TEMED	tetramethylethylenediamine
TG	transgenic
TnC	troponin C
TnI	troponin inhibitor
TnT	troponin T
Tris	Trishydroxymethylaminomethane
TTM	tautomycin
U	unit
V	volt
vs.	versus
WT	wild-type

9.2 Amino acid abbreviations

Alanine	Ala	A
Arginine	Arg	R
Asparagine	Asn	N
Aspartic acid	Asp	D
Cysteine	Cys	C
Glutamic acid	Glu	E

Glutamine	Gln	Q
Glycine	Gly	G
Histidine	His	H
Isoleucine	Ile	I
Leucine	Leu	L
Lysine	Lys	K
Methionine	Met	M
Phenylalanine	Phe	F
Proline	Pro	P
Serine	Ser	S
Threonine	Thr	T
Tryptophan	Trp	W
Tyrosine	Tyr	Y
Valine	Val	V

9.3 Indication of particular risks (R)

- 1: Explosive when dry
- 2: Risk of explosion by shock, friction, fire or other sources of ignition
- 3: Extreme risk of explosion by shock, friction, fire or other sources of ignition
- 4: Forms very sensitive explosive metallic compounds
- 5: Heating may cause an explosion
- 6: Explosive with or without contact with air
- 7: May cause fire
- 8: Contact with combustible material may cause fire
- 9: Explosive when mixed with combustible material
- 10: Flammable
- 11: Highly Flammable
- 12: Extremely Flammable
- 14: Reacts violently with water
- 15: Contact with water liberates extremely flammable gases
- 16: Explosive when mixed with oxidizing substances
- 17: Spontaneously flammable in air
- 18: In use may form flammable/explosive vapor-air mixture

-
- 19: May form explosive peroxides
 - 20: Harmful by inhalation
 - 21: Harmful in contact with skin
 - 22: Harmful if swallowed
 - 23: Toxic by inhalation
 - 24: Toxic in contact with skin
 - 25: Toxic if swallowed
 - 26: Very Toxic by inhalation
 - 27: Very Toxic in contact with skin
 - 28: Very Toxic if swallowed
 - 29: Contact with water liberates toxic gas
 - 30: Can become highly flammable in use
 - 31: Contact with acids liberates toxic gas
 - 32: Contact with acids liberates very toxic gas
 - 33: Danger of cumulative effects
 - 34: Causes burns
 - 35: Causes severe burns
 - 36: Irritating to the eyes
 - 37: Irritating to the respiratory system
 - 38: Irritating to the skin
 - 39: Danger of very serious irreversible effects
 - 40: Limited evidence of a carcinogenic effect
 - 41: Risk of serious damage to eyes
 - 42: May cause sensitization by inhalation
 - 43: May cause sensitization by skin contact
 - 44: Risk of explosion if heated under confinement
 - 45: May cause cancer
 - 46: May cause heritable genetic damage
 - 48: Danger of serious damage to health by prolonged exposure
 - 49: May cause cancer by inhalation
 - 50: Very Toxic to aquatic organisms
 - 51: Toxic to aquatic organisms
 - 52: Harmful to aquatic organisms

-
- 53: May cause long-term adverse effects in the aquatic environment
 - 54: Toxic to flora
 - 55: Toxic to fauna
 - 56: Toxic to soil organisms
 - 57: Toxic to bees
 - 58: May cause long-term adverse effects in the environment
 - 59: Dangerous for the ozone layer
 - 60: May impair fertility
 - 61: May cause harm to the unborn child
 - 62: Possible risk of impaired fertility
 - 63: Possible risk of harm to the unborn child
 - 64: May cause harm to breast-fed babies
 - 65: Harmful: May cause lung damage if swallowed
 - 66: Repeated exposure may cause skin dryness or cracking
 - 67: Vapors may cause drowsiness and dizziness
 - 68: Possible risk of irreversible effects

9.4 Indication of safety precautions (S)

- 1: Keep locked up
- 2: Keep out of the reach of children
- 3: Keep in a cool place
- 4: Keep away from living quarters
- 5: Keep contents under... (appropriate liquid to be specified by the manufacturer)
- 6: Keep under ... (inert gas to be specified by the manufacturer)
- 7: Keep container tightly closed
- 8: Keep container dry
- 9: Keep container in a well-ventilated place
- 12: Do not keep the container sealed
- 13: Keep away from food, drink and animal feeding stuffs
- 14: Keep away from...(incompatible materials to be indicated by the manufacturer)
- 15: Keep away from heat
- 16: Keep away from sources of ignition - No smoking
- 17: Keep away from combustible material

-
- 18: Handle and open container with care
 - 20: When using, do not eat or drink
 - 21: When using, do not smoke
 - 22: Do not breathe dust
 - 23: Do not breathe gas/fumes/vapor/spray (appropriate wording to be specified by the manufacturer)
 - 24: Avoid contact with skin
 - 25: Avoid contact with eyes
 - 26: In case of contact with eyes, rinse immediately with plenty of water and seek medical advice
 - 27: Take off immediately all contaminated clothing
 - 28: After contact with skin, wash immediately with plenty of ... (to be specified by the manufacturer)
 - 29: Do not empty into drains
 - 30: Never add water to this product
 - 33: Take precautionary measures against static discharges
 - 35: This material and its container must be disposed of in a safe way
 - 36: Wear suitable protective clothing
 - 37: Wear suitable gloves
 - 38: In case of insufficient ventilation, wear suitable respiratory equipment
 - 39: Wear eye/face protection
 - 40: To clean the floor and all objects contaminated by this material use ... (to be specified by the manufacturer)
 - 41: In case of fire and/or explosion do not breathe fumes
 - 42: During fumigation/spraying wear suitable respiratory equipment (appropriate wording to be specified)
 - 43: In case of fire, use ... (indicate in the space the precise type of fire-fighting equipment. If water increases the risk add - Never use water)
 - 45: In case of accident or if you feel unwell, seek medical advice immediately (show label where possible)
 - 46: If swallowed, seek medical advice immediately and show this container or label

-
- 47: Keep at temperature not exceeding .. E C (to be specified by the manufacturer)
 - 48: Keep wetted with ... (appropriate material to be specified by the manufacturer)
 - 49: Keep only in the original container
 - 50: Do not mix with ... (to be specified by the manufacturer)
 - 51: Use only in well-ventilated areas
 - 52: Not recommended for interior use on large surface areas
 - 53: Avoid exposure - obtain special instruction before use
 - 56: Dispose of this material and its container to hazardous or special waste collection point
 - 57: Use appropriate container to avoid environmental contamination
 - 59: Refer to manufacturer/supplier for information on recovery/recycling
 - 60: This material and/or its container must be disposed of as hazardous waste
 - 61: Avoid release to the environment. Refer to special instructions safety data sheet
 - 62: If swallowed, do not induce vomiting: seek medical advice immediately and show this container or label
 - 63: In case of accident by inhalation, remove casualty to fresh air and keep at rest
 - 64: If swallowed, rinse mouth with water (only if the person is conscious)

9.5 Curriculum vitae

Personal information

Surname, First name	Sotoud, Hannieh
Address	45a Frohmestr. 22457 Hamburg
Phone(-s)	Fixed: +49 40 741058131 Mobile: +49 176 20373383
E-mail	hanisotood@yahoo.com
Nationality(-ies)	German/Iranian
Personal status	married, 1 child
Date of birth	21.03.1978

Education and training

Dates	2007-2012
Title of qualification	PhD
Title of thesis	Development of an <i>in vitro</i> assay system for protein phosphatase inhibitor 1 antagonists.
Name and address of organisation	Department of Experimental Pharmacology and Toxicology University Medical Center Hamburg-Eppendorf (UKE) 52 Martinistr. 20246 Hamburg

Dates	2009-2011
Title of qualification	Certificated in Molecular Biology
Name and address of organization	The Center for Molecular Neurobiology Hamburg (ZMNH) 94 Falkenried 20251 Hamburg

Dates	1997-2003
Title of qualification	Pharm.D.
Title of doctoral research	Study of protective roles of renin-angiotensin system inhibitors on diabetic nephropathy.
Name and address of organisation	Pharmaceutical Sciences of Azad University 99 Jasaman, Jakhchal Shariati Tehran-Iran

Work experience

2004-2006	Pharmacist at Seoul pharmacy in Tehran-Iran
-----------	---

9.6 Congress participations

H. Sotoud, T. Eschenhagen, A. El-Armouche. Development of an *in vitro* assay system for screening for protein-phosphatase-inhibitor-1 inhibitory compounds.

49. Jahrestagung der Deutschen Gesellschaft für Experimentelle und Klinische Pharmakologie und Toxikologie, Mainz, März 2008. **Poster presentation**

H. Sotoud, Björn Windshügel, L. Kattner, T. Eschenhagen, A. El-Armouche. Colorimetric protein phosphatase inhibition assay for specific detection of phosphatase-inhibitor-1 inhibitory compounds.

50. Jahrestagung der Deutschen Gesellschaft für Experimentelle und Klinische Pharmakologie und Toxikologie, Mainz, März 2009. **Poster presentation**

H. Sotoud, Björn Windshügel, L. Kattner, T. Eschenhagen, A. El-Armouche. Development of an *in vitro* assay for protein-phosphatase-1.

51. Jahrestagung der Deutschen Gesellschaft für Experimentelle und Klinische Pharmakologie und Toxikologie, Mainz, März 2010. **Poster presentation**

H. Sotoud, A. El-Armouche, Björn Windshügel, L. Kattner, T. Eschenhagen. Screening for inhibitors of protein phosphatase inhibitor-1 with a new microplate assay.

7th annual Screening Europe conference and exhibition. Barcelona, February 2010. **Poster presentation**

H. Sotoud, A. El-Armouche, Philip Gribbon, Björn Windshügel, L. Kattner, T. Eschenhagen. Development of an *in vitro* assay for protein-phosphatase-1.

2nd PhD Student Exchange Meeting in London. October 2010. **Poster presentation**

H. Sotoud, A. El-Armouche, P. Gribbon, J. Reinshagen, F. Halley, B. Windshügel, L. Kattner and T. Eschenhagen. Development of an *in vitro* assay system for protein-phosphatase-inhibitor-1 inhibitory compounds.

6th Annual Winter Research Meeting on Translational Basic Science. Les Diablerets, January 2011. **Poster presentation**

H. Sotoud, A. El-Armouche, P. Gribbon, J. Reinshagen, B. Windshügel, and T. Eschenhagen. Development of an *in vitro* assay system for PP1-I-1 inhibitory compounds. Biomarker and Translational Research Workshop. Hamburg, September 2011. **Oral presentation**

10 Acknowledgement

Sometimes the best opportunities are achieved simply unplanned. I experienced this fact in one summer day, as I entered the “Institut für Experimentelle Pharmakologie und Toxikologie” to ask for a PhD position. I was extraordinary fortunate to meet Prof. Dr. Thomas Eschenhagen who was generous towards my unconventional way of application and gave me this unique chance to be a member of his big family. His enthusiasm, strong willingness, and immense knowledge guided me through my thesis. His exemplary manner was always inspiring, and I would be deeply grateful to him.

I thank Prof. Dr. Peter Heisig for his kind supervision of my thesis in the Department of Chemistry in the University of Hamburg.

I would like to express my heartfelt gratitude to Prof. Dr. Ali El-Armouche for his excellent supervision during the first two years of my thesis and his never-ending supports in the all time. Through his patient and confidence, I could improve my performance. Writing of this thesis would not have been possible without him.

My special thanks go to Prof. Dr. Lucie Carrier for her useful comments and advices, in particular, her untiringly commitment of IonOptix measurements.

I would like to acknowledge Dr. Philip Gribbon, Dr. Uwe Borgmeyer, Dr. Christian Schulze, Dr. Björn Winshügel, Dr. Peter Boknik and Dr. Lars Kattner for their invaluable collaborations.

I offer my regards to all my colleagues who made the “Institute of Experimental Pharmacology & Toxicology” as a second home for me. Particularly, my warm thanks go to Jutta Starbatty, Dr. Christiane Neuber, Thomas Schulze, Dr. Katrin Wittköpper, Dr. Saskia Schlossarek, Elisabeth Krämer, Dr. Alexandra Eder, Dr. Sebastian Schaaf and Dr. Giulia Mearini for their tremendous dedication and adorable friendliness. I wish to express my great delights in having Andrea Stöhr who was my soulmate, despite our different backgrounds. She was such sunshine in all my dark moments. I always enjoyed our time together, particularly our interesting discussions either related to work or about the sense of life.

I also wish to thank Frank Neumann and Gerlinde Raasch for their kind supports of the administrative efforts.

Last but by no means least, my deepest appreciation to my family for general education and providing the opportunity to start and pursue a career in science. First, I like to remember my mother whose ambition was my felicity and success in life and in a high-level education. She is always in my heart wishing her soul is blessed. Also, I would like to pay my respects and blessings to my father. His suffering made me aware of people who require not only improved medical treatments, also emotional supports. Very importantly, I would like to deeply acknowledge my adorable husband, Amir, for his ongoing supports, motivating encouragements, and enormous patient. Without him I would not be there where I am now. Therefore, I dedicate this thesis to him and also to my beloved son, Parsa, for his great understanding and tolerance towards my inadequate attention. His sweet proudness of my work in the lab as a “super scientist” was a big comfort for me. Also, I like to express the greatest thanks to my grandmother who raised me and still loves me at the most. Without her maybe I was not existed. I am also very indebted to my uncle, who was always poised to help me.

Finally, I would like to thank all people that were involved in accomplishing this thesis either directly or indirectly, and I could not mention personally one by one.

Hannieh Sotoud

Hamburg May 2012

“Success is never final. Failure is never fatal. It’s courage that counts.”

John Wooden